Exploring the transcriptional function of mTOR in prostate cancer

Yonghong Chen

Department of Biochemistry, McGill University, Montreal

April 2023

A thesis submitted to McGill University in partial fulfillment of the requirements of the degree of Doctor of Philosophy.

11.5. Chapter 3 Supplemental Tables 1-5

Abstract

mTOR (mechanistic target of rapamycin) is a critical kinase to coordinate the upstream signals (growth factors and nutrients) with the downstream metabolic processes to promote cell growth and survival. In addition to its known roles in controlling translation, mTOR is capable of regulating transcription. Here my PHD project demonstrates two distinct but not mutually exclusive ways of mTOR transcriptional function. On one hand, mTOR indirectly regulates transcription by phosphorylating HOXB13. mTOR dependent HOXB13 phosphorylation decreases HOXB13 protein stability but increases its transcriptional activity, dictating a specific oncogenic gene program to drive prostate cancer cell growth in vitro and in murine xenografts. It is a kinase dependent mechanism. On the other hand, mTOR directly regulates transcription by complexing on chromatin. mTOR can translocate into the nucleus and interact with multiple cofactors such as AR and FOXA1 on the cis-regulatory elements of target genes, modulating the downstream gene expression regardless of its kinase activity. NLS (nuclear localization signaling) tagged mTOR specifically increases nuclear mTOR abundance and activity, functionally inhibiting AR signaling and promoting androgen independent prostate cancer progression. Taken together, both kinase activity and transcriptional activity are two important characteristics that determine mTOR nuclear function, which could be therapeutically targeted for treating mTOR-driven prostate cancer.

Version française

mTOR (mechanistic target of rapamycin) est une kinase essentielle pour coordonner les signaux en amont (facteurs de croissance et nutriments) avec les processus métaboliques en aval pour favoriser la croissance et la survie des cellules. En plus de ses rôles connus dans le contrôle de la traduction, mTOR est capable de réguler la transcription. Ici, mon projet de doctorat démontre deux mécanismes distincts mais non mutuellement exclusifs de la fonction transcriptionnelle de mTOR. D'une part, mTOR régule indirectement la transcription en phosphorylant HOXB13. La phosphorylation de HOXB13 dépendante de mTOR diminue la stabilité de la protéine HOXB13 mais augmente son activité transcriptionnelle, dictant un programme d'oncogènes spécifiques pour stimuler la croissance des cellules cancéreuses de la prostate in vitro et dans les xénogreffes murines. D'autre part, mTOR régule directement la transcription en se complexant sur la chromatine. mTOR peut se transloquer dans le noyau et interagir avec plusieurs cofacteurs tels que le récepteur aux androgènes (AR) et FOXA1 sur les éléments cis-régulateurs des gènes cibles, modulant étroitement l'expression des gènes en aval. mTOR marqué avec un NLS (signalisation de localisation nucléaire) augmente spécifiquement l'abondance et l'activité de mTOR nucléaire, inhibant fonctionnellement la signalisation AR et favorisant la progression du cancer de la prostate indépendamment des androgènes. Ensemble, les activités kinase et transcriptionnelle sont deux caractéristiques importantes pour déterminer la fonction nucléaire de mTOR, qui pourraient être ciblées thérapeutiquement pour le traitement du cancer de la prostate.

Acknowledgements

I wish to thank my supervisor (Dr. Vincent Giguere) who provided the platform for my PHD study. Thanks to all the lab members for the help in the daily time and the discussion in the lab meeting. Thanks to the funding agencies (CIHR and Terry Fox Foundation) for providing the funding support. Thanks to my RAC members (Dr. Michel Tremblay and Dr. Jose Teodoro) for giving important research suggestions. Thanks to the Department of Biochemistry and Goodman Cancer Institute for the great graduate education.

Also, I want to thank all the co-authors in my two papers who helped me complete the experiments and publication. Specifically, thanks to Ms. Catherine Dufour for bioinformatics analysis, data organization and manuscript correction. Thanks to Dr. Ting Li, Dr. Hui Xia and Lingwei Han for help on the experiments (more details in the "Author Contributions" part).

Certainly, only with all these helps and supports above can I accomplish my PHD projects and graduate smoothly.

Contributions to original knowledge

In Chapter 2, I identified previously unknown phosphorylation sites for HOXB13 at T8/T41/S31. It was first time to show that mTOR could interact with and phosphorylate HOXB13 in a sequential order. HOXB13 phosphorylation led to its protein destabilization but also transcriptional activation, dictating specific oncogenic gene programs. My work highlighted that it is the phosphorylated HOXB13 level but not the total protein level that determines its oncogenic function in prostate cancer, which would undoubtedly reconcile the conflicts about the role of HOXB13 previously ascribed in prostate cancer. Notably, phosphorylated HOXB13 may be used as a biomarker to monitor prostate cancer aggressiveness.

In Chapter 3, I for the first time added NLS and NES tags to mTOR to modulate its abundance and activity specifically in the nucleus and cytoplasm of prostate cancer cells, respectively. Comparing NLS-mTOR dependent gene signature with that of NES-mTOR, I was able to differentiate nuclear mTOR function from its cytosolic mTOR function. Nuclear mTOR majorly downregulated the androgen response genes regardless of its kinase activity. This previously unappreciated kinase independent nuclear mTOR function played significant roles in promoting androgen independent prostate cancer progression. It helped explain the unsatisfactory efficacy of mTOR kinase inhibitors in clinical trials, and suggested that combination therapy targeting both kinase activity and transcriptional activity of mTOR could provide more and better therapeutic benefits to prostate cancer patients.

Author Contributions

In the first paper (Chapter 2), I performed most of the experimental work under the supervision of Dr. Vincent Giguère. Catherine Dufour analyzed the RNA-seq data. I prepared cells for xenograft models; Lingwei Han monitored the tumor growth; Dr. Ting Li and Dr. Hui Xia dissected the tumors at endpoint. I designed the experiments and organized the data with the help of Catherine Dufour and Dr. Giguère. I wrote the original draft of the manuscript with edits from Catherine Dufour and Dr. Giguère.

In the second paper (Chapter 3), I established the NLS-mTOR tool and performed most of the experiments. I prepared the samples for mTOR RNA-seq and ChIP-seq. Catherine Dufour helped in the analysis of the omics datasets. Lingwei Han performed some mTOR ChIP-qPCR assays. I designed the experiments and organized the data under the guidance of Catherine Dufour and Dr. Giguère. I wrote the original draft of the manuscript with correction from Catherine Dufour and Dr. Giguère.

Chapter 1. Background Introduction

Prostate cancer

Prostate cancer (PCa) is one of the most prevalent cancer types among men worldwide and a major cause of cancer related death in men. Charles Huggins and colleagues in 1941 demonstrated the remarkable benefit of androgen deprivation therapy (ADT) via surgical or medical castration for men with advanced metastatic prostate cancer [1, 2]. He was thus awarded the Nobel Prize in Physiology or Medicine in 1966. After that, ADT has become the mainstay treatment for PCa patients. Surgical castration means the removal of testes by surgery to block androgen production [3], while medical castration uses LHRH/GnRH (Luteinizing Hormone Releasing Hormone/ Gonadotropin Releasing Hormone) agonists to reduce serum androgen level [4]. Despite the initial successful response rate (80%-90%) [5], ADT is palliative but not curative. After short-term tumor shrinkage, all patients will eventually develop into castration resistant prostate cancer (CRPC) which is more aggressive and lethal. Two distinct but not mutually exclusive models are proposed to explain the mechanisms for CRPC progression [6]. One is adaptation model suggesting the acquisition of several oncogenic alterations to survive in androgen depleted condition, the other is the selection model showing the outgrowth of pre-existing androgen independent cancer cells during the castration treatment.

Adaptation model

The adaptation model describes multiple mechanisms for castration resistance including restored AR activity, bypass of AR signaling and complete AR independence [4]. Restoring AR activity occurs at two facets (the ligand and the receptor). In the context of the ligand, testosterone is majorly produced by the testes (90%) but still some can be derived from the adrenal gland (10%)

[3]. Although androgen level decreased drastically after surgical castration, the residual androgens were primarily adrenal Dehydroepiandrosterone (DHEA) and androstenedione (AD), which can be converted into testosterone and dihydrotestosterone (DHT) in the prostate to sustain tumor growth [7, 8]. As for the receptor, AR gene amplification has been identified in a significant portion of CRPC patients (20%-70%) [6], which enables tumors to be hypersensitive to low level of androgens [9]. Multiple AR hotspot point mutations (such as L702H, W742C, H875Y and T878A) in its LBD (Ligand Binding Domain) were also found in 15%-20% of CRPC cases to confer drug resistance [4, 10]. These mutants could turn AR antagonists into AR agonists to paradoxically activate AR, or confer AR androgen hypersensitivity, or broaden AR ligand specificity [11, 12]. Alternative splicing of AR mRNA is another mechanism. Numerous AR splicing variants are identified in clinical specimens, of which all share one common feature by truncating or exon skipping the carboxyl- terminal LBD to gain constitutive androgen-independent activity [13-15].

In addition, signaling bypass means the initially important signaling pathway could be alternatively activated by a different driver. In the context of AR signaling, studies found other hormone receptors including the Glucocorticoid Receptor (GR), Progesterone Receptor (PR) and Mineralocorticoid Receptor (MR) could replace AR to regulate the shared target gene expression because of the substantial homology within the DNA Binding Domain [16, 17]. Furthermore, complete AR independence reveals that prostate adenocarcinoma could develop into AR null PCa particularly in tumors undergoing neuroendocrine differentiation (NEPC). Molecular profiling of NEPC has uncovered several other oncogenic alterations including loss of *RB1*

(Retinoblastoma) and *TP53* (Tumor Protein 53) as well as amplification of *MYCN* and *AURKA* (Aurora Kinase A) which can promote PCa progression in the absence of AR function [18-23].

Selection model

The selection model comes from the complexity and heterogeneity of prostate cancer on which the AR pathway inhibition therapy could exert selective pressure. Only tumor cells with low or no dependency on AR activity for growth and survival will be eventually selected to expand [24, 25]. It is quite similar to the concept of cancer stem cells [26, 27]. Due to the very low frequency of these therapy resistant cells ($1/10^5$-$1/10^6$), the progression from androgen dependence to androgen independence theoretically needs two steps [24]. The first is the apoptotic cell death of the majority of androgen responsive cells and the second is the outgrowth of these minority of androgen insensitive cells. Additionally, the hormone naive PCa cells display different responses to castration mimicking the property of normal prostate epithelial cells which comprise three major cell types (basal cells, luminal cells and neuroendocrine cells) [28]. The luminal cells constituting the major part of the prostate glandular structure are highly dependent on androgen signaling for growth [29], while the basal cells forming a layer between luminal cells and the basement membrane show very limited requirement of AR function for homeostasis [30]. The third neuroendocrine cells distributing throughout the basal layer represent the minor group of epithelial cells with complete androgen independence [31]. Prostate cancer cells originating from these different prostate epithelial cells after the long-time accumulation of oncogenic mutations certainly inherit their parental heterogeneous features with diverse degree of castration resistance [32, 33].

NEPC and its treatment

As shown in Figure 1, there are three major stages during PCa progression, from the initial androgen responsive adenocarcinoma (treated with ADT), to AR hyperactive CRPC (treated with abiraterone and enzalutamide), to the lethal androgen negative prostate cancer (including NEPC, no targeted therapy available) [34]. In order to treat the late stage of PCa, intensive studies have been done to uncover the mechanisms for NEPC development and screen the possible druggable therapeutic targets. Several transcription factors and epigenetic factors were found to be involved in controlling lineage plasticity towards NEPC. Transcription factors including SOX2, MYC, BRN2 and ONECUT2 were reported to induce neuroendocrine differentiation and androgen independence [34-38]. Epigenetic factor EZH2 could downregulate and even abrogate AR gene expression by adding H3K27me3 repressive marks on the AR promoter [23]. Therapeutically, re-expression of AR in AR negative PCa is advised to treat the lethal and most aggressive form of PCa. Drugs inhibiting DNA methylation, histone deacetylation (HDACs inhibitors) and histone methylation (EZH2 inhibitors) are proposed to reactivate AR expression in AR negative PCa [39-41]. However, these drugs can not only modulate AR expression, but also many other genes expression, which will cause many side effects and definitely complicate the treatment outcome. Thus, more precise, and direct approaches to specifically increase AR expression and re-sensitize AR negative PCa to androgen targeting therapy should be explored.

Figure 1

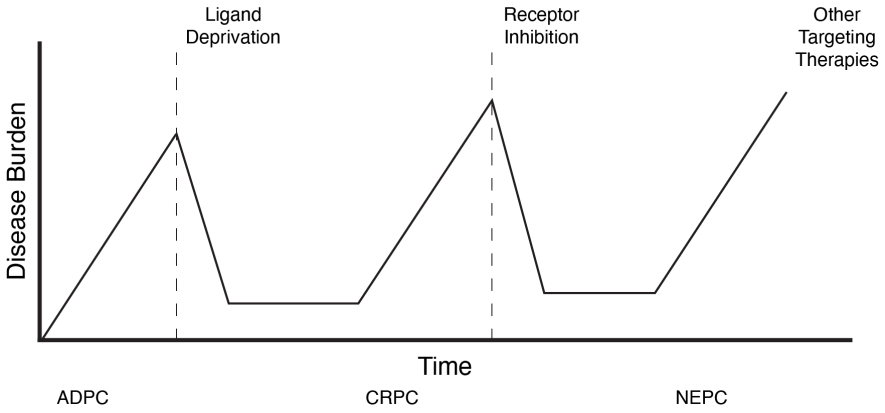

Figure 1. Prostate cancer progresses upon AR pathway inhibition over time. Ligand Deprivation can be mediated by surgical or medical castration. Receptor Inhibition uses Enzalutamide as the second-generation inhibitor of AR. ADPC: Androgen Dependent Prostate Cancer; CRPC: Castration Resistance Prostate Cancer; NEPC: Neuroendocrine Prostate Cancer.

Prostate cancer cell lines

Relatively few human prostate cancer cell lines have been established and used. The classic and widely used cells are LNCaP, DU145, PC3 and 22RV1 cells. They are different in regard of AR expression, PTEN expression and androgen responsiveness. LNCaP and 22RV1 cells can express AR proteins, while DU145 and PC3 cells do not express AR proteins. LNCaP and PC3 cells are PTEN negative cells, while 22RV1 and DU145 cells are PTEN positive cells. LNCaP cells are sensitive to androgen treatment, but 22RV1 cells are weakly dependent on AR function because of the additional expression of AR-V7. Therefore, LNCaP cells can recapitulate the features of ADPC (Androgen Dependent Prostate Cancer), and 22RV1 cell line can be a model to study CRPC (Castration Resistance Prostate Cancer). Both DU145 and PC3 cells can be models to study advanced prostate cancer such as NEPC (Neuroendocrine Prostate Cancer) in which AR is no longer expressed.

Biomarkers

Biomarkers constitute another important aspect of PCa (a non-cutaneous cancer type) research to monitor its disease progression and therapeutic response. Prostate specific antigen (PSA) encoded by *KLK3*, is an androgen regulated serine protease that could liquefy the seminal fluid, of which blood level test is widely used for PCa screening and monitoring [42]. However, other benign prostate diseases could also increase PSA level in blood, which leads to a wrong diagnosis of PCa. In addition, PSA screening by detecting some of these insignificant prostate cancers (without any health threats) could cause unnecessary cancer treatment and increase patient mental pressure [43]. It may not help early diagnosis but induce over diagnosis. Therefore, some improvements for PSA testing or other biomarkers are needed for better PCa diagnosis. One way to improve PSA test is to differentiate free PSA from protease inhibitor complexed PSA (more stable in blood). In proportion to total PSA (measured by conventional PSA assay), free PSA is much lower in prostate cancer than other benign prostate diseases [44]. Another way is to measure the PSA dynamics (velocity to change or doubling time in blood) [45, 46], which can help determine disease aggressiveness and monitor disease progression. Furthermore, speaking of novel markers, hK2 is proposed to be one of the candidates because of its property similar to PSA [47], which also depends on androgen for its production, is released to seminal fluid and increases in serum after cancer initiation. Altogether, conventional PSA test is generally beneficial and frequently used for prostate cancer diagnosis, which should be combined with some improvements and other accurate screening methods for better performance in treating PCa.

Androgen Receptor

AR gene on Chromosome X q11-12 region encodes a protein with molecular weight around 110KD [3]. AR (also known as NR3C4) belongs to the nuclear hormone receptor transcription factor family. AR contains four functional domains which are the amino-terminal transactivation domain (NTD), the central DNA binding domain (DBD), the flexible hinge region and the carboxyl-terminal ligand binding domain (LBD) (Figure 2A) [48]. The AR NTD contains the AF1 (Activation Function 1) region that can constitutively activate AR when separated from the LBD [49], while the AR LBD contains the AF2 region as the major protein-protein interaction surface to recruit LXXLL-motif containing coactivators [50]. The AR DBD contains two zinc fingers that determine the specificity of DNA recognition and the dimerization [51], whereas the hinge region contains a bipartite NLS (nuclear localization signal) that enables its nuclear translocation in a ligand-dependent manner [52]. Therefore, upon ligand binding, the inactive cytoplasmic form of AR will be activated by dissociating from the chaperone heat shock proteins (HSP90), dimerizing and translocating into the nucleus [53]. Inside the nucleus, AR binds with specific DNA sequences designated as androgen response elements (ARE) in the promoters or enhancers of target genes, with core repeated sequences of 5'-TGTTCT-3' [51]. ChIP-seq (Chromatin Immunoprecipitation coupled with high-throughput sequencing) as a powerful method can be used to identify genome-wide binding patterns for AR. First, DNA-AR interaction needs to be crosslinked by formaldehyde. Second, chromatin should be fragmented under 500 base pairs by sonication in order to get high quality DNA pieces for ChIP analysis. Third, beads-antibody mediated immunoprecipitation could pull down AR and its bound DNA specifically. Fourth, AR bound DNA should be de-crosslinked with AR protein and extracted.

Lastly, the purified DNA fragments can be analyzed by qPCR or second-generation sequencing, which can provide important information about the direct genomic binding sites for AR. This direct interaction with the genome regulatory regions can lead to the up-regulation or down-regulation of target genes, which is also affected by the co-recruitment of AR cofactors. Comprehensive proteomic analysis identified over 300 AR cofactors, many of which are general transcription factors, chromatin remodeling factors and histone modifying factors (Figure 2B) [54].

Figure 2A

Figure 2B

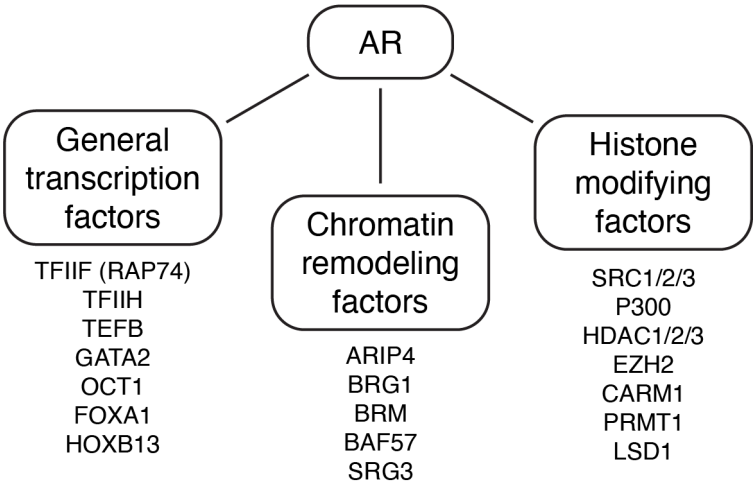

Figure 2. Information for AR**. A**, schematic shows AR has four functional domains. NTD: N-terminal Domain; DBD: DNA Binding Domain; H: Hinge region; LBD: Ligand Binding Domain. **B**, AR interacts with various cofactors including General Transcription Factors, Chromatin Remodeling Factors and Histone Modifying Factors.

General transcription factors

Since enhanced transcription by AR requires the recruitment of RNA polymerase II to promoters of its target genes, AR could undoubtedly interact and collaborate with several key components of the transcriptional PIC (Preinitiation Complex). AR binds with RAP74 subunit of TFIIF to recruit coactivator SRC1 and binds with TFIIH to enhance the phosphorylation of RNA polymerase CTD (Carboxyl Terminal Domain) [55, 56]. AR also recruits TEFB (Transcription Elongation Factor B) to phosphorylate the largest subunit of the RNA polymerase II, necessitating the transcription progression from initiation to elongation [57]. In addition, DNA binding motif analysis of AR bound genomic sites reveals that transcription factor GATA2, OCT1 and FOXA1 could interact and co-recruit with AR to the same target genes for transcriptional regulation [58]. Deletion of GATA2 and OCT1 results in the suppression of AR target gene expression, while FOXA1 acts upstream of GATA2 and AR to reprogram their cistrome [59]. Pioneer factor FOXA1 and HOXB13 physically interacting with AR possess important functions in dictating AR genomic binding sites to be more tumorigenic [60, 61].

Chromatin remodeling factors

Due to the structural features of nucleosome that restrict the accessibility of DNA to transcription factors in quiescent state, chromatin remodeling complexes are needed to unwrap histone-DNA contacts in an ATP dependent manner and reorganize the chromatin to be more permissive for transcription [62]. The first chromatin remodeler identified to bind with AR is ARIP4 (AR Interacting Protein 4), a nuclear ATPase that belongs to SNF2-like protein family [63, 64]. ARIP4 mutants lacking ATPase activity behave as the dominant negative regulators for AR function. Two other ATPases BRG1 (also known as SMARCA4) and BRM, two core

components of SWI/SNF (Switching /Sucrose Non-Fermenting) chromatin remodeling complex, are shown to interact with and stimulate AR activity [65]. Other subunits such as BAF57 (BRG1 Associated Factor 57) and SRG3 (SWI3 Related Gene) are also able to bind with AR and enhance its transactivation [66, 67].

Histone modifying factors

Modifications on histone residues are known to affect the transcription efficiency by changing the net charges of nucleosome to lighten or tighten the histone-DNA interactions [68]. Histone acetyltransferase SRC1/2/3 (Steroid Receptor Coactivator 1/2/3, also known as NCOA1/2/3) and P300 could bind with AR to increase AR transcriptional activity [69-72]. Histone deacetylase HDAC1/2/3 and methyltransferase EZH2 (Enhancer of Zeste Homolog 2) are also found to bind with AR and attenuate AR transcriptional activity critical for epithelial differentiation, leading to aggressive prostate cancer metastasis [73, 74]. Another two methyltransferases CARM1 (Coactivator Associated Arginine Methyltransferase 1) and PRMT1 (Protein Arginine Methyltransferase 1) are initially identified to interact with SRC1 coactivators, thereby acting as the secondary coactivator for AR transactivation [75, 76]. Histone demethylase LSD1 (Lysine Specific Demethylase 1) corecruits with AR to a conserved site in the second intron of AR gene itself to directly suppress AR mRNA expression [77].

AR in prostate cancer

AR is widely believed as the oncogenic driver for PCa progression. AR promotes G1-S cell cycle progression through androgen dependent regulation of Cyclin D1 expression in primary prostate adenocarcinoma [78], while AR positively regulates G2-M transition by activating UBE2C

expression in CRPC [79]. As a transcription factor, AR can control multiple target genes expression to accomplish its genomic signaling. TMPRSS2-ERG fusion is one of the most common molecular alterations in early prostate cancer which puts the androgen response elements of TMPRSS2 at the upstream of ETS family oncogene (including ERG) by chromosomal rearrangements [80, 81]. Thus, AR could directly upregulate the expression of ERG which drives prostate cancer progression. Additionally, AR has been implicated in crosstalk with various oncogenic pathways to complete its non-genomic signaling. Growth factors like EGF (Epidermal Growth Factor) and IGF (Insulin-like Growth Factor) and cytokines like IL6 could activate AR independent of its ligand and sustain PCa cell growth despite castrate level of androgen [82, 83]. Several kinases including MAPK (Mitogen Activated Protein Kinase) and mTOR (mechanistic Target of Rapamycin) could be activated by AR non-genomic function to coordinate cell growth with cell metabolism [84, 85]. However, contradictory studies also show that AR can function as a tumor suppressor and high doses of androgen can suppress PCa cell growth. High level of AR is found to directly repress the expression of genes required for DNA replication through the co-recruitment of hypo-phosphorylated RB (Retinoblastoma) to AR binding sites [86]. AR is also found to repress the expression of itself via the co-recruitment of LSD1 [77]. Restoring AR in PC3 cells (AR negative PCa cells) results in decreased invasion in bone lesion assays and in vivo mouse models [87]. In summary, on one hand AR promotes proliferation and inhibits apoptosis, but on the other hand AR impedes PCa invasion and metastasis by inducing differentiation to maintain epithelial phenotype [73].

AR mutations

Intensive efforts have revealed that AR undergoes point mutations with hotspots in the LBD in response to AR targeting therapy [88, 89]. These mutants are exclusively found in CRPC patients but not in those with primary PCa. Mechanistically, four key point mutations (L702H, W742C, H875Y and T878A) are shown to turn AR antagonists into AR agonists so that treating with AR inhibitors (Bicalutamide or Enzalutamide) could activate rather than inhibit AR-driven PCa growth [4]. Mutations in AR LBD could also affect the ligand specificity to allow AR activation by other steroid ligands such as progesterone and glucocorticoid [12]. In addition, various AR splicing variants (ARVs) have been identified in several PCa cell lines, xenograft tumors and clinical patient samples [15, 90]. All the ARVs retain NTD and DBD, but truncate LBD with different degrees. Only those with intact NLS sequence located in the hinge region can have constitutive, ligand independent nuclear localization, while variants having incomplete or even no NLS sequence can translocate into the nucleus differentially through unknown mechanisms. ARV7 as the best characterized variant can be induced by ADT, possibly contributing to CRPC [91]. Considering these alterations of AR occur mainly in the LBD region to cause therapeutic resistance, drugs targeting AR NTD or DBD could be rationally developed.

AR post translational modifications

Intensive studies have uncovered that AR undergoes various PTMs (post-translational modifications) that alter its transcription activity, nuclear translocation and protein stability [92, 93]. For example, AR could be phosphorylated by CDK1 at Ser81, leading to protein stabilization and androgen sensitization [94]. AR could be acetylated by P300 at Lys632 and Lys633, increasing its transcriptional activity [69]. AR could be methylated by SET9 at Lys632, facilitating its recruitment to androgen target genes [95]. AR could be ubiquitinated by RNF6 at

Lys845 and Lys847, enhancing its transcriptional activity [96]. AR could be SUMOylated by PIAS1 at Lys386 and Lys520, repressing androgen dependent transcription [97]. Altogether, PTMs have undoubtedly provided critical insights for the mechanisms regulating AR activation in addition to androgen ligand mediated activation, which suggests that these epigenetic enzymes of AR could be potentially novel drug targets for better control of AR function in CRPC.

AR targeting therapies

Currently there are several widely and clinically used agents for ARPI (AR Pathway Inhibition) [3]. Abiraterone is an inhibitor for cytochrome P450 family enzyme CYP17A1, which can inhibit intraprostatic androgen synthesis particularly originating from adrenal gland [98, 99]. Overexpression or mutations of CYP17A1 are shown to contribute to abiraterone resistance. Bicalutamide as the AR first generation inhibitor could compete with androgen for the binding to AR and promote the recruitment of AR corepressors [100, 101], while Enzalutamide as the AR second generation inhibitor could have higher efficiency by suppressing androgen binding to AR, AR nuclear translocation, AR DNA binding and co-activator recruitment [102, 103]. AR splicing variations or mutations in the LBD are found to cause enzalutamide resistance. Therefore, inhibitors targeting AR NTD or DBD should be designed [104-106]. Emerging evidence suggest huge potentials of AR antisense oligonucleotides and AR PROTAC degrader that could be alternative approaches to directly reduce AR protein level and activity in treating AR driven prostate cancer [107, 108]. Considering the importance of these enzymes post-translationally modifying AR and these coregulators modulating AR activity, multiple drugs (such as SWI/SNF inhibitors, EZH2 inhibitors, P300 inhibitors and HDACs inhibitors) are also being enthusiastically tested in clinic [109-113].

FOXA1

FOXA1 (also termed as HNF3a) is a transcription factor belonging to forkhead box protein family [114]. It is known as a pioneer factor of which structure closely resembles that of histones [115], so that it can bind with condensed chromatin and subsequently pry it open [116, 117]. FOXA1 recruitment to chromatin is governed by its consensus forkhead (FKHD) DNA binding motif and further facilitated by the presence of histone methylation (particularly H3K4me1 and H3K4me2) and the loss of DNA methylation [118, 119]. After creating an open and easily accessible chromatin region, FOXA1 could promote the DNA binding of hormonal transcription factors including estrogen receptor α (ERα) and AR [120, 121]. In ERα positive breast cancer, FOXA1 is required for ERα DNA binding and its transcriptional activity because loss of FOXA1 abolishes most ERα association with chromatin and overexpression of FOXA1 enhances ERα regulated transcriptome and cell growth [122, 123]. However, in prostate cancer, FOXA1 roles in regulating AR signaling and cancer progression are much more complex [124]. Instead of simply inhibiting AR total binding events, FOXA1 depletion intensively reprograms AR cistrome by losing some binding sites but also gaining many new binding sites [121]. Three classes of AR binding sites have been categorized, which are FOXA1 independent binding sites (not changing binding regardless of FOXA1 loss), FOXA1 augmented binding sites (losing binding upon FOXA1 loss) and FOXA1 attenuated binding sites (gaining binding upon FOXA1 loss). One explanation is that FOXA1 preferentially recruits AR to genomic sites primarily containing FKHD motif but AR will be liberated to bind its own target sites with ARE motif after FOXA1 depletion [125]. One drawback for this hypothesis is that excessive expression of FOXA1 is also found to increase AR binding to new sites because of the hyperactive pioneering

activity of FOXA1 to open immensely more chromatin regions. Therefore, whether FOXA1 facilitates or inhibits AR DNA binding is dependent on the genomic context of target regions and the equilibrium of FOXA1/AR nearby.

FOXA1 in prostate cancer

FOXA1 has been shown to have dual roles in PCa biology [126]. Some report that high level of FOXA1 expression is associated with aggressive PCa and poor prognosis [127-130], while others show that loss of FOXA1 promotes metastatic PCa progression [131-133]. In the presence of androgen, FOXA1 promotes cell proliferation in concert with AR function by inducing cell cycle genes expression [79, 134]. However, in the absence of androgen, downregulation of FOXA1 still leads to androgen independent cell growth [121]. Additionally, FOXA1 harbors androgen independent function to inhibit cell invasion and migration by directly repressing SLUG expression [135]. FOXA1 is found to inhibit PCa neuroendocrine differentiation [136], but it is also suggested to be an essential factor for NEPC and potentiate lineage specific enhancer activation [137, 138]. Also, FoxA2 as a closely related family member to FOXA1 is reported to drive lineage plasticity in NEPC [139], which may have competing or compensating effects with FOXA1 to regulate NEPC progression. Taken together, FOXA1 expression level and function should be more carefully examined by taking into considerations of androgen condition, treatment history and disease stage.

FOXA1 mutations

Intensive studies uncover that FOXA1 is frequently mutated in both coding and noncoding regions, which significantly impacts PCa development and drug treatment [140-142]. Among all

these coding mutations, around 50% mutations map to the forkhead DBD particularly the Wing2 region, which primarily are point mutations, while over 20% mutations enrich at the CTD (Carboxyl Terminal Domain) which are truncating frameshifting mutations [143]. Intriguingly, DBD point mutants are originated in primary prostate cancer, whereas CTD truncating mutants are found in metastatic prostate cancer, implying the information possibly correlating FOXA1 mutation status with disease stage. FOXA1 coding mutations could affect its DNA and cofactors binding, remodel accessible chromatin landscapes and change its transcriptional activity [144]. As the pioneering factor for AR, FOXA1 mutants could also disturb androgen signaling but the effects are complex. Both promoting and inhibiting functions were reported, and the phenotypic outcomes vary among these mutants. For instance, DBD mutants including D226G, H247Y and M253K prevent AR DNA binding and suppress some AR target genes expression [145], and CTD truncating mutants promote EMT (Epithelial Mesenchymal Transition) and cancer metastasis [143]. However, the underlying mechanisms remain largely elusive and need to study case by case. For non-coding mutations, if occurring at these CREs (Cis Regulatory Elements) of FOXA1, they likely result in dysregulated FOXA1 mRNA expression [146, 147]. Chromosomes reposition or gene translocation nearby FOXA1 CREs could hijack FOXA1 cis-regulatory activity to increase certain oncogene expression. Also, if non-coding mutations are found in the CREs of FOXA1/AR target genes, the DNA binding of FOXA1/AR will certainly be affected (either induced or reduced), leading to diverse expression profiles [140].

FOXA1 post translational modifications

FOXA1 has been reported to have multiple post-translational modifications (PTMs) to regulate its activity, such as acetylation, phosphorylation and SUMO (Small Ubiquitin-like Modification)

[148-150]. More importantly, FOXA1 can be methylated by EZH2 at Lys295 to enable the de-ubiquitination by USP7, which consequently enhances FOXA1 protein stability and promotes FOXA1-driven PCa growth [151]. Also, FOXA1 can be de-methylated by LSD1at Lys270 to enhance its DNA binding, which positively regulates AR transcriptional output and promote CRPC progression [152]. Considering these advances in the mechanisms of regulating FOXA1 above, drugs can be designed and screened to target these epigenetic enzymes, which help bypass the obstacles to inhibit transcription factor FOXA1 directly. Indeed, EZH2 inhibitors or LSD1 inhibitors, partly by inhibiting FOXA1 activity to suppress PCa cell growth, are currently tested in clinical trials, showing promising effects on PCa treatment.

HOXB13

HOXB13 is a pioneer transcription factor, belonging to homeodomain box protein family which orchestrates developmental programming along the anterior-posterior and proximal-distal axes of vertebrates in temporally- and spatially-regulated manners [153, 154]. It can bind with specific chromatin sites by recognizing A/T rich sequences, often with a core sequence of 5'-TAAT-3' [155]. The DNA binding affinity and transcriptional activity of HOXB13 can be further modulated by other transcription factors including MEIS1 [156]. HOXB13 is expressed in prostate epithelium to promote differentiation into mature luminal epithelial cells, lack of which leads to defective lobe morphology and abnormal secretory function of ventral prostate [157]. HOXB13 could physically interact with AR and confer target genes androgen response [158, 159].

HOXB13 in prostate cancer

For HOXB13 in PCa, both oncogenic function and tumor suppressive role have been reported [160-164]. In the presence of androgen, HOXB13 inhibits PCa cell growth by downregulating the expression of TCF4 and its responsive genes (c-MYC and Cyclin D1) [165]. HOXB13 acts as an AR repressor to modulate the complex AR signaling and consequent growth [166]. In the absence of androgen, HOXB13 promotes androgen independent PCa growth by reducing the expression of p21 and activating cell cycle E2F signaling [167]. HOXB13 also decreases intracellular zinc and increases NF-KB signaling to promote PCa metastasis [168]. Additionally, overexpression or lost expression of HOXB13 is found in clinical PCa patient tumors compared with adjacent normal prostate tissues. One study shows that HOXB13 immunohistochemistry

staining is negative in approximately 30% of CRPC patient tumors because of its gene hypermethylation status, implying its tumor suppressive role in CRPC [169]. On the contrary, exogenous expression of HOXB13 together with FOXA1 in transformed prostate epithelial cells significantly reprograms AR cistrome away from normal prostate associated AR sites to tumor associated AR sites, thereby driving PCa initiation and progression [61]. HOXB13 is also shown to be universally required and colocalize with AR-V7 binding to upregulate the target oncogenes [170]. HOXB13 silencing significantly decreases CRPC growth through inhibition of AR-V7 oncogenic function, suggesting that HOXB13 may be a novel therapeutic target for AR-V7 driven PCa. Taken together, deciphering HOXB13 accurate roles in PCa should take into consideration of androgen presence, molecular context, and disease stage [68, 171].

HOXB13 mutations

Several mutations of HOXB13 have been identified from clinical patient tumors, possibly promoting PCa progression [172, 173]. One germline mutation for HOXB13 (G84E) is revealed to be associated with increased PCa risks [174, 175]. This rare variant is predominantly found among individuals of European descent, with an initially reported prevalence of 1.4% in prostate cancer patients [174]. Despite that this mutation occurs at the MEIS interacting domain of HOXB13, it seems not to disturb the interaction between MEIS1 and HOXB13 [156]. Remarkably, it is G84E but not WT HOXB13 that could activate de novo lipogenesis to promote PCa metastasis by diminishing the interaction with HDAC3 and thereby releasing the inhibition on FASN (Fatty Acid Synthase) expression [169].

HOXB13 post translational modifications

PTMs are another important aspect for the regulation of HOXB13 activity. HOXB13 can be acetylated by P300 at Lys277 to increase its stability and confer tamoxifen resistance in breast cancer [176]. HOXB13 can be de-phosphorylated by calcineurin at Ser204 to promote its nuclear translocation and facilitate cardiomyocyte cell cycle arrest [177]. However, little is known about HOXB13 PTM in the context of prostate cancer. Understanding the mechanisms regulating HOXB13 PTM will certainly help reconcile HOXB13 conflicting roles in PCa and enable better PCa management.

mTOR

mTOR (mechanistic Target of Rapamycin) is a serine/threonine kinase belonging to PI3K related kinase family [178, 179]. This protein with 289KD has several domains including N-terminal HEAT (Huntingtin, Elongation factor 3, Protein phosphatase-2A subunit and TOR1) domain, FAT (FRAP, ATM and TRRAP) domain, FRB (FKBP12 Rapamycin Binding) domain, C-terminal Kinase domain and FATC (FAT Carboxyterminal) domain (Figure 3A) [180]. It usually functions as the catalytic subunit of two distinct complexes known as mTORC1 and mTORC2 [181-183]. This two complexes are defined by their special structural components (mTOR, RAPTOR, mLST8 for mTORC1, and mTOR, RICTOR, mLST8 and mSIN1 for mTORC2) [184]. RAPTOR (Regulatory Associated Protein of mTOR) is the unique component for mTORC1 [185, 186], while RICTOR (Rapamycin Insensitive Companion of mTOR) is the component specific for mTORC2 [187] [188]. mLST8 (mammalian Lethal with SEC13 protein 8, also known as GβL) is a common core component for both complexes to positively contribute to their functions [189]. DEPTOR (DEP domain containing mTOR interacting protein) is found to act an intrinsic inhibitor for the two complexes [190]. Also, mTORC1 is very sensitive to acute treatment of rapamycin, an anti-fungi and immunosuppressive bacterial macrolide originally isolated from the soil samples from the island of Rapa Nui (Easter Island) [191]. In contrast, mTORC2 is quite resistant to short-time rapamycin treatment but prolonged treatment can still inhibit mTORC2 activity possibly by blocking the assembly of newly synthesized mTOR into the complex [192]. In addition, mTORC1 and mTORC2 translocate to different sub-cellular localizations to have distinct substrates to phosphorylate and diverse biological processes to regulate [193, 194]. Active mTORC1 is largely localized on the surface of lysosome, whereas

mTORC2 primarily functions at MAM (Mitochondria Associated ER Membrane) and plasma membrane [193].

Figure 3A

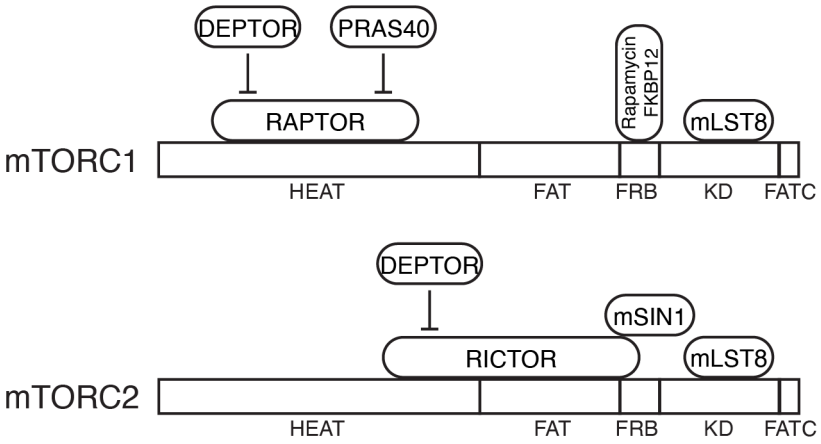

Figure 3B

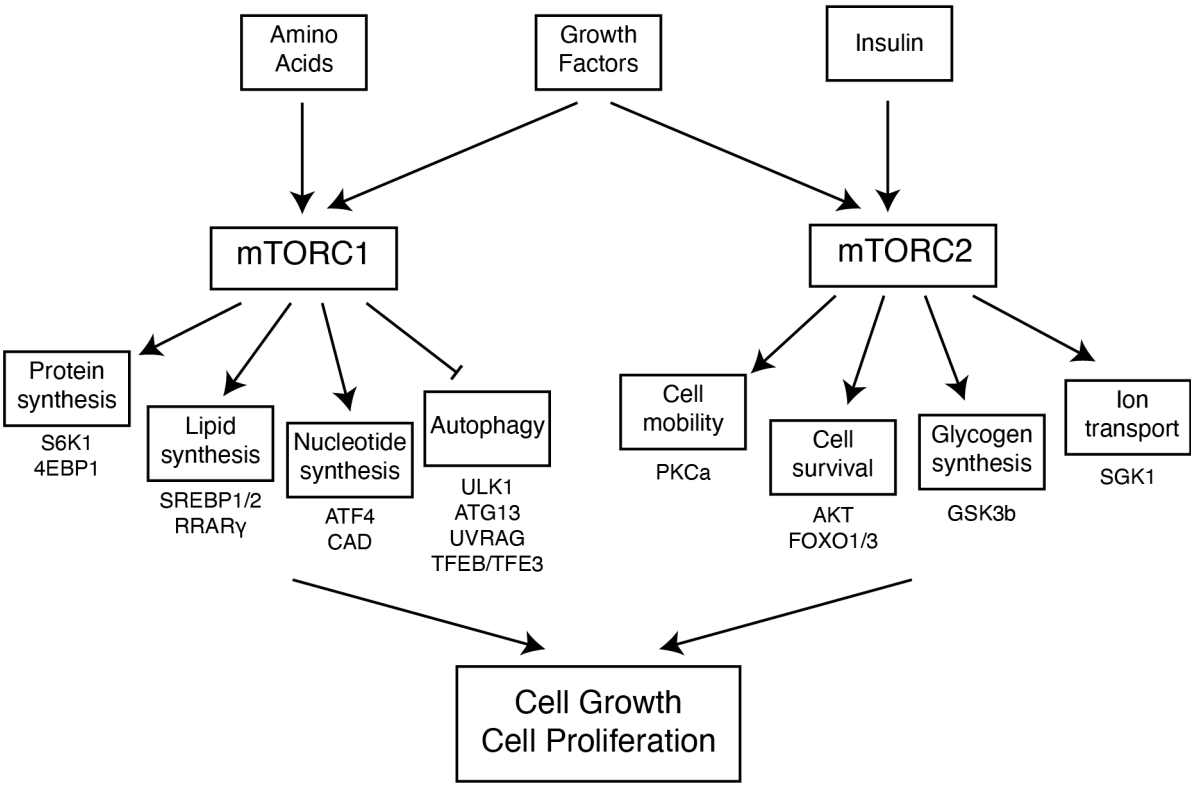

Figure 3. Information for mTOR. **A**, mTOR has several important domains. HEAT: Huntingtin, Elongation factor 3, Protein phosphatase-2A subunit and TOR1; FAT: FRAP, ATM and TRAP;

FRB: FKBP12 Rapamycin Binding domain; KD: Kinase Domain; FATC: FAT C-terminal domain. mTOR forms two distinct complexes. mTORC1 contains mTOR, RAPTOR and mLST8, while mTORC2 contains mTOR, RICTOR, mLST8 and mSIN1. DEPTOR is an intrinsic inhibitor for both complexes. PRAS40 is an inhibitor for mTORC1. **B**, Upstream signals and downstream regulated processes for mTORC1 and mTORC2. mTORC1 senses Amino Acids and Growth Factors to promote synthesis of protein, lipid and nucleotide, but inhibit autophagy. mTORC2 acts downstream of Growth Factors and Insulin to regulate cell mobility, cell survival, glycogen synthesis and ion transport. mTORC1 and mTORC2 cooperate and coordinate with each other to promote cell growth and cell proliferation.

mTORC1 function

Protein synthesis

mTORC1 promotes protein synthesis largely through the phosphorylation of two important effectors (4EBP1 and S6K1) (Figure 3B) [195]. 4EBP1 is the cellular intrinsic inhibitor for eukaryotic initiation factor 4E by direct binding and sequestering. When it is not phosphorylated, 4EBP1 could block the formation of eIF4F cap-binding complex and the consequent initiation of translation [196]. However, upon phosphorylation by mTORC1, 4EBP1 releases eIF4E and therefore activates the translation of mRNAs [197]. For S6K1, mTORC1 phosphorylates its hydrophobic motif (T389) to stimulate the kinase activity [195]. Activated S6K1 consequently phosphorylates its substrate S6 (a ribosome protein constituting 40S subunit) [198]. Phosphorylated S6 is believed to up-regulate the expression of genes involved in ribosome biogenesis. Also, mTORC1-S6K1 promotes rRNA transcription to enhance ribosome biogenesis by phosphorylating several regulatory factors such as UBF (Upstream Binding Factor), TIF1A

(Transcription Initiation Factor 1A) and MAF1 [199-202]. Although both 4EBP1 and S6K1 contribute to the control of translation, 4EBP1 seems to have more prominent roles because 4EBP1 knockout but not S6K1 inhibition causes much stronger effects for global translation inhibition [203, 204]. Additionally, mTOR inhibitor rapamycin abrogates S6K1 but not 4EBP1 phosphorylation completely [205, 206]. Additionally, S6K1 and 4EBP1 act as the downstream effectors of mTORC1 but have quite differential impacts on mTORC1 controlled cell growth and proliferation. S6K1 is reported to play key roles in controlling cell growth (increase in cell size), while 4EBP1 dominantly regulates cell proliferation (increase in cell number) [207].

Lipid and nucleotide synthesis

mTOR stimulated cell growth requires not only enhanced protein synthesis but also increased lipid and nucleotide synthesis. Lipids are needed for plasma membrane and other organelles membrane formation, while nucleotides support efficient DNA replication during cell division [208]. mTORC1 promotes de novo lipid synthesis majorly through transcription factor SREBP1/2 (Sterol Responsive Element Binding Protein) and PPARγ (Peroxisome Proliferator Activated Receptor γ). In response to low level of sterol, SREBPs translocate into the nucleus to positively regulate the transcription of genes involved in fatty acid and cholesterol biosynthesis [209]. mTORC1 could enhance SREBPs transcriptional activity either by phosphorylating SREBPs inhibitor Lipin1 to exclude it from the nucleus [210], or by promoting the processing and nuclear translocation of SREBPs [211, 212]. Likewise, mTORC1 could modulate the expression and activity of PPARγ to control lipid homeostasis [213, 214]. For nucleotide synthesis, mTORC1 could activate transcription factor ATF4 and downstream target MTHFD2 (Methylenetetrahydrofolate Dehydrogenase 2) to drive de novo purine synthesis [215], and

phosphorylate CAD (Carbamoyl-α phosphate synthetase 2, Aspartate transcarbamoylase, Dihydroorotase) to increase pyrimidine biosynthesis [216, 217].

Autophagy

Anabolism and catabolism are two critically reversible and coordinated processes in cells. mTORC1 promotes anabolism by positively enhancing the synthesis of protein, lipid and nucleotide as mentioned above, but at the same time it needs to suppress catabolism to avoid a futile cycle. Autophagy is the well-known mechanism for catabolism by degrading proteins and organelles [218], and indeed mTORC1 directly inhibits this process [219]. Targeting early autophagy, mTORC1 phosphorylates ULK1 and ATG13 to inactivate both effectors in the induction of autophagy [220, 221]. For late autophagy, mTORC1 phosphorylates UVRAG to block the maturation of autophagosome and the conversion of endosome to lysosome [222]. Also, mTOR phosphorylates transcription factor TFEB and TFE3 and sequester them with scaffolding protein 14-3-3 in the cytoplasm, which consequently inhibits gene expression for lysosome biogenesis and autophagy machinery [223, 224].

mTORC2 function

While mTORC1 precisely controls cell growth and metabolism, mTORC2 instead positively regulates cell mobility and survival primarily by phosphorylating several members for AGC (PKA/PKG/PKC) kinase family (Figure 3B). The first substrate identified for mTORC2 was PKCa, a regulator to remodel actin cytoskeleton [225]. The most important substrate for mTORC2 was later found to be AKT. mTORC2 phosphorylates AKT at S473 for activation in response to upstream signaling such as insulin signaling [226]. Then, active AKT promotes cell

survival via the phosphorylation of several key downstream substrates including FOXO1/3a and GSK3β. AKT phosphorylates FOXO1/3 to cause their nuclear exclusion and protein degradation, which leads to apoptosis suppression [227]. GSK3β phosphorylation by AKT is inhibitory, thereby releasing the inhibition on the glycogen synthesis [228]. In addition, mTORC2 phosphorylates SGK1 (Serum/Glucocorticoid Regulated Kinase 1) to regulate ion transport [229].

mTORC1 upstream regulation

mTORC1 is responsive to and regulated by two main upstream signals (growth factors and nutrients including amino acids) (Figure 4A) [230]. For growth factor branch to regulate mTORC1, signals converge on TSC (Tuberous Sclerosis Complex), a heterotrimeric complex that is composed of TSC1, TSC2 and TBC1D7 [231]. TSCs act as the GAP (GTPase Activating Protein) for lysosome RHEB (Ras Homolog Enriched in Brain) to inhibit the function of RHEB (an mTORC1 activator) [232, 233]. TSCs stimulate the conversion of RHEB from GTP-bound active state to GDP-bound inactive state [234, 235]. Upon insulin or IGF1 (Insulin like Growth Factor 1) stimulation, AKT is activated and hence directly phosphorylates and dissociates TSCs from lysosome surface, relieving the inhibition for downstream RHEB and mTORC1 [236]. For amino acids arm to regulate mTORC1, Rags (Ras-related GTPase) are uncovered to be the essentially core components [237, 238]. There are four mammalian Rag genes (encoding Rag A-D), among which Rag A or Rag B forms heterodimers with Rag C or Rag D. Rag complexes are necessary and sufficient to activate mTORC1 in response to nutrient signals only in their active state (GTP-loaded Rag A/B in complex with GDP loaded Rag C/D). The GTP binding to one subunit of the dimer could induce conformational change that excludes the binding of a second

GTP to the other subunit, likely facilitating the rapid response to amino acid signals [239]. Altogether, amino acids activated Rag GTPases interact with RAPTOR and thereby recruit mTORC1 from cytoplasm onto lysosome surface where growth factors activated RHEB is ready to switch on mTORC1 activity [240, 241], highlighting that both amino acids and growth factors are required for mTORC1 activation.

Consistent with the crucial role of Rag GTPases in mTORC1 activation, shifting between active and inactive nucleotide bound states, some have recently identified several Rag GTPases regulators (Figure 4B), including GEF (Guanine Exchange Factor) to confer Rags GTP binding and GAP (GTPase Activating Protein) to hydrolyze GTP into GDP [184]. Ragulator pentameric complex (p18, p14, MP1, C7orf59 and HBXIP, also known as LAMTOR1-LAMTOR5) has been shown to act as the GEF for Rag A/B that is further regulated by v-ATPase [242]. Since Rag GTPases lack a lipid-targeting signal, Ragulator complex can help anchor Rag GTPases on lysosome surface, which also recruits mTORC1 there [243]. GATOR (GTPase Activating Protein Toward Rags) can be divided into two multiprotein subcomplexes, called GATOR1 and GATOR2. GATOR1 is comprised of DEPDC5, NPRL2 (harboring GAP activity) and NPRL3, whereas GATOR2 contains MIOS, WDR24, WDR59, SEH1L and SEC13 [244]. GATOR1 directly interacts with and acts as the GAP for Rag A/B, leading to the inhibition of mTORC1 [245]. GATOR2 binds with and antagonizes GATOR1 function through an unknown mechanism, which results in the activation of mTORC1. Another large KICSTOR complex (containing KPTN, ITFG2, C12orf66 and SZT2) was revealed as the scaffold to tether GATOR1 to the lysosome surface [246]. FLCN complex comprising FLCN and FNIP1/2 (FLCN Interacting Proteins 1 and 2) functions as the GAP for Rag C/D, thereby stimulating mTORC1

activity [247]. Also, LARS (Leucyl-tRNA synthetase) has been suggested to be the intracellular leucine sensor to regulate mTORC1 activity by acting as a GAP for Rag D [248].

Despite the insights mentioned above, the identities of direct amino acid sensors directing mTORC1 activation through Rag GTPases remained elusive until recently (Figure 4B) [249]. The lysosomal arginine sensor SLC38A9 interacts with Rag GTPase-Ragulator-v-ATPase complex, by which it senses the arginine level inside the lysosome lumen and is required for lysosomal arginine to activate mTORC1 [250-252]. The cytosolic leucine sensor Sestrin1/2, SAR1B and cytosolic arginine sensor CASTOR1/2 both could regulate mTORC1 activity via GATOR2 (a positive upstream regulator for mTORC1) [253-255]. In the absence of their corresponding amino acid, Sestrin1/2 and CASTOR1/2 could interact with and inhibit GATOR2. However, when leucine or arginine is present, Sestrin1/2 or CASTOR1/2 will bind with their target amino acid and dissociate with GATOR2, releasing the inhibition on mTORC1 [256, 257]. The SAM (S-adenosylmethionine) sensor SAMTOR could regulate mTORC1 activity through the interaction with GATOR1 [258]. Methionine starvation reduces SAM levels and promotes SAMTOR-GATOR1 binding to suppress mTORC1. In addition, mitochondrial TARS2 (Threonyl-tRNA Synthetase) is found to sense threonine level and modulate mTORC1 activity by preferentially interacting with GTP-Rag C and increasing GTP loading of Rag A [259].

mTORC2 upstream regulation

Compared to mTORC1, mTORC2 regulation by upstream factors is much less appreciated. mTORC2 is majorly regulated by growth factors via PI3K (Figure 4B). The mTORC2 core component mSIN1 contains a phosphoinositide binding PH (Pleckstrin Homology) domain,

which can bind with PIP3 generated by PI3K and thereby recruit mTORC2 to plasma membrane [260, 261]. Without PIP3 binding, the PH domain of mSIN1 interacts with mTOR kinase domain to autoinhibit mTORC2 [262]. However, PIP3 bound mSIN1 releases the inhibition of mTOR, allowing mTORC2 activation [263]. Also, mTORC1 could feedback downregulate PI3K signaling and dampen mTORC2 activity via IRS1 and GRB10 axis as mentioned before [264-267].

Crosstalk between mTORC1 and mTORC2

mTORC2 substrate AKT phosphorylates TSC2 (one upstream inhibitor for mTORC1) to release the inhibition for mTORC1 (Figure 4C) [268]. AKT phosphorylates another one mTORC1 inhibitor PRAS40 (Proline-Rich AKT Substrate of 40 kDa), leading to its sequestration by scaffolding protein 14-3-3 and restoration of mTORC1 activity [269, 270]. AKT also directly phosphorylates mTOR at S2448 to increase its kinase activity [271]. Reversely, mTORC1 substrate S6K1 could phosphorylate IRS1 (Insulin Receptor Substrate 1) as negative feedback to block insulin stimulated PI3K-mTORC2-AKT signaling [266, 267]. Likewise, mTORC1 could phosphorylate and activate GRB10, a negative regulator of Insulin/IGF1 signaling upstream of AKT and mTORC2 [264, 265]. S6K1 also phosphorylates RICTOR and mSIN1 at site T1135 and T86/T398, respectively, to destabilize mTORC2 [272, 273]. In addition, as the Yin-Yang metabolism opponent for mTOR (promoting anabolism), AMPK (promoting catabolism) is found to regulate mTORC1 and mTORC2 differentially [274]. AMPK could phosphorylate TSC2 at two sites (T1271 and S1387) [275], and also phosphorylate RAPTOR at two sites (S722 and S792) [276], thereby all resulting in the suppression of mTORC1 activity. However, AMPK instead could promote mTORC2 activity by directly phosphorylating mTOR at S1261 [277].

mTORC1 is additionally found to directly phosphorylate AMPK catalytic subunit a1 (at site S347) or a2 (at site S345 and S377) that diminishes AMPK active phosphorylation (at site T172) and limits AMPK activity [278].

Figure 4A

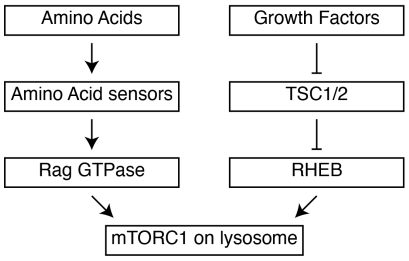

Figure 4B

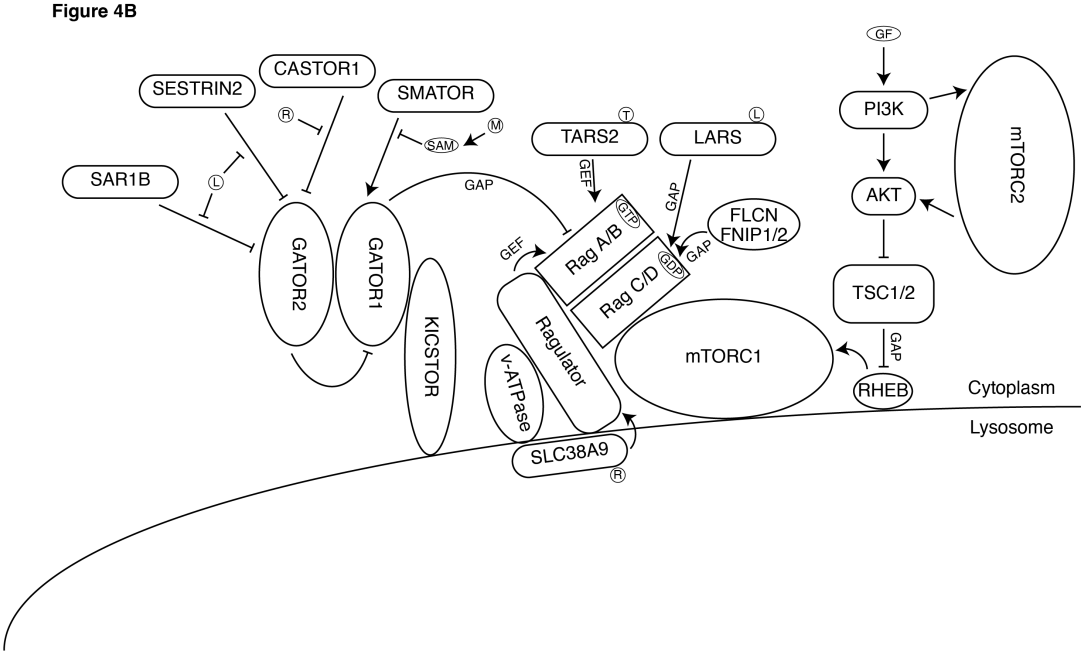

Figure 4C

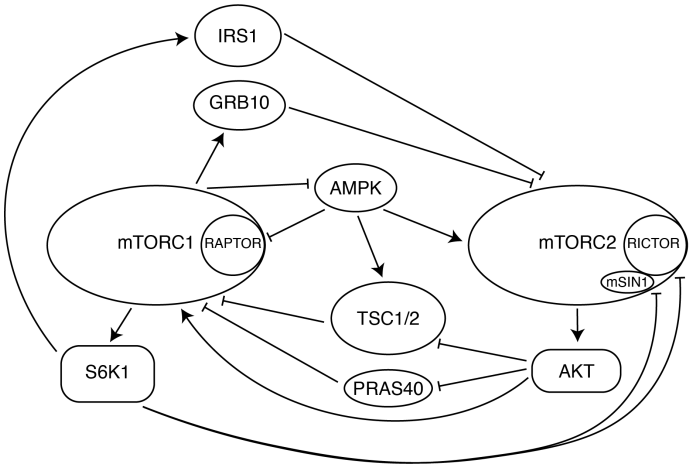

Figure 4. Upstream signals for mTORC1 and mTORC2. **A**, mTORC1 has two arms of upstream signals. Amino Acids bind with their corresponding sensors to activate Rag GTPases which recruit mTORC1 onto lysosome surface. Growth Factors signal into cells to inactivate TSC1/2 which releases the inhibition on RHEB, so that RHEB is ready to activate mTORC1 on lysosome surface. These two upstream signals are required for mTORC1 activation. **B**, mTORC1 has various upstream Amino Acid sensors to sense the level of amino acids. mTORC2 is majorly stimulated by Growth Factors. L: Leucine; R: Arginine; M: Methionine; SAM: S-Adenosyl Methionine; T: Threonine. GEF: Guanine Exchange Factor; GAP: GTPase Activating Protein. **C**, crosstalk between mTORC1 and mTORC2.

mTOR pathway mutations

mTOR signaling is hyperactive in up to 80% cancers, in which context it plays significant roles in sustaining cancer cell growth and survival. Mutations of the upstream regulators of mTORC1 have been characterized, such as TSC1/2 in tuberous sclerosis [279], the GATOR1 complex in glioblastoma [244], Rag C in follicular lymphoma [280], and FLCN in the Birt-Hogg-Dubé hereditary cancer syndrome [281]. mTORC2 signaling was also shown to be dysregulated in cancer, such as *PTEN* loss, and oncogenic *PI3K* and *AKT* mutations [230, 282]. Additionally, mTOR itself has been observed to undergo mutation in cancer cells conferring pathway hyperactivation [283]. Considering the important functions of mTOR in regulating almost all the aspects of biological processes in cells, drugs inhibiting aberrant mTOR activity in cancer could provide significant benefits to patients [284].

mTOR inhibitors

The first generation mTOR inhibitors approved for cancer treatment are derived from rapamycin, termed Rapalogs [285]. Unfortunately, the clinical efficiency of Rapalogs has been disappointing. One reason is that they are allosteric inhibitors only suppressing mTORC1 activity. mTORC1 inhibition could unexpectedly activate PI3K-AKT signaling via a feedback mechanism to support cell survival. The second generation of mTOR inhibitors such as Torin1 are ATP competitive inhibitors which suppress mTOR kinase activity of both mTORC1 and mTORC2 [286]. mTOR mutations in its kinase domain may cause drug resistance to these inhibitors [287]. Therefore, the third generation mTOR inhibitors (called Rapalink) linking first generation inhibitor (rapamycin) with second generation inhibitor (TORKi) have been shown to greatly increase drug efficacy and decrease drug resistance [288], emphasizing the potentials of dual mTOR inhibitors for cancer treatment.

Nuclear mTOR

Despite the canonical cytosolic mTOR functions mentioned above, emerging evidence reveals mTOR localization in the nucleus [289-292], thereby possibly regulating gene transcription more directly [293]. mTORC1 was found to interact with PGC-1α (PPARγ Coactivator 1) and YY1 (Yin Yang 1) in the nucleus to promote mitochondrial biogenesis and metabolism [294]. Tumor suppressor PML inhibits mTOR activity through physical interaction and co-localization in the nucleus and consequently inhibits neoangiogenesis [295]. Nuclear mTOR could phosphorylate acetyltransferase P300 to inhibit autophagy but activate lipogenesis [296]. Nuclear mTOR regulates ERRα activity and stability by directly controlling the transcription of genes involved in ubiquitin proteasome pathway [297]. ERα binds with RAPTOR and recruits mTOR onto the promoter of its target genes, resulting in the upregulation of estrogenic gene expression in breast

cancer [298]. Likewise, AR induces mTOR nuclear translocation and directs mTOR genomic binding, leading to the activation of AR-driven energy metabolism in prostate cancer cells [299]. Moreover, nuclear mTOR has been shown to be involved in the direct transcriptional regulation of RNA Pol I and RNA Pol III genes [300, 301]. Nuclear mTOR is also known to phosphorylate the RNA pol III repressor MAF1 to relieve the inhibition on tRNA and 5s rRNA expression [202, 302, 303].

Crosstalk among AR, FOXA1, HOXB13 and mTOR

AR, FOXA1 and HOXB13

Both FOXA1 and HOXB13 are pioneer transcription factors interacting with AR to co-regulate androgen signaling. Exogenous expression of FOXA1 and HOXB13 in transformed prostate epithelial cells reprograms AR cistrome from normal prostate specific binding sites to prostate tumor specific binding sites, driving prostate carcinogenesis [61]. Also, both FOXA1 and HOXB13 are reported to play complex functions in PCa. In the presence of androgen, FOXA1 promotes but HOXB13 inhibits PCa cell proliferation via the dependency on AR [135, 166]. In the absence of androgen, both can promote androgen independent PCa cell growth [121, 167]. One possible reason could be attributed to the dual roles of AR which could be differentially modulated by FOXA1 and HOXB13. FOXA1 acts as the upstream regulator of AR to alter its transcriptional activity [124], while HOXB13 recruits AR to target genes to confer them androgen response [159]. Clinically relevant mutations of FOXA1 and HOXB13 undoubtedly result in dysregulated AR transactivation, as demonstrated by the observation that AR induces a distinct transcriptional program in CRPC [79, 304]. Additionally, several epigenetic enzymes could modify and modulate the activity of these three factors simultaneously but differentially, leading to mixed outcomes that may increase the difficulty to interpret the results of distinct studies. For example, LSD1 represses AR expression by binding to the second intron of AR gene and demethylates FOXA1 at Lys270 to enhance its regulation on AR signaling [77, 152]. P300 could acetylate AR and HOXB13 to increase their activity but acetylate FOXA1 to attenuate its DNA binding [69, 148, 176]. EZH2 directly binds onto the HOXB13 promoter and induces trimethylation of H3K27 to inhibit the HOXB13 expression [169], while EZH2 methylates

FOXA1 at Lys295 to enhance FOXA1 protein stability and promote FOXA1-driven PCa growth [151]. Moreover, FOXA1 is shown to regulate HOXB13 gene expression directly by binding to the conserved chromatin site with forkhead motif downstream HOXB13 coding region [305]. Altogether, future studies need to carefully examine the intricate functional crosstalk among AR, FOXA1, HOXB13 and their closely related co-regulators.

AR and mTOR

Upon androgen activation, AR upregulates mTOR expression and kinase activity via AR-mediated transcription of nutrient transporters [306, 307]. AR also induces mTOR nuclear translocation and chromatin interaction, by which AR collaborates with mTOR to control energy metabolism directly in the nucleus of PCa cells [299]. Reversely, inhibition of mTORC1 by rapamycin increases the expression and activity of AR [308, 309]. mTORC1 was also shown to phosphorylate AR at Ser96 to promote the stability, nuclear localization and transcriptional activity of AR in HCC (Hepatocellular Carcionma) [310]. Furthermore, AR functionally interacts with PI3K-AKT-mTOR signaling pathway at multiple levels [311]. AR inhibits AKT activation by increasing its target gene FKBP5 expression, stabilizing AKT phosphatase PHLPP and consequently decreasing AKT phosphorylation [312, 313]. Reciprocally, AKT can repress AR protein expression and transcriptional activity through the reduction of its upstream activator HER2/3 [313, 314]. Likewise, PTEN loss leading to hyperactive AKT and mTOR inhibits androgen responsive genes expression and promotes androgen independent prostate cancer progression [315]. However, conflicting studies report that AR could induce PI3K activity too, possibly occurring via Src (proto-oncogene tyrosine-protein kinase) mediated non-genomic signaling [316]. Moreover, mTOR could function upstream and downstream of AKT due to the

complex interplays between mTORC1 and mTORC2. mTORC2 phosphorylates AKT at Ser473 to boost its activation [226]. Activated AKT can further phosphorylate TSC2 and PRAS40 to release inhibition on mTORC1 [268, 270]. mTORC1 activation feedback phosphorylates IRS1 and GRB10 to block PI3K-mTORC2-AKT signaling [264-267]. In summary, the crosstalk between AR and mTOR recapitulates one aspect of the complexity of PCa initiation and progression, implying that combination therapy inhibiting both oncogenic pathways is required to achieve a good clinical outcome [313].

mTOR, AR, FOXA1 and HOXB13

One mTOR proteomics study uncovers AR, FOXA1 and HOXB13 as novel interactors for nuclear mTOR in PCa [317]. DNA binding motifs analysis of mTOR ChIP-sequencing data also reveals that AR, FOXA1 and HOXB13 motif are the top enriched motifs among those mTOR genomic binding sites [299]. These data suggest that these three factors may be vital for mTOR-chromatin interaction since mTOR does not have a DBD. Experimental evidences are needed to confirm mTOR interaction with AR, FOXA1 and HOXB13, validate their colocalization onto the same chromatin regions and identify the functional output.

Questions to answer

My thesis is focused on investigating the underlying mechanisms on how mTOR regulates transcription in concert with AR, FOXA1 and HOXB13 in PCa. Several interesting questions need to be answered. First, does mTOR phosphorylate AR, FOXA1 and HOXB13 since mTOR possibly directly interacts with them? Second, mTOR is known to phosphorylate transcription factors to indirectly regulate gene transcription. If so, what function can be associated with their

phosphorylation? Third, mTOR can be induced by androgen to translocate into the nucleus, by which mTOR could regulate gene transcription directly. Could FOXA1 and HOXB13 as pioneer factors facilitate mTOR DNA binding and modulate its transcriptional activity? If so, what are the target genes and biological processes dependent on nuclear mTOR function? Fourth, does nuclear mTOR requires its kinase activity to control transcription? Fifth, how significant is the transcriptional activity of mTOR in regulating PCa progression? Data presented in Chapter 2 and 3 begin the process to provide clear answers to these important questions.

Rationales

mTOR was previously reported to go into the nucleus and form complex with AR (androgen receptor), possibly regulating gene transcription and controlling energy metabolism in prostate cancer. DNA binding motifs analysis of the mTOR bound peaks in mTOR ChIP-seq data uncovered that the top enriched motifs were those recognized by FOXA1, HOXB13 and AR, suggesting the three factors could be involved in mTOR transcriptional function. It is known that FOXA1, HOXB13 and AR can reprogram gene expression and drive prostate cancer progression, but how nuclear mTOR could influence the transcriptional activity of these factors was completely unknown. Therefore, my PHD project was focused on investigating the underlying mechanisms about how mTOR regulates gene transcription in prostate cancer, particularly in collaboration and coordination with HOXB13, FOXA1 and AR, with the hope to enhance our understanding of prostate cancer biology (Figure 5).

Figure 5

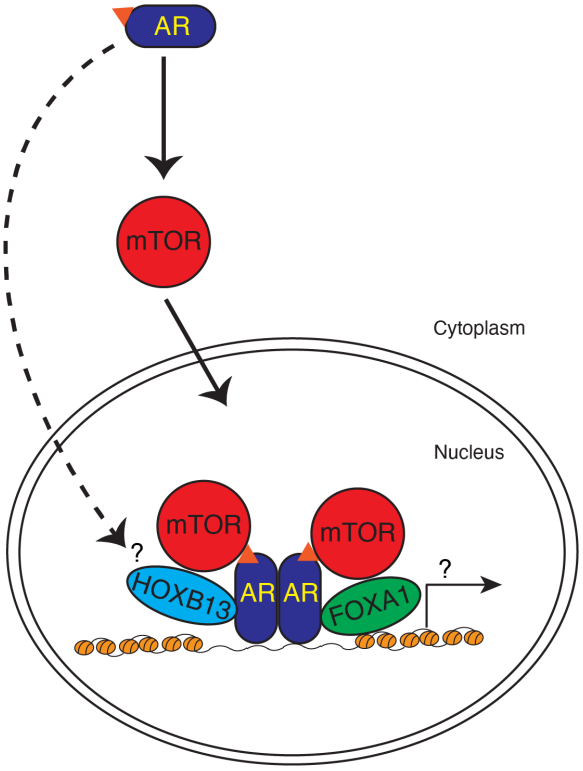

Figure 5. Working model for my study is proposed. AR activation induces mTOR nuclear translocation. Nuclear mTOR may complexes with AR, FOXA1 and HOXB13 on chromatin to potentially regulate target gene transcription. Two major questions are needed to answer. One is whether mTOR as a kinase could phosphorylate these three factors. The other is what target genes are dependent on nuclear mTOR function. Chapter 2 is focused on the first question, and Chapter 3 is studying the second question.

Hypothesis

We hypothesize that nuclear mTOR works in concert with HOXB13, FOXA1 and AR and other regulatory factors to alter the transcriptional landscape of PCa cells and promote an oncogenic gene program driving the progression of the disease.

Objectives

Objective 1: Identify the mechanisms governing the functional crosstalk among mTOR and HOXB13, FOXA1 and AR. mTOR as a kinase may possibly phosphorylate these three factors to modulate their transcriptional activity and thereby indirectly alter the target gene program.

Objective 2: Define the downstream pathways and individual components regulated by mTOR transcriptional function. mTOR may co-recruit with HOXB13, FOXA1 and AR to the regulatory regions of diverse target genes to directly control oncogenic pathways for prostate cancer progression.

Chapter 2.

Hierarchical phosphorylation of HOXB13 by mTOR dictates its activity and oncogenic function in prostate cancer

Yonghong Chen[1,2], Catherine Rosa Dufour[1], Lingwei Han[1,2], Ting Li[1], Hui Xia[1,2] and Vincent Giguère[1,2,*]

[1]Goodman Cancer Institute, McGill University, Montreal, Québec, H3A 1A3, Canada.

[2]Department of Biochemistry, Faculty of Medicine, McGill University, Montréal, Québec, H3G 1Y6, Canada.

*Correspondence: vincent.giguere@mcgill.ca

Keywords: Prostate cancer; E3 ligase; androgen receptor; SKP2, gene signature

Abstract

Dysregulation of mTOR signaling plays a critical role in promoting prostate cancer (PCa) growth. HOXB13, a homeodomain transcription factor, is known to influence the androgen response and PCa development. Recently, HOXB13 was found to complex with mTOR on chromatin. However, the functional crosstalk between HOXB13 and mTOR remains elusive. We now report that mTOR directly interacts with and hierarchically phosphorylates HOXB13 at threonine 8 and 41 then serine 31 to promote its destabilization by the E3 ligase SKP2 while enhancing its oncogenic properties. Expression of HOXB13 harboring phosphomimetic mutations at the mTOR-targeted sites stimulates PCa cellular growth both *in vitro* and in murine xenografts. Transcriptional profiling studies revealed a phospho-HOXB13-dependent gene signature capable of robustly discriminating between normal prostate tissues, primary and metastatic PCa samples. This work uncovers a previously unanticipated molecular cascade by which mTOR directly phosphorylates HOXB13 to dictate a specific gene program with oncogenic implications in PCa.

Introduction

Prostate Cancer (PCa) is one of the most diagnosed cancers in men worldwide. Androgen and its receptor (AR) play important roles in the progression of PCa; hence androgen deprivation therapy (ADT) is used as the first standard treatment for PCa patients. Despite the initial success, it eventually develops into castration-resistant prostate cancer (CRPC) (1), which is often metastatic with poor prognosis and lethal with minimal therapy. Although AR remains hyperactive in CRPC, the emergence of drug resistance to AR inhibitors confers PCa androgen-independent properties that lead to AR cistrome and transcriptome reprogramming by dysregulated cofactors (2). Therefore, in addition to AR-targeted therapies, alternative therapeutic targets are urgently needed (3,4), with AR cofactors being promising rational targets for exploration into their underlying regulatory mechanisms (5).

HOXB13, a homeobox family transcription factor, is a well-known AR cofactor which confers cellular responses to androgen (6,7). It exerts dual roles in AR signaling by both activating and suppressing the transcription of AR target genes (8-10). Paradoxically, HOXB13 has been shown to either promote or suppress PCa cell growth and metastasis (11-14). These discrepancies may be attributed to the different experimental strategies (overexpression versus knockdown) that were used to assess the role of HOXB13 in PCa cells (7). In addition, long-term versus short-term effects of HOXB13 modulation may also play a key role in determining its function in PCa biology. While known mechanisms controlling HOXB13 activity are limited, recent studies have pointed towards post-translational modifications (PTMs). In particular, acetylation of HOXB13 at K277 by p300 increases its stability and confers tamoxifen resistance in breast cancer cells (15) and its de-phosphorylation at S204 by calcineurin promotes its nuclear translocation and facilitates

cardiomyocyte cell cycle arrest (16). Little is known about regulation of HOXB13 activity by PTMs in the context of PCa.

mTOR, mechanistic target of rapamycin, is a serine/threonine kinase belonging to the PI3K-related kinase family (17). It functions as the central catalytic subunit in two distinct protein complexes, mTORC1 and mTORC2. mTORC1 is defined by its unique component RAPTOR while RICTOR is specific to mTORC2 (18). Each complex usually phosphorylates a different set of substrates in different subcellular localizations, mainly in the cytoplasm, to regulate cell growth by promoting anabolic processes including protein, lipid and nucleotide synthesis, and by suppressing catabolic processes like autophagy (19-21). In addition, emerging evidence highlights that mTOR and mTORC1/2 components can translocate into the nucleus and that nuclear mTOR can functionally interact with transcriptional regulators to coordinate gene transcription with cellular metabolism in a more direct manner (22,23). Notably, we have previously shown that androgen signaling drives PCa progression in part by promoting mTOR nuclear localization and its genomic reprogramming in part by enhancing mTOR-AR interaction on DNA (24,25). HOXB13 binding motif were found to be enriched at mTOR-bound loci, suggesting a functional genomic association between mTOR and HOXB13, a notion further corroborated by the identification of HOXB13 as a mTOR interactor in the recent characterization of the mTOR chromatin-bound interactome by rapid immunoprecipitation mass spectrometry of endogenous protein (RIME) in PCa cells (26). Furthermore, canonical mTOR signaling has been shown previously to be activated by androgens, including by the synthetic androgen R1881 (24,27,28).

In this study, we sought to further investigate the functional connection between nuclear mTOR and HOXB13. We show that mTOR directly interacts with and phosphorylates HOXB13 in the nucleus of PCa cells. Phosphorylation of HOXB13 by mTOR at threonine 8 and 41 primes

its further phosphorylation at serine 31, which consequently triggers E3 ligase SKP2 licensed proteasome-mediated protein degradation. Remarkably, although this mTOR-mediated phosphorylation cascade promotes HOXB13 destabilization, it augments HOXB13 oncogenic function. We provide evidence that expression of a HOXB13 phosphomimetic mutant involving the three mTOR-targeted residues, but not the non-phosphorylatable mutant, promotes PCa cellular growth *in vitro* and tumor growth *in vivo* in a xenograft model system. RNA-sequencing (RNA-seq) analyses identified a phospho-HOXB13-targeted gene signature capable of discriminating normal prostate tissue, primary and metastatic tumors in three human clinical cohorts. Taken together, our results reveal a previously unrecognized oncogenic regulatory circuit involving mTOR-mediated phosphorylation and destabilization of HOXB13, which could be envisaged as a therapeutic avenue in PCa.

RESULTS

mTOR regulates HOXB13 protein stability

To explore a possible role for mTOR in regulating the activity of HOXB13, we first tested whether perturbing mTOR activity could influence the expression of HOXB13 in PCa cells. Three HOXB13 positive human PCa cell lines were used to monitor the effect of mTOR inhibitors, Torin 1 and rapamycin, on HOXB13 expression: LNCaP ($AR^+/PTEN^-$), 22Rv1 (AR and AR variant$^+$/$PTEN^+$) and PC3 ($AR^-/PTEN^-$). Treatment with either Torin 1 or rapamycin for 24h led to increased HOXB13 expression, most prominently in LNCaP and PC3 cells (Supplementary Figure 1A), two cell lines retained for further study. The increase in HOXB13 expression was rapid, augmenting as early as 2h following treatment with Torin 1 with maximal levels attained by 8h (Figure 1A). The increase in HOXB13 was inversely correlated with the inhibition of S6K1 phosphorylation by mTOR inhibitors (Figure 1A and Supplementary Figure 1A). Consistent with pharmacological inhibition of mTOR, genetic knockdown of mTOR using shRNAs also increased HOXB13 protein levels in both LNCaP and PC3 cells (Figure 1B). Activation of canonical mTOR signaling by the synthetic androgen R1881 decreased HOXB13 levels, an effect rescued by co-treatment with Torin 1 (Figure 1C). Torin 1 had no significant impact on the expression of *HOXB13* mRNA levels, indicating that its regulation of HOXB13 expression in PCa cells is likely post-transcriptional (Supplementary Figure 1B). In a similar fashion, serum stimulation of mTOR activity decreased HOXB13 protein levels which was rescued by addition of Torin1 in PC3 cells (Supplementary Figure 1C). In addition, stimulation of mTOR signaling by either overexpression of Rheb or knockdown of TSC1/2, two important but opposite regulators of mTOR activity, led to a reduction in HOXB13 levels in both LNCaP and PC3 cells (Figure 1D, 1E and Supplementary Figure 1D, 1E). This reduction in HOXB13 expression was dependent on mTOR kinase activity

since co-treatment with Torin1 abolished the observed effects (Figure 1D and Supplementary Figure 1D). Furthermore, shRNA-mediated genetic disruption of specific mTORC1 and mTORC2 component, Raptor and Rictor, respectively, provoked an increase in HOXB13 levels (Supplementary Figure 1F, 1G). It suggested that both canonical mTOR complexes were involved in regulating HOXB13. We next investigated whether the regulation of HOXB13 expression by mTOR involves changes in poly-ubiquitination of HOXB13. As shown in Figure 1F and 1G, both pharmacological inhibition (Torin1) and genetic disruption of mTOR (shRNAs) led to a sharp reduction in HOXB13 poly-ubiquitination, indicating less targeting of HOXB13 to the proteasome and its protection from degradation.

mTOR physically interacts with HOXB13

The presence of HOXB13 recognition motifs within mTOR chromatin-bound regions (24) together with the identification of HOXB13 and mTOR as partners from two recent proteomics studies probing the mTOR and HOXB13 interactomes, respectively (26,29), support the notion that mTOR and HOXB13 are components of the same complex. To explore mTOR and HOXB13 association further, we first performed co-immunoprecipitation (co-IP) assays in 293T cells confirming that exogenously expressed V5-tagged HOXB13 complexes with mTOR (Figure 2A), a finding further validated by co-IPs in LNCaP cells using endogenous proteins (Figure 2B). In addition, both endogenous Raptor and Rictor also co-IP’d with HOXB13 in LNCaP cells (Figure 2C). Importantly, *in vitro* GST pulldown assay established that the interaction between HOXB13 and mTOR is direct (Figure 2D). To further map the functional domains involved in the interaction, we performed Co-IP experiments in 293T cells co-expressing HOXB13 and mTOR full-length or truncation mutants which showed that the amino-terminal domain of HOXB13 is required to

interact with mTOR and reciprocally, the carboxyl-terminal domain mTOR, which includes the kinase domain, is necessary to interact with HOXB13 (Figure 2E-2G).

mTOR phosphorylates HOXB13

We next examined whether mTOR can phosphorylate HOXB13. *In vitro* kinase assay confirmed that HOXB13 is indeed a substrate of the mTOR kinase, with a higher degree of phosphorylation observed when mTOR was IP’d from extracts of Hela cells previously treated with insulin, an effect abolished by adding Torin1 directly to the reaction (Figure 3A). Mass spectrometry (MS) analysis of the detected phospho-HOXB13 band from the mTOR kinase assay identified two prominent HOXB13 phosphorylation sites, threonine 8 and 41 (Figure 3B). Mutations of these sites to alanine residues, individually or together, led to a partial reduction in HOXB13 phosphorylation by mTOR in the *in vitro* kinase assay (Figure 3C). Although with a lower confidence score, serine 31 was also identified as a candidate HOXB13 phosphorylation site by MS, suggesting that mTOR phosphorylation at the primary sites, threonine 8 and 41, could induce subsequent phosphorylation at nearby sites. To test this hypothesis, we first mutated threonine 8 and 41 to aspartic acid residues to introduce phosphomimic sites in HOXB13. Interestingly, expression of the HOXB13 phosphomimic mutants T8D, T41D, and T8D+T41D in LNCaP cells resulted in the detection of an additional upper protein band, revealed to be the result of another phosphorylation event as the novel upper band vanished upon treatment with lambda phosphatase (Figure 3D, 3E). Aside from the potential HOXB13 S31 phosphorylation site detected by MS, there are possible prospective false-negative phosphosites including S35, S250, and S254 that also warrant consideration. As such, we employed a mutagenesis screening by mutating these potential phosphorylated residues to alanine within the HOXB13 T8D+T41D phosphomimic mutant.

Mutating serine residues at positions 250 and 254 to alanine did not eliminate the upper band (Figure 3F). In stark contrast, mutating the HOXB13 phosphomimic T8D+T41D mutant at positions 31 and 35 from serine to alanine resulted in the complete disappearance of the upper band, implying that either S31 or S35 is the additional phosphorylation site(s) (Figure 3F). HOXB13 T8D+T41D mutants harboring individual mutation of serine 31 or 35, confirmed that phosphorylation of S31 is responsible for the appearance of the additional upper band (Figure 3G), thus supporting the MS data (Figure 3B). Similar results were observed when the serine 31 to alanine mutation was introduced independently in the HOXB13 T8D or T4D mutant (Supplementary Figure 2A). Importantly, the additional phosphorylation at serine 31 primed by phosphorylation at threonine residues 8 or 41 was not abolished by single alanine mutations at these sites, denoting that phosphorylation of either T8 or T41 could trigger phosphorylation at S31 (Figure 3H). No additional upper phosphorylation band was observed in a triple alanine mutant ($HOXB13^{3A}$) of the three phosphorylation sites T8, T41, and S31 (Figure 3I). Notably, the additional phosphorylation of S31 was still found dependent on mTOR, because pharmacological inhibition or genetic knockdown of mTOR inhibited the appearance of the upper band sparked by the HOXB13 phosphomimic mutants (Supplementary Figure 2B, 2C). Further analysis showed that knockdown of Raptor, but not Rictor, could reduce HOXB13 S31 phosphorylation (Supplementary Figure 2D, 2E). A simplified model of HOXB13 phosphorylation by mTOR is illustrated in Figure 3J.

HOXB13 phosphorylation promotes its degradation by SKP2

We next tested whether HOXB13 phosphorylation at the mTOR-targeted sites affects its protein stability. As shown by a cycloheximide chase assay in 293T cells, expressed levels of the triple

phosphomimic mutant HOXB13^{3D} degraded at a faster pace than both HOXB13 and HOXB13^{3A} (Figure 4A). Likewise, depriving doxycycline (Dox) from LNCaP cells (Dox off assay) with pre-induced expression of either HOXB13, HOXB13^{3A}, or HOXB13^{3D} confirmed that HOXB13^{3D} was more unstable than HOXB13^{3A} (Supplementary Figure 3A). Consistently, HOXB13^{3D} showed markedly enhanced polyubiquitination compared to HOXB13 and HOXB13^{3A}, indicating its increased recognition by the proteasome for degradation (Figure 4B). To identify potential E3 ligase(s) targeting HOXB13 for degradation, we used the ubiquitin ligase-substrate interaction tool Ubibroswer$^{1.0}$ (http://ubibrowser.bio-it.cn/ubibrowser). We were particularly interested in the 3rd top ranked candidate E3 ligase SKP2 (Supplementary Figure 3B) as it is known to lead to the degradation of its substrates in a phosphorylation-dependent manner (30,31). SKP2, also referred to as FBXL1, is a member of the F-box E3 ligase family which usually forms a SCF complex with SKP1/Cullin1 to trigger substrate ubiquitination and subsequent degradation (32,33). Fittingly, a recent proteomics study identified the SKP2 family member SKP1 as a potential HOXB13 interactor (29). Co-IP experiments confirmed that both exogenously expressed HOXB13 in 293T cells and endogenous HOXB13 in LNCaP and PC3 cells interact with SKP2 (Figure 4C, 4D and Supplementary Figure 3C). Overexpression of SKP2 promoted HOXB13 polyubiquitination and destabilization (Figure 4E and Supplementary Figure 3D-3F), while both genetic and pharmacological inhibition of SKP2 stabilized HOXB13 protein levels in LNCaP and PC3 cells (Figure 4F and Supplementary Figure 3G-3I). In support that mTOR control of HOXB13 stability is SKP2-dependent, both genetic knockdown and pharmacological inhibition of mTOR in LNCaP cells impaired HOXB13-SKP2 interaction (Figure 4G, 4H), while HOXB13^{3D} interacted more strongly with SKP2 compared to HOXB13 and HOXB13^{3A} in 293T cells (Figure 4I). Crucially, SKP2-induced HOXB13 degradation was abolished upon co-treatment with Torin 1 in LNCaP

cells (Figure 4J), underscoring the necessity of mTOR-mediated HOXB13 phosphorylation for SKP2-mediated HOXB13 degradation (Figure 4K).

HOXB13 phosphorylation specifies the HOXB13-dependent transcriptome

HOXB13, an important co-regulator of AR, is well-known to play a critical role in the control of gene expression. To establish whether HOXB13 phosphorylation at T8/T41/S31 affects its transcriptional activity, we conducted RNA-seq analyses of inducible LNCaP cell lines in which endogenous HOXB13 was depleted by shRNA-mediated knockdown and rescued by exogenous expression of HOXB13 or the HOXB13^{3A} mutant with YFP as the empty vector (EV) control in cells exposed to either vehicle (EtOH) or R1881 for 24h to stimulate mTOR signaling (Supplementary Table 1). Our analysis revealed a phospho-HOXB13-dependent gene signature ± R1881 comprised of 200 up-regulated and 154 down-regulated differentially expressed genes (DEGs, $p< 0.05$, $|Log2FC|> 0.5$) which were significantly and specifically driven by HOXB13 re-expression compared to EV control but also significantly reversed by the phospho-deficient HOXB13^{3A} mutant (Figure 5A and Supplementary Table 1). Notably, 72% of the 354 gene signature was established from R1881-treated cells, a condition leading to the simultaneous enhancement of both AR and mTOR activity, upstream regulators of HOXB13 protein destabilization found herein to involve mTOR-mediated phosphorylation. Functional interrogation of the 354-gene set uncovered several important enriched molecular signature database (MSigDB) Hallmark terms including the down-regulation of the androgen response signature and bi-directional regulation of TNFα/NF-κB signaling (Figure 5B). RT-qPCR confirmed that both HOXB13 and the phospho-mimic HOXB13^{3D} mutant but not HOXB13^{3A} could repress androgen-mediated upregulation of the IκBα-encoding gene *NFKBIA*, a key inhibitor of NF-κB

transcriptional activity via its cytoplasmic sequestration (Supplementary Figure 4A). Reversely, pharmacological inhibition of mTOR by Torin1 or Rapamycin promoted *NFKBIA* expression, supporting mTOR as an upstream kinase directing phospho-HOXB13-mediated regulation of NF-κB signaling (Supplementary Figure 4B). Consistently, HOXB13 promoted the nuclear translocation and activation of NF-κB (p65 and p50) in a phospho-dependent manner by releasing the inhibitory effect of NFKBIA (Supplementary Figure 4C).

To reinforce the molecular link between phospho-HOXB13 T8/T41/S31 with mTOR kinase, we established inducible shRNA-mediated mTOR knockdown LNCaP cell lines rescued with mTOR or YFP as the empty vector control (Supplementary Figure 4D) to observe functional overlap between phospho-HOXB13- and mTOR-driven gene signatures. mTOR activation led to a robust up-regulation of 1704 genes and down-regulation of 2108 genes ($p< 0.05$, $|Log2FC|> 0.5$) in cells exposed to either vehicle (EtOH) or R1881 for 24h (Figure 5C and Supplementary Table 2). Importantly, 30% of the phospho-HOXB13-driven genes (106 of 354) were also regulated by mTOR in a consistent manner ± R1881 (Figure 5D, Supplementary Figure 4E, and Supplementary Table 2). The majority of the 106 shared co-targets were down-regulated by p-HOXB13 and mTOR of which several were validated by RT-qPCR including androgen response genes *KLK2* and *STEAP4* and lipid metabolic genes *HMGCS2* and *ACSL3* (Figure 5E, 5F). The repressive action of HOXB13 on the examined genes were mimicked by the $HOXB13^{3D}$ mutant but lost by the $HOXB13^{3A}$ mutant, indicating the necessary and dominate effect of HOXB13 phosphorylation on their transcriptional control (Figure 5E). In contrast to mTOR activation, all four genes examined were found de-repressed by mTOR inhibition with Torin1 or Rapamycin (Figure 5G).

HOXB13 phosphorylation promotes its oncogenic function

To investigate the impact of HOXB13 phosphorylation on PCa cell growth and tumorigenesis, we made use of genetically engineered LNCaP cell lines with stable knockdown of endogenous HOXB13 rescued by the inducible expression of HOXB13, HOXB13^{3A}, and HOXB13^{3D} (Figure 6A). In addition, cells re-expressing HOXB13^{G84E} harboring a G84E mutation, a variant associated with increased PCa risk (34), were used as a control for comparison (Figure 6A). Cell colony formation assay showed a decreased LNCaP cell growth rate upon HOXB13 depletion, found rescued and even enhanced by re-introduction of HOXB13^{3D} and HOXB13^{G84E} phosphomimic mutants but not the phospho-deficient HOXB13^{3A} mutant (Figure 6B). Similarly, HOXB13^{3D} and HOXB13^{G84E} mutants promoted HOXB13-depleted LNCaP cell proliferation unlike the HOXB13^{3A} mutant (Figure 6C). To further support the *in vitro* findings, the distinct LNCaP clones were inoculated subcutaneously in NSG-nude mice and xenograft tumor development was monitored to evaluate the oncogenic potential of the HOXB13 mutants in an *in vivo* model system. The tumor incidence was 100% (6/6) for all xenograft models. Critically, in stark contrast to HOXB13^{3A}, HOXB13 and HOXB13^{3D} phosphomimic mutant significantly enhanced xenograft tumorigenicity compared to the HOXB13 knockdown model (Figure 6D-6F), thus recapitulating the phenotypes observed *in vitro*. Although LNCaP cells expressing the HOXB13^{G84E} mutant displayed enhanced cellular growth and proliferation *in vitro*, its impact on tumor growth *in vivo* was not significant (Figure 6D-6F). This observation is consistent with previous reports demonstrating that HOXB13^{G84E} confers a greater PCa risk without obvious phenotypic changes (35).

Together, the data demonstrate that phosphorylation of T8, T41, and S31 on HOXB13 promotes its oncogenic activation. Due to the lack of commercially available antibodies and

difficulty in generating specifically targeting the identified HOXB13 phosphorylated residues, we evaluated the clinical relevance of the identified phospho-HOXB13 354-gene signature on PCa progression and aggressiveness in human clinical specimens. First, we performed unsupervised hierarchical clustering analysis on patient samples from the Tomlins et al. cohort (36) (GSE6099) resulting in a strong discrimination (90%) between normal and epithelial benign cells, localized PCa and hormone-refractory (CRPC) metastatic PCa using 127 of 354 mapped genes with available expression data (Figure 6G). Next, using this validated phospho-HOXB13 driven 127-gene subset, we were also able to robustly distinguish normal benign prostate tissue, localized primary PCa and metastatic PCa tissue in two independent cohorts, GSE3325 (37) and GSE8511 (Figure 6G), reinforcing the connection between oncogenic phospho-HOXB13 action and PCa progression.

Discussion

HOXB13 is known to exert both oncogenic and tumor suppressive roles in PCa development through its interaction with AR, MEIS1 and the HDAC3-NCoR/SMART complex (7,29,38). In recent work, we found strong evidence supporting genomic interaction between chromatin-bound mTOR and HOXB13 in several PCa cell lines (24,26) whereas mTOR was also identified as a potential regulatory cofactor of HOXB13 in LNCaP cells (29). However, how these interactions affect the activity of each component of this complex and, more importantly, how a potential mTOR-HOXB13 axis transcriptional axis could influence PCa progression remained to be investigated. Herein, we report that mTOR and HOXB13 directly interact with each other and that mTOR-mediated phosphorylation of HOXB13 activates its oncogenic function in PCa cells.

Mechanistically, we showed that the mTOR-HOXB13 interaction involves the carboxyl-terminal region of mTOR harboring the kinase domain and the amino-terminal region encoding the MEIS domain of HOXB13. Our results demonstrated that this interaction leads to the phosphorylation by mTOR of three residues within the amino-terminal domain of HOXB13, and that phosphorylation of T8/T41 by mTOR primed its subsequent phosphorylation at S31. Serine 31 of HOXB13 is followed by a proline residue and mTOR is known to phosphorylate its substrates in a proline-directed manner (19,39). Although S31 phosphorylation was found sensitive to mTOR inhibition, it is also plausible that other kinases contribute to the phosphorylation of these residues. Along these lines, CDK1 and CDK9 were identified as possible HOXB13 interactors in a recent HOXB13 interactome study (29) and CDKs are proline-directed kinases. In addition, the sequences surrounding HOXB13 S31 and S35 also predict recognition by GSK3α/β given their kinase consensus motif, Ser/Thr-x-x-x-Ser/Thr. However, our results indicate that GSK3α/β is not the second kinase implicated in HOXB13 S31 phosphorylation as GSK3α/β would first require

phosphorylation at S35 to phosphorylate S31 and our results showed that the S35A mutation did not abolish the upper band (S31 phosphorylation) of HOXB13 (Figure 3G). In effect, mTOR-mediated phosphorylation of HOXB13 is better aligned with 4EBP1 phosphorylation by mTOR, whereby T37/T46 phosphorylation primes its further phosphorylation at T70/S65 with the second kinase proposed to be mTOR or another proline-directed kinase like ERK2 (40-42). Phosphorylation of HOXB13 at T8/T41/S31 was found to increase its association with E3 ligase SKP2, thus triggering its polyubiquitination and subsequent degradation. Proteosome-mediated turnover of transcription factors has been shown to contribute significantly to transcriptional activation (43,44), and may thus constitute an important mechanism by which HOXB13 activity is controlled in both normal and transformed cells. Indeed, SKP2 has been shown to act as a coactivator of the oncoprotein Myc uniting its transcriptional activity and degradation (45,46). Since phosphorylation and de-phosphorylation are two reversible and dynamic reactions transpiring within cells, it will also be of great interest to identify potential phosphatase(s) for HOXB13 that may participate in the regulation of HOXB13 protein stability in addition to possible involvement of other E3 ligases and deubiquitinases in this process. Recently, the phosphatase calcineurin was shown to dephosphorylate HOXB13 at S204 (16), suggesting that the identification of the phosphatase(s) responsible for removing the phosphate group from HOXB13 at T8, T41 and S31 can be achieved in the near future.

RNA-seq profiling revealed that genes associated with androgen response, TNFα/NF-κB signaling, and lipid metabolism were among molecular signatures found modulated among the 354-geneset likely governed by HOXB13 phosphorylation. While HOXB13 has previously been shown to promote PCa metastasis through upregulation of NF-κB signaling via *NFKBIA* down-regulation (12) as well as act as a key modulator of the androgen response (7), our findings

emphasize the importance of mTOR-mediated phosphorylation of HOXB13 in dictating the PCa transcriptome, undoubtedly altering PCa oncogenesis. Nearly one third of the phospho-HOXB13-dependent gene signatures was similarly regulated by mTOR, thus reinforcing the functional link of mTOR acting as an upstream kinase of HOXB13. Ultimately, the profound transcriptional reprogramming driven by phospho-competent HOXB13 resulted in an acceleration of LNCaP cellular growth and proliferation *in vitro* as well as LNCaP xenograft tumor growth *in vivo* as compared to the non-phosphorylatable HOXB13 mutant. Notably, the $HOXB13^{3D}$ phosphomimic mutant (T8D/T41D/S31D) displayed greater xenograft tumorigenesis compared to the phosphomimicking mutant $HOXB13^{G84E}$, although the precise underlying oncogenic mechanisms require further study. It is conceivable that phosphorylation of HOXB13 at T8/T41/S31 influences its interactome on the chromatin and distinct AR/HOXB13 protein complexes combined with other cofactors could be responsible for the differential transcriptional effects observed. HDAC3 was recently found to interact specifically with HOXB13 but not $HOXB13^{G84E}$, in an AR-independent manner, underlying the ability of HOXB13 to suppress *de novo* lipogenesis and inhibit PCa metastasis (29). In this report, the authors showed that re-introduction of HOXB13 following HOXB13 knockdown transcriptionally repressed key lipogenic genes including FASN, SREBF2, and KLK3, an effect lost with the oncogenic HOXB13G84E mutant. Our transcriptomic data show that repression of FASN and KLK3 but not SREBF2 was found to require HOXB13 T8/T41/S31 phosphorylation (Supplementary Figure 4F), suggesting the existence of phosphorylation specific HOXB13 transcription complexes.

As noted above, HOXB13 has been shown to have both growth-inducing and inhibiting effects on PCa cell growth. Here we show that introduction of phosphomimetic mutations at mTOR-dependent phosphorylation sites in HOXB13 promotes PCa cellular growth *in vitro* and

tumor growth *in vivo* in a xenograft model system. mTOR kinase is a homeostatic sensor that plays a major role in the control of cell growth (19), and dysregulation of the canonical mTOR pathway and activity in the nucleus have linked to PCa aggressiveness and poor outcome (24,47-49). Here we identified a critical link between mTOR activation, HOXB13 phosphorylation and PCa cell growth. Significantly, we showed that expression of a HOXB13 triple phosphomimetic mutant involving the mTOR-targeted residues, but not the non-phosphorylatable mutant, promotes PCa cellular growth *in vitro* and tumor growth *in vivo* in a xenograft model system. In addition, we established that a functional phospho-HOXB13-dependent gene signature can robustly differentiate normal prostate tissues, primary PCa, and metastatic PCa in three independent human clinical cohorts emphasizing the importance of the previously unrecognized mTOR/HOXB13 regulatory axis during PCa development. While activation of canonical mTOR signaling takes place in the cytoplasm, recent work clearly demonstrated that mTOR and HOXB13 associate on chromatin in PCa cells (26), indicating that mTOR most likely encounters HOXB13 and phosphorylates HOXB13 in the nucleus. In any case, this work exposed a previously unrecognized mTOR-dependent phosphorylation cascade dictating HOXB13 oncogenic activity in PCa.

Limitation of the study

Our data demonstrates that mTOR-dependent phospho-HOXB13 T8/T41/S31 is oncogenic, but whether this HOXB13 phosphorylation state directly correlates with poor prognosis and worse PCa malignancy that could be observed in clinical specimens awaits further elucidation given the current lack of suitable HOXB13 phospho-specific antibodies.

Methods

Reagents

A complete list of reagents used in this study are presented in Supplementary Table 3.

DNA constructs and transfection

shRNAs targeting TSC1, TSC2, Raptor, Rictor, and SKP2 as well as pLX317 V5-tagged ORF of Rheb, SKP2, HOXB13, and GFP were originally from the Genetic Perturbation Platform of Broad Institute at MIT, and provided by the Genetic Perturbation Service of the Goodman Cancer Institute at McGill University. Inducible shRNAs of mTOR and HOXB13 were self-cloned by inserting the short hairpin sequence into the inducible shRNA pLKO-TetON backbone (Addgene, Cat#21915). Inducible V5-tagged ORF of HOXB13 was made by inserting HOXB13-V5 sequence into a pCW57-Blasticidine inducible backbone (Addgene, Cat#80921). HOXB13 mutants (including shRNA2-resistant mutant, 3A, 3D, G84E and other point mutations) were mutated from WT HOXB13-V5 constructs by using a Q5 site-directed mutagenesis kit (NEB, Cat#E0554S). GST-HOXB13 WT and mutants (T8A, T41A and T8A+T41A) were cloned into a pGEX-5X-3 backbone. HOXB13 domain fragments (N-terminal and C-terminal) were cloned into a pLPC-3xFlag backbone, while mTOR domain fragments (N-terminal, Middle, and C-terminal) were generated by deletion strategy using a Q5 mutagenesis kit. HA-Ubiquitin (Cat#18712) and YFP-mTOR (Cat#73384) were purchased from Addgene. See also Supplementary Table 3 for further details.

Plasmid transfection

Calcium Phosphate Precipitation was used to transiently transfect 293T cells. Viral infections consisted of co-transfection of lentivirus packaging vector psPAX2 (Addgene, Cat#12260) and envelop vector pMD2.G (Addgene, Cat#12259) with shRNAs or ORFs of target genes into 293T cells to first generate lentivirus. Then, virus soup was collected and filtered. PCa cells (LNCaP and PC3 cells) were next infected by the virus supplemented with 8ug/ml polybrene and selected by 1ug/ml puromycin or blasticidine to establish stable cell lines.

Stable LNCaP cells

LNCaP cells were infected with lentivirus containing HOXB13 inducible shRNA (produced in 293T cells) to knockdown endogenous HOXB13. These cells were selected by puromycin to be stable. Then, lentivirus containing inducible HOXB13 mutants (produced in 293T cells) were used to infect LNCaP-shHOXB13 stable cells for rescuing expression. These cells were selected by blasticidine to be stable. For experiments, 1ug/ml Doxycycline was added to these stable LNCaP cells to induce the expression of HOXB13 shRNA and HOXB13 mutants simultaneously whereby endogenous HOXB13 is knocked down and rescued with exogenous HOXB13 mutants. Exogenous HOXB13 mutants had a V5 tag, thus their expression levels were validated using a V5 antibody and migrated slightly higher than endogenous HOXB13 which could be detected using a HOXB13 antibody (if separated well during migration).

Cell culture

PCa cell lines (LNCaP, PC3, 22RV1) were originally purchased from ATCC and routinely cultured in phenol-red free RPMI medium (Wisent, Cat#350-046CL) supplemented with 10% FBS

(Thermo Fisher Scientific, Cat#12483020). The 293T and Hela cell lines were maintained in DMEM medium (Wisent, Cat#319-005CL) supplemented with 10% FBS. Mycoplasma was regularly monitored using a mycoplasma PCR detection kit (Applied Biological Materials, Cat#G238) and no contamination was detected. For treatment with the synthetic androgen R1881 (Steraloids, Cat#E3164-000), LNCaP cells were plated and grown in 150mm culture dishes to ~75% confluency before switching to medium containing 2% Charcoal-Stripped Serum (CSS medium) for 48h to steroid deprivation prior to treatment with 10nM R1881 in freshly added CSS medium for another 24h or as indicated.

Immunoblotting

Cell culture medium was discarded, and cells were washed once with ice-cold 1xPBS prior to protein lysate preparation. For cytosolic/nuclear fractionation, 1ml Harvest Buffer (10mM Hepes, 50mM NaCl, 0.5M Sucrose, 10mM EDTA, 0.5% Triton X-100 and protease inhibitors) was added per 150mm plate for cell lysis. Cells were rapidly scraped, and lysates were transferred into 1.5ml eppendorf tubes and incubated on ice for 8min before being centrifuged at 3000rpm, 4^{o}C for another 8min. The supernatants were collected and centrifuged further at 12000rpm, 4^{o}C for 15min. The resulting supernatants were kept as the cytosolic fractions and the nuclear pellets were washed twice with Buffer A (10mM Hepes, 10mM KCl, 0.1mM EDTA and 0.1mM EGTA). Finally, the nuclear pellets were re-suspended in Buffer K (20mM phosphate buffer PH7.4, 150mM NaCl, 0.1% NP40, 5mM EDTA and protease inhibitors) supplemented with 0.6% CHAPS and rotated at 4^{o}C for at least 40min to extract the nuclear proteins. Brief sonication was used to ensure more efficient extractions. The nuclear lysates were collected after centrifugation at 12000rpm, 4^{o}C for 15min. For whole cell lysates, cells were directly lysed in Buffer K

supplemented with 0.6% CHAPS for at least 40min on ice. The supernatants were collected after being centrifuged at 12000rpm, 4° C for 15min.

For IP, at least 5 confluent 150mm plates (per treatment condition) of LNCaP or 22rv1 cells were extracted in Buffer K supplemented with 0.6% CHAPS for nuclear IPs. For each nuclear IP, 2ug antibody was pre-incubated with 1mg Protein G magnetic beads (Invitrogen, Cat# 10009D) at room temperature for 1h, then ~0.3-1mg nuclear protein was added to the antibody-beads mixture and left to rotate at 4° C overnight. The next day, the beads were washed three times with 1x PBST containing 0.1% Tween and heated to 70° C for 5min in 1x Western Loading Buffer.

Protein concentration was measured using Bradford reagent (Bio-Rad, Cat#500-0006). Generally, 20-30μg of proteins were mixed with 1x Western Loading Buffer and heated at 95° C for 5min before being loaded on 6%-9% SDS-PAGE gels for immunoblotting. Denatured proteins were separated by electrophoresis and transferred onto PVDF membranes (Bio-Rad, Cat#162-0177). Membranes were blocked with 5% milk (BIOSHOP, Cat#SK1400.500) for 1h at room temperature then incubated with primary antibody overnight at 4° C. The next day, membranes were incubated with anti-rabbit or anti-mouse HRP-linked secondary antibodies for 1h at room temperature then washed efficiently with 1xPBS containing 0.1% Tween 20. Proteins were detected by chemiluminescence using Western ECL substrate mix (Bio-Rad, Cat#1705061, #1705062) and results were obtained using film or a ChemiDoc MP imaging system (Bio-Rad, Cat# 12003154). Primary and secondary antibodies are listed in Supplementary Table 3. Portions of uncropped blots (indicated by red boxes) used to generate the figures are shown in Supplementary Figure 5.

Lambda phosphatase treatment

293T cells were transiently transfected with and expressing HOXB13 mutants (WT, T8D, T41D or T8D+T41D). After extracting the whole cell lysates, we did V5 tag immunoprecipitation to pull down these exogenous HOXB13 mutants and used lambda phosphatase to digest the immunoprecipitates directly in the tubes for 30 minutes. Then, we ran for western blot and observed that the upper band completely disappeared after brief phosphatase treatment. It implied that the upper band was a phosphorylation band.

mTOR *in vitro* kinase assay

GST-HOXB13 WT (pGEX-5x-3 backbone) and mutants were transformed into BL21 bacteria and their expression was induced by 0.4mM IPTG for 4h at 30^{o}C after reaching a 0.6 O.D. (600nm) absorbance at 37^{o}C. Bacteria were collected and lysed in STE buffer (10mM Tris-HCl pH 8.0, 1mM EDTA, 100mM NaCl, 5mM DTT, and protease inhibitors) with 1 mg/ml lysozyme (Roche, Cat#10837059001) and 1.5% Sarcosyl (Sigma, Cat#L5125) for 30-45min prior to sonication.

Glutathione Sepharose beads (GE Healthcare, Cat#17-0756-01) were washed twice with NETN buffer (10mM Tris-HCl pH 8.0, 1mM EDTA, 100mM NaCl, 0.5% NP-40) and rotated together with bacterial lysate containing GST-HOXB13 protein at 4° C for 2 h. Beads were then washed twice with NETN buffer, twice with high salt NETN buffer (10mM Tris-HCl pH 8.0, 1mM EDTA, 500mM NaCl, 0.5% NP-40), and once more with NETN buffer. After washing, GST-HOXB13 protein was eluted from the beads by adding freshly prepared pH 8.8 Elution Buffer (25mM glutathione, 50mM Tris pH 8.8, 200mM NaCl) and rotating at 4° C for 30 min. After

brief centrifugation, the supernatant containing pure GST-HOXB13 protein was collected as the substrate for an mTOR kinase assay described below.

mTOR was IP’d from Hela cells (with or without 300nM insulin stimulation for 30min) lysed in mTOR lysis buffer (40mM HEPES pH 7.4, 2mM EDTA, 10mM Pyrophosphate, 10mM Glycerophosphate, 0.3% CHAPS). Briefly, magnetic Protein G beads (Invitrogen, Cat# 10009D) bound with target proteins were washed three times with low salt wash buffer (40mM HEPES PH 7.4, 2mM EDTA, 10mM Pyrophosphate, 10mM Glycerophosphate, 0.3% CHAPS, and 150mM NaCl) and twice with equilibrium buffer (25mM HEPES pH 7.4, 20mM KCl). The mTOR kinase assay was then performed by mixing Protein G beads containing mTOR kinase, 0.5μg GST-HOXB13 protein purified from bacteria, 50μM unlabeled ATP and 5μCi P^{32}-ATP together in mTOR kinase buffer (25mM HEPES PH 7.4, 50mM KCl, 10mM MgCl2, 4mM MnCl2, 1mM DTT, 20% Glycerol) at 30° C for 40min. The reaction was stopped by the addition of Western loading buffer and the mixture was boiled at 95° C for 5min. Heat-denatured samples were separated on a 12% SDS-PAGE gel. The radioactive gel was dried, exposed to Fuji Storage Phosphor Screen, and viewed by the Typhoon TRIO Variable Mode Imager (Amersham Biosciences). The gel was also stained with Coomassie brilliant blue to confirm that an equal amount of GST-HOXB13 protein substrate was used in each reaction.

GST pull-down

During protein extraction and purification from bacteria, GST-tagged HOXB13 protein or the GST tag only were bound with Glutathione Sepharose Beads (GE Healthcare, Cat#17-0756-01) which served as the bait. For the prey proteins, we used 293T whole cell lysates which were pre-cleared with unbound Glutathione Sepharose Beads. Then, pre-cleared supernatant (prey) was directly

added to and mixed with GST-HOXB13 or GST-bound Glutathione Sepharose Beads (bait). Binding buffer (1xPBS+ 0.1% Tween 20, 0.25mM DTT) was added to a final volume of 1ml and the mixture was rotated at 4° C overnight. The next day, the beads were washed three times with binding buffer by pipetting up and down. Then, Western loading buffer was added, and the beads were boiled at 95° C for 5min before loading on the gel.

Mass spectrometry (in gel digestion)

Following the mTOR *in vitro* kinase assay (with only unlabeled ATP) using GST-HOXB13 as the substrate, denatured proteins were separated by SDS-PAGE. Coomassie Brilliant Blue R250 was used for gel staining to visualize the protein bands. A small piece around 60 kDa (size of GST-HOXB13) was cut and sent for MS analysis (in gel digestion) conducted by Dr. Denis Faubert at the Institut de Recherches Cliniques de Montréal (IRCM). Chymotrypsin was selected for efficient digestion of HOXB13 for phosphorylation site identification. Phosphopeptides detected with >80% probably were considered high-confident phosphosites.

RT-qPCR

Total RNA from cells was isolated using a RNeasy Mini Kit (Qiagen, Cat#74106). RNA (1μg) was reverse transcribed using ProtoScript II Reverse Transcriptase (NEB, Cat#M0368X) and measured by quantitative real-time PCR using SYBR Green Master Mix (Roche, Cat#4887352001) on a LightCycler 480 instrument (Roche). The relative expression levels of target genes were normalized to the average expression of two human housekeeping genes (*TBP* and *ACTB*). For RNA-seq samples, a DNase I (Qiagen, Cat#79254) digestion step was additionally

performed during RNA extraction to eliminate DNA contamination. Specific human RT-qPCR primer sequences are listed in Supplementary Table 3.

RNA-sequencing and analysis

Messenger RNA-seq profiling was performed by Novogene Bioinformatics Technology Co., Ltd. Sample libraries prepared using the NEBNext Ultra II RNA Library Prep kit according to manufacturer's recommendations were sequenced on an Illumina platform (NovaSeq 6000) and 150bp paired-end reads were generated. Raw data (raw reads) of fastq format were processed through in-house perl scripts to remove reads containing adapter and poly-N sequences and reads with low quality. Hisat2 software (version 2.0.5) was used to align paired-end clean reads to the Homo Sapiens reference genome hg38 and Feature Counts software (version 1.5.0-p3) was used to count the number of reads mapped per gene. FPKM (Fragments per kilobase of transcript sequence per millions base pairs sequenced) of each gene was calculated based on the length of the gene and read counts mapped to this gene. Differential expression analysis between the groups was performed using the DESeq2 R package (version 1.20.0). Significant DEGs between groups (n=3 per group) were determined using DESeq2 p-value < 0.05 and an absolute log2 fold-change > 0.5. Additionally, probes with an attributed value of zero in expression found in at least 1 sample among the comparative groups were filtered out. HOXB13- and mTOR-dependent DEGs ± vehicle (EtOH) or R1881 for 24h are presented in Supplementary Tables 1 and 2, respectively. Total DEGs found dependent on phospho-HOXB13 (354 genes) ± R1881 are presented in Supplementary Table 1. Total DEGs found dependent on mTOR (3812 genes) or common to phospho-HOXB13 and mTOR (106) ± R1881 are presented in Supplementary Table 2. Note that Heatmaps of DEGs using z-scaled log2(FPKM+1) values were generated using Morpheus

(https://software.broadinstitute.org/morpheus/). Functional enrichment analysis of DEGs was performed using Enrichr (50) (https://maayanlab.cloud/Enrichr/) to identify enriched Molecular Signature Database (MSigDB) hallmark signatures (v 2020). For clustering analyses, microarray data from public clinical datasets were first filtered to include probes associated with phospho-HOXB13-dependent genes. In Gene Cluster 3.0 (51), probes with expression values present across 80% of the samples and a MaxVal-MinVal cutoff > 1.0 were retained and hierarchical clustering using average linkage and the distance metric correlation (uncentered) was performed on log transformed data with genes centered on means. Clustering results were visualized using Java TreeView 3.0 (v beta 1) (https://doi.org/10.5281/zenodo.1303402). Interrogated datasets were GSE6099 (36), GSE3325 (37) and GSE8511. The 354-geneset regulated by phospho-HOXB13 was first assessed on the Tomlins et al. cohort and the resulting validated list of 127 mapped genes were used to further interrogate the cohorts in GSE3325 and GSE8511.

Colony formation assay

A total of 6,000 LNCaP cells were seeded evenly per well in 6-well plates. After ~3 weeks (changing the medium every 5 days) cell colonies grew out. Then, the cells were gently washed once with cold 1xPBS and 100% methanol was added for 20min at room temperature to fix the colonies in the plates. Next, three washes with cold 1xPBS were done to remove the methanol before adding Crystal Violet (Sigma, Cat#V5265) for 10min at room temperature to stain the colonies Again, cold 1xPBS was used to wash out the unbound Crystal Violet at least 3 times to get achieve a clear background. The plates were air dried at room temperature and pictures were taken.

Incuyte cell proliferation assay

A total of 3,000 LNCaP cells were seeded evenly per well in 96-well plates. Six replicates were prepared for each experimental condition. Cell plates were incubated in an Incucyte incubator where cellular growth was monitored over one week and cell confluency was quantified. Higher confluency is correlated with faster cell proliferation. A proliferation curve (relative confluency) was generated by normalizing the value of each time point over the value at time 0. One-way ANOVA test was used to calculate the statistical significance.

Xenograft tumor growth

All mouse manipulations were performed in accordance with procedures approved by the McGill Facility Animal Care Committee and complied with ethical guidelines set by the Canadian Council of Animal Care. Thirty NSG mice (14-weeks old) were purchased from Dr. William Muller's laboratory and used as a model to study the growth and development of LNCaP tumor xenografts. Stable LNCaP cell lines were established by inducible shRNA-mediated HOXB13 knockdown and rescued by inducible expression of either Empty Vector (EV) or WT-HOXB13, 3A-HOXB13, 3D-HOXB13 and G84E-HOXB13. Cells were cultured and maintained in an incubator set at 37^{o} C and 5% CO_2. Prior to injection in mice, cells were first trypsinized and resuspended in PBS. Three million cells were mixed with Matrigel (VWR, Cat#354262) (v/v is 2/1, 100ul in total per mouse) and subcutaneously injected into the right side of each mouse. Six mice were injected for each of the 5 established LNCaP cell lines. Doxycycline (Wisent Bio-products, Cat#450-185) was administered in the drinking water at 2mg/ml (Dox water) and given to mice following injection to induce gene expression. Every 6 days, the Dox water was freshly replaced considering the instability of doxycycline at room temperature. Around 16 days after the cell injections, the first

tumor was observed, after which tumors were monitored and volumes were measured every 3 days. Tumor volume was determined by caliper measurements of two dimensions and calculated using the formula V=L*W*W/2 where V= volume, L = length and W = width. When the largest tumor reached the maximal permitted size (2 cm^3), all mice were sacrificed at the same time. Tumors were collected, weighed, snap-frozen in liquid nitrogen and stored at -80^o C.

Statistics

GraphPad Prism 9 software was used to draw graphs and for statistical analyses. The number of independent experiments or biological replicates used are indicated in the figure legends. Unless otherwise specified, differences were considered significant when p-value calculated by One-way ANOVA analysis was less than 0.05.

Data availability

RNA-seq data of HOX13 shRNA-mediated knockdown in LNCaP cells rescued with either WT HOXB13, HOXB13^{3A}, HOXB13^{3D} or empty vector (EV) control ± 10nM R1881 for 24h as well as RNA-seq data of mTOR shRNA-mediated knockdown in LNCaP cells rescued with either WT mTOR or empty vector (EV) control ± 10nM R1881 for 24h have been deposited in NCBI's Gene Expression Omnibus (GEO) and are accessible through GEO SuperSeries accession number GSE225207 encompassing SubSeries GSE225206 (HOXB13 RNA-seq) and GSE225205 (mTOR RNA-seq). Public human clinical microarray data used in this study are available from the GEO database: GSE6099 (36), GSE3325 (37) and GSE8511.

Source data underlying the graphs are presented in Supplementary Table 4. Uncropped immunoblots are shown in Supplementary Figure 5.

Author Contributions

Y.C. performed most of the experimental work under the supervision of V.G. C.R.D. analyzed the RNA-seq data. Y.C. prepared cells for xenograft models; L.H. monitored the tumor growth; T.L and H.X dissected the tumors in the end. Y.C. designed the experiments and organized the data with the help of C.R.D. and V.G. Y.C. wrote the original draft of the manuscript with edits from C.R.D. and V.G. All authors commented on the manuscript.

Acknowledgments

We thank all the members from Dr. Giguère's laboratory for daily assistance and helpful discussions; Mr. Carlo Ouellet for the injections of cells in murine xenografts; Dr. Denis Faubert and his team at the IRCM (Institut de Recherches Cliniques de Montréal) for Mass Spectrometry analysis; Drs. Michel Tremblay and Jose Teodoro (McGill University) for advice on the project; and Dr. Etienne Audet-Walsh (Laval University) for suggestions on clinical correlation analysis. This work was supported by a Foundation grant from the Canadian Institutes of Health Research (CIHR) to V.G. (FDT-156254), a Terry Fox Research Institute Team Grant (PPG-1091), and a co-funded operating grant from the Cancer Research Society and Génome Québec (CRS-25085). Lingwei Han is supported by a Canderel studentship. Xia Hui received a studentship from the Fond de recherches Québec – Santé.

Declaration of Interests

The authors declare no conflict of interests.

References

1. Harris WP, Mostaghel EA, Nelson PS, Montgomery B. Androgen deprivation therapy: progress in understanding mechanisms of resistance and optimizing androgen depletion. Nat Clin Pract Urol **2009**;6:76-85
2. Pomerantz MM, Li F, Takeda DY, Lenci R, Chonkar A, Chabot M*, et al.* The androgen receptor cistrome is extensively reprogrammed in human prostate tumorigenesis. Nat Genet **2015**;47:1346-51
3. Ku SY, Gleave ME, Beltran H. Towards precision oncology in advanced prostate cancer. Nat Rev Urol **2019**;16:645-54
4. Teo MY, Rathkopf DE, Kantoff P. Treatment of Advanced Prostate Cancer. Annu Rev Med **2019**;70:479-99
5. Giguère V. DNA-PK, Nuclear mTOR, and the Androgen Pathway in Prostate Cancer. Trends Cancer **2020**;6:337-47
6. Yu M, Zhan J, Zhang H. HOX family transcription factors: Related signaling pathways and post-translational modifications in cancer. Cell Signal **2020**;66:109469
7. Norris JD, Chang CY, Wittmann BM, Kunder RS, Cui H, Fan D*, et al.* The homeodomain protein HOXB13 regulates the cellular response to androgens. Mol Cell **2009**;36:405-16
8. Chen Z, Wu D, Thomas-Ahner JM, Lu C, Zhao P, Zhang Q*, et al.* Diverse AR-V7 cistromes in castration-resistant prostate cancer are governed by HOXB13. Proc Natl Acad Sci U S A **2018**;115:6810-5

9. Huang Q, Whitington T, Gao P, Lindberg JF, Yang Y, Sun J*, et al.* A prostate cancer susceptibility allele at 6q22 increases RFX6 expression by modulating HOXB13 chromatin binding. Nat Genet **2014**;46:126-35

10. Yao J, Chen Y, Nguyen DT, Thompson ZJ, Eroshkin AM, Nerlakanti N*, et al.* The Homeobox gene, HOXB13, Regulates a Mitotic Protein-Kinase Interaction Network in Metastatic Prostate Cancers. Sci Rep **2019**;9:9715

11. Kim YR, Oh KJ, Park RY, Xuan NT, Kang TW, Kwon DD*, et al.* HOXB13 promotes androgen independent growth of LNCaP prostate cancer cells by the activation of E2F signaling. Mol Cancer **2010**;9:124

12. Kim YR, Kim IJ, Kang TW, Choi C, Kim KK, Kim MS*, et al.* HOXB13 downregulates intracellular zinc and increases NF-kappaB signaling to promote prostate cancer metastasis. Oncogene **2014**;33:4558-67

13. Jung C, Kim RS, Lee SJ, Wang C, Jeng MH. HOXB13 homeodomain protein suppresses the growth of prostate cancer cells by the negative regulation of T-cell factor 4. Cancer Res **2004**;64:3046-51

14. Jung C, Kim RS, Zhang HJ, Lee SJ, Jeng MH. HOXB13 induces growth suppression of prostate cancer cells as a repressor of hormone-activated androgen receptor signaling. Cancer Res **2004**;64:9185-92

15. Liu B, Wang T, Wang H, Zhang L, Xu F, Fang R*, et al.* Oncoprotein HBXIP enhances HOXB13 acetylation and co-activates HOXB13 to confer tamoxifen resistance in breast cancer. J Hematol Oncol **2018**;11:26

16. Nguyen NUN, Canseco DC, Xiao F, Nakada Y, Li S, Lam NT*, et al.* A calcineurin-HOXB13 axis regulates growth mode of mammalian cardiomyocytes. Nature **2020**;582:271-6

17. Imseng S, Aylett CH, Maier T. Architecture and activation of phosphatidylinositol 3-kinase related kinases. Curr Opin Struct Biol **2018**;49:177-89

18. Blenis J. TOR, the Gateway to Cellular Metabolism, Cell Growth, and Disease. Cell **2017**;171:10-3

19. Battaglioni S, Benjamin D, Walchli M, Maier T, Hall MN. mTOR substrate phosphorylation in growth control. Cell **2022**;185:1814-36

20. Kim J, Guan KL. mTOR as a central hub of nutrient signalling and cell growth. Nat Cell Biol **2019**;21:63-71

21. Wan W, You Z, Xu Y, Zhou L, Guan Z, Peng C*, et al.* mTORC1 Phosphorylates Acetyltransferase p300 to Regulate Autophagy and Lipogenesis. Mol Cell **2017**;68:323-35 e6

22. Giguère V. Canonical signaling and nuclear activity of mTOR: a teamwork effort to regulate metabolism and cell growth. Febs J **2018**;285:1572-88

23. Laribee RN, Weisman R. Nuclear Functions of TOR: Impact on Transcription and the Epigenome. Genes (Basel) **2020**;11

24. Audet-Walsh E, Dufour CR, Yee T, Zouanat FZ, Yan M, Kalloghlian G*, et al.* Nuclear mTOR acts as a transcriptional integrator of the androgen signaling pathway in prostate cancer. Genes Dev **2017**;31:1228-42

25. Audet-Walsh E, Vernier M, Yee T, Laflamme C, Li S, Chen Y*, et al.* SREBF1 activity Is regulated by an AR/mTOR nuclear axis in prostate cancer. Mol Cancer Res **2018**;16:1396-405

26. Dufour CR, Scholtes C, Yan M, Chen Y, Han L, Li T*, et al.* The mTOR chromatin-bound interactome in prostate cancer. Cell Rep **2022**;38:110534

27. Xu Y, Chen SY, Ross KN, Balk SP. Androgens induce prostate cancer cell proliferation through mammalian target of rapamycin activation and post-transcriptional increases in cyclin D proteins. Cancer Res **2006**;66:7783-92

28. Massie CE, Lynch A, Ramos-Montoya A, Boren J, Stark R, Fazli L*, et al.* The androgen receptor fuels prostate cancer by regulating central metabolism and biosynthesis. EMBO J **2011**;30:2719-33

29. Lu X, Fong KW, Gritsina G, Wang F, Baca SC, Brea LT*, et al.* HOXB13 suppresses de novo lipogenesis through HDAC3-mediated epigenetic reprogramming in prostate cancer. Nat Genet **2022**

30. Carrano AC, Eytan E, Hershko A, Pagano M. SKP2 is required for ubiquitin-mediated degradation of the CDK inhibitor p27. Nat Cell Biol **1999**;1:193-9

31. Chan CH, Li CF, Yang WL, Gao Y, Lee SW, Feng Z*, et al.* The Skp2-SCF E3 ligase regulates Akt ubiquitination, glycolysis, herceptin sensitivity, and tumorigenesis. Cell **2012**;149:1098-111

32. Yumimoto K, Yamauchi Y, Nakayama KI. F-Box Proteins and Cancer. Cancers (Basel) **2020**;12

33. Hunter T. The age of crosstalk: phosphorylation, ubiquitination, and beyond. Mol Cell **2007**;28:730-8

34. Ewing CM, Ray AM, Lange EM, Zuhlke KA, Robbins CM, Tembe WD*, et al.* Germline mutations in HOXB13 and prostate-cancer risk. N Engl J Med **2012**;366:141-9

35. Cardoso M, Maia S, Paulo P, Teixeira MR. Oncogenic mechanisms of HOXB13 missense mutations in prostate carcinogenesis. Oncoscience **2016**;3:288-96

36. Tomlins SA, Laxman B, Dhanasekaran SM, Helgeson BE, Cao X, Morris DS*, et al.* Distinct classes of chromosomal rearrangements create oncogenic ETS gene fusions in prostate cancer. Nature **2007**;448:595-9

37. Varambally S, Yu J, Laxman B, Rhodes DR, Mehra R, Tomlins SA*, et al.* Integrative genomic and proteomic analysis of prostate cancer reveals signatures of metastatic progression. Cancer Cell **2005**;8:393-406

38. VanOpstall C, Perike S, Brechka H, Gillard M, Lamperis S, Zhu B*, et al.* MEIS-mediated suppression of human prostate cancer growth and metastasis through HOXB13-dependent regulation of proteoglycans. Elife **2020**;9

39. Hsu PP, Kang SA, Rameseder J, Zhang Y, Ottina KA, Lim D*, et al.* The mTOR-regulated phosphoproteome reveals a mechanism of mTORC1-mediated inhibition of growth factor signaling. Science **2011**;332:1317-22

40. Gingras AC, Raught B, Gygi SP, Niedzwiecka A, Miron M, Burley SK*, et al.* Hierarchical phosphorylation of the translation inhibitor 4E-BP1. Genes Dev **2001**;15:2852-64

41. Gingras AC, Gygi SP, Raught B, Polakiewicz RD, Abraham RT, Hoekstra MF*, et al.* Regulation of 4E-BP1 phosphorylation: a novel two-step mechanism. Genes Dev **1999**;13:1422-37

42. Qin X, Jiang B, Zhang Y. 4E-BP1, a multifactor regulated multifunctional protein. Cell Cycle **2016**;15:781-6

43. Lonard DM, Nawaz Z, Smith CL, O'Malley BW. The 26S proteasome is required for estrogen receptor-a and coactivator turnover and for efficient estrogen receptor-a transactivation. Mol Cell **2000**;5:939-48

44. Wang X, Arceci A, Bird K, Mills CA, Choudhury R, Kernan JL*, et al.* VprBP/DCAF1 Regulates the Degradation and Nonproteolytic Activation of the Cell Cycle Transcription Factor FoxM1. Mol Cell Biol **2017**;37

45. Kim SY, Herbst A, Tworkowski KA, Salghetti SE, Tansey WP. Skp2 regulates Myc protein stability and activity. Mol Cell **2003**;11:1177-88

46. von der Lehr N, Johansson S, Wu S, Bahram F, Castell A, Cetinkaya C*, et al.* The F-box protein Skp2 participates in c-Myc proteosomal degradation and acts as a cofactor for c-Myc-regulated transcription. Mol Cell **2003**;11:1189-200

47. Taylor BS, Schultz N, Hieronymus H, Gopalan A, Xiao Y, Carver BS*, et al.* Integrative genomic profiling of human prostate cancer. Cancer Cell **2010**;18:11-22

48. Grasso CS, Wu YM, Robinson DR, Cao X, Dhanasekaran SM, Khan AP*, et al.* The mutational landscape of lethal castration-resistant prostate cancer. Nature **2012**;487:239-43

49. Kumar A, Coleman I, Morrissey C, Zhang X, True LD, Gulati R*, et al.* Substantial interindividual and limited intraindividual genomic diversity among tumors from men with metastatic prostate cancer. Nat Med **2016**;22:369-78

50. Chen EY, Tan CM, Kou Y, Duan Q, Wang Z, Meirelles GV*, et al.* Enrichr: interactive and collaborative HTML5 gene list enrichment analysis tool. BMC Bioinformatics **2013**;14:128

51. de Hoon MJ, Imoto S, Nolan J, Miyano S. Open source clustering software. Bioinformatics **2004**;20:1453-4

Figure Legends

Figure 1.

mTOR negatively regulates HOXB13 protein stability. **A,** Time course treatment of LNCaP and PC3 cells with mTOR inhibitor Torin 1 (100nM). **B,** Detection of HOXB13 protein levels in LNCaP and PC3 cells with mTOR knockdown using two inducible shRNAs (induced by 1ug/ml Doxycycline for 3 days). **C,** Assessment of HOXB13 protein levels in LNCaP cells that were androgen deprived for 48h prior to treatment with the synthetic androgen R1881 (10nM) and/or Torin1 (100nM) for another 24h. **D,** HOXB13 immunoblot analysis in LNCaP cells with genetic overexpression of mTOR upstream activator Rheb ± pharmacological inhibition of mTOR with Torin 1 (250nM, 6h). **E,** Effect of shRNA-mediated knockdown of mTOR upstream inhibitors TSC2 and TSC1 on HOXB13 expression in LNCaP cells. **F,** HOXB13 polyubiquitination was examined in response to mTOR inhibitor Torin1 (100nM) for 24h in LNCaP cells. **G,** HOXB13 polyubiquitination following inducible shRNA-mediated mTOR knockdown (1ug/ml Dox, 3 days) in LNCaP cells.

See also **Supplementary Figure 1**.

Figure 2.

mTOR physically interacts with HOXB13. **A,** mTOR co-IP with exogenously expressed HOXB13 in 293T cells. **B,** Co-IPs showing endogenous interaction between mTOR and HOXB13 in LNCaP cells ±10nM R1881 for 48h. **C,** Specific mTORC1 (Raptor) and mTORC2 (Rictor) components interact with HOXB13 in LNCaP cells ± 10nM R1881 for 48h by co-IP. **D,** GST-HOXB13 protein purified from bacteria BL21 was used to pull-down mTOR from 293T whole cell lysates.

E, HOXB13 N-terminal domain (NTD) interacts with mTOR in 293T cells. **F,** mTOR C-terminal kinase domain interacts with HOXB13 in 293T cells. HOXB13 also interacted with mTOR Middle domain but to a lesser extent. **G,** Schematic illustrating mTOR and HOXB13 interacting domains.

Figure 3.

mTOR directly phosphorylates HOXB13. **A,** mTOR *in vitro* kinase assay with GST-HOXB13 as the substrate. mTOR purified from Hela cells treated with insulin showed higher kinase activity, an effect abolished by co-treatment with mTOR inhibitor Torin 1. **B,** Mass spectrometry analysis of phosphorylated HOXB13 in (**A**) identified two HOXB13 phosphorylation sites (T8 and T41) with high probability. MIS, Mascot ion score. **C,** Alanine mutation of HOXB13 on T8 and T41 disabled its mTOR-mediated phosphorylation *in vitro*. **D,** HOXB13 phosphorylation mimics T8D, T41D and T8D+T41D (plasmid) were transfected and stably expressed in LNCaP cells. Whole cell lysates were extracted for immunoblotting and one additional upper band was observed. **E,** HOXB13 phosphorylation mimics T8D, T41D and T8D+T41D (plasmid) were transfected and transiently expressed in 293T cells. After extracting the whole cell lysates, V5 tag immunoprecipitation was used to pull down these HOXB13 mutants and Lambda phosphatase was used to digest the immunoprecipitates directly in the tubes for 30 minutes. Immunoblots showed that the upper band completely disappeared after brief phosphatase treatment, implicating the upper band was another phosphorylation band triggered by T8 or T41 phosphorylation. **F,** Serine (S) residues at sites 250/254 or sites 31/35 were mutated to Alanine (A) or Aspartic Acid (D) in HOXB13 T8D+T41D phosphomimic mutant. **G,** Single Alanine mutation was introduced to Serine 31 or Serine 35 of HOXB13 T8D+T41D phosphomimic mutant. **H,** Alanine mutation of T41 and T8 was introduced to HOXB13 phosphomimic T8D and T41D, respectively. **I,**

Immunoblots showing one additional band from V5-tagged HOXB13 immunoprecipitates of WT but not the 3A phospho-deficient mutant. Lambda phosphatase was used to confirm the upper band was a phosphorylation band. **J,** Schematic of HOXB13 phosphorylation primed by mTOR.

See also **Supplementary Figure 2**.

Figure 4.

HOXB13 phosphorylation promotes its degradation by SKP2. **A,** Protein synthesis inhibitor Cycloheximide was used to evaluate the protein stability of HOXB13 WT, phospho-deficient mutant (3A) and phospho-mimicking mutant (3D). **B,** Polyubiquitination of HOXB13 mutants were examined using 293T whole cell lysates. **C,** Exogenous HOXB13 interacted with E3 ligase SKP2 in 293T cells. **D,** HOXB13 and E3 ligase SKP2 interact endogenously in LNCaP cells ± 10nM R1881 for 24h. **E,** SKP2 overexpression decreased HOXB13 protein levels which were rescued by proteasome inhibitor MG132 (20uM, 6h) in LNCaP cells. **F,** Genetic knockdown of SKP2 increased HOXB13 protein levels in LNCaP cells. **G,** Inducible shRNA-mediated knockdown (1ug/ml Dox, 3 days) of mTOR decreased HOXB13 interaction with SKP2 in LNCaP cells. **H,** Pharmacological inhibition (100nM Torin1, 24h) of mTOR impaired HOXB13 interaction with SKP2 in LNCaP cells. **I,** HOXB13 phosphomimic mutant 3D interacted more strongly with SKP2 in 293T cells compared to WT or phospho-deficient mutant 3A. **J,** Diminished HOXB13 protein levels provoked by SKP2 overexpression was rescued by Torin1 treatment (250nM, 6h) in LNCaP cells. **K,** Schematic of mTOR primed and SKP2 licensed HOXB13 degradation.

See also **Supplementary Figure 3**.

Figure 5.

HOXB13 phosphorylation regulates its target genes transcription. **A,** Heatmaps showing 354 DEGs ($p < 0.05$, $|Log2FC| > 0.5$) specifically altered by HOXB13 WT rescue in HOXB13 KD LNCaP cells under vehicle (EtOH) and/or R1881 24h conditions compared to empty vector (EV) with levels also contrasting significantly compared to rescue with the phospho-deficient HOXB13 3A mutant. Heatmaps represent z-scaled Log2(FPKM+1) values. Pie chart showing the subset of up- (200) and down-regulated (154) DEGs dependent on phospho-HOXB13. **B,** Significantly enriched MSigDB Hallmark terms ($p < 0.05$) among the 354 DEGs identified in (**A**) with the number of associated up- and down-regulated genes indicated. **C,** Heatmaps showing 3812 DEGs ($p < 0.05$, $|Log2FC| > 0.5$) significantly altered by mTOR rescue in mTOR KD LNCaP cells under vehicle (EtOH) and/or R1881 24h conditions relative to empty vector (EV). Heatmaps represent z-scaled Log2(FPKM+1) values. Pie chart showing the subset of up- (2108) and down-regulated (1704) mTOR-dependent DEGs. **D,** Cross-examination of phospho-HOXB13- (**A**) and mTOR-dependent (**C**) gene signatures ± R1881 revealed a set of 106 commonly regulated genes, representing ~30% of phospho-HOXB13-dependent DEGs. **E,** RT-qPCR analysis of phospho-HOXB13 and mTOR co-regulated genes in HOXB13 KD LNCaP cells rescued with HOXB13 WT or mutants ± 10nM R1881 for 24h. Statistical significance was calculated by comparing HOXB13 mutants to empty vector (EV) in vehicle (EtOH) or R1881 conditions. **F,** RT-qPCR analysis of phospho-HOXB13 and mTOR co-regulated genes in mTOR KD LNCaP cells rescued with mTOR ± 10nM R1881 for 24h. Statistical significance was calculated by comparing mTOR rescue to empty vector (EV) in vehicle (EtOH) or R1881 conditions. **G,** RT-qPCR examination of LNCaP cells treated with mTOR inhibitor Torin 1 (100nM) or Rapamycin (40nM) for 24h on the

expression of phospho-HOXB13 and mTOR co-regulated genes. Statistical significance was calculated by comparing Torin 1/Rapamycin to DMSO in either vehicle (EtOH) or R1881 conditions. Data in E-G represent means ± SEM of four independent experiments. Statistics was calculated by one-way ANOVA test. *, $p < 0.05$. **, $p < 0.01$. ns, not significant.

See also **Supplementary Figure 4**.

Figure 6.

HOXB13 phosphorylation promotes its oncogenic function. **A,** HOXB13 KD LNCaP cells were rescued by either empty vector (EV), WT-HOXB13, 3A-HOXB13, 3D-HOXB13, or G84E-HOXB13. Both knockdown and overexpression were simultaneously induced by 1ug/ml Doxycycline for 3 days. **B,** Colony formation assay was performed using stable LNCaP cells in (A) for ~3 weeks. **C,** Incucyte cell proliferation assay was performed using HOXB13 KD LNCaP cells rescued with different HOXB13 mutants. Statistical significance was calculated by comparing HOXB13 mutants with empty vector (EV) at 144h (n=6 replicates). **D,** Xenograft tumor growth assay was performed using HOXB13 KD LNCaP cells rescued with either WT HOXB13 or different HOXB13 mutants. Immuno-deficient NSG mice were given 2mg/ml Doxycycline water. Statistical significance was calculated by comparing HOXB13 mutants with empty vector (EV) at day 43 from six biological replicates from each group. **E,** Image of end-point xenograft tumors from (**D**). **F,** Quantification of tumor weight from (**E**). **G,** Unsupervised hierarchical clustering analysis with the 354 phospho-HOXB13-dependent gene signature as defined in Figure 5A was first tested on the Tomlins et al. cohort (GSE6099), resulting in 127 mapped genes capable of discriminating between normal or peri-tumoral epithelial cells (Normal), localized primary PCa tissues (Primary PCa), and hormone-refractory metastatic PCa (HR Metastatic PCa). The validated

127 gene subset was subsequently used on two independent clinical cohorts Varambally et al. (GSE3325) and Poisson et al. (GSE8511) also capable of distinguishing between normal benign prostate tissues, localized primary PCa tissues and metastatic PCa tissues. Data in C, D, and F represent means ± SEM. Statistics was calculated by one-way ANOVA test. *, $p < 0.05$. **, $p < 0.01$. ns, not significant.

Supplemental Information

Supplementary Tables 1-4 (excel files)

Supplementary Figures 1-5

Supplementary Table 1. RNA-seq analysis of LNCaP HOXB13 KD cells rescued with either empty vector (EV), HOXB13 WT or phospho-deficient mutant 3A ± R1881 for 24h.

Supplementary Table 2. RNA-seq analysis of LNCaP mTOR KD cells rescued with either empty vector (EV) or mTOR ± R1881 for 24h.

Supplementary Table 3. List of reagents, plasmids, antibodies, and human RT-qPCR primers used in this study.

Supplementary Table 4. Source data.

Supplementary Figure Legends

Supplementary Figure 1.

mTOR negatively regulates HOXB13 protein stability. **A,** Immunoblot analysis of HOXB13 expression in LNCaP, 22RV1, and PC3 cells following treatment with mTOR inhibitors Torin 1 (100nM) and Rapamycin (Rapa, 40nM) for 24h. HOXB13 protein level was obviously changed only in LNCaP and PC3 cells, therefore both cell lines were kept using for the following study. H.E., high exposure; L.E., low exposure. **B,** RT-qPCR quantification of *HOXB13* mRNA levels in response to 10nM R1881 and/or 100nM Torin 1 treatment for 24h in LNCaP cells from four independent experiments. **C,** PC3 cells were serum-starved for 24h and then stimulated by 10% serum ± 100nM Torin 1 for another 24h. **D,** HOXB13 immunoblot analysis in PC3 cells with genetic overexpression of mTOR upstream activator Rheb ± pharmacological inhibition of mTOR with Torin 1 (250nM, 6h). **E,** Effect of shRNA-mediated knockdown of mTOR upstream inhibitors TSC2 and TSC1 on HOXB13 expression in PC3 cells. **F,** Two independent shRNAs were used to knockdown Raptor or Rictor in LNCaP or PC3 cells. **G,** Detection of HOXB13 protein levels in LNCaP and PC3 cells with stable knockdown of Raptor and Rictor, components of mTORC1 and mTORC2, respectively. LNCaP cells were androgen deprived for 48h and then treated with 10nM R1881 for another 24h. PC3 cells were serum-starved for 24h and then stimulated with 10% serum for another 24h. Data in B represent means ± SEM. Statistics was calculated by one-way ANOVA test. *, $p < 0.05$. ns, not significant.

See also **Figure 1**.

Supplementary Figure 2.

HOXB13 additional phosphorylation at S31 is still dependent on mTOR activity. **A,** Single Alanine mutation was introduced to S31 or S35 of HOXB13 phosphomimic T8D or T41D mutant. **B,** 293T cells expressing different HOXB13 phosphomimics were treated with Torin1 (250nM) for 1h. **C,** Effect of shRNA-mediated mTOR knockdown in 293T cells on the expression of different HOXB13 phosphomimics. **D,** Effect of shRNA-mediated Raptor knockdown in 293T cells on the expression of different HOXB13 phosphomimics. **E,** Effect of shRNA-mediated Rictor knockdown in 293T cells on the expression of different HOXB13 phosphomimics.

See also **Figure 2**.

Supplementary Figure 3.

SKP2 is an E3 ligase for HOXB13. **A,** HOXB13 WT, 3A and 3D were induced in LNCaP cells in a doxycycline (Dox) inducible manner for 3 days and then Dox was deprived for the indicated times. **B,** Top 3 predicted HOXB13-targeting E3 ligases by Ubibroswer[1.0]. **C,** Endogenous HOXB13 interacts with SKP2 in PC3 cells. *, indicates IgG heavy chain. **D,** SKP2 overexpression increases HOXB13 polyubiquitination in LNCaP cells. **E,** SKP2 overexpression decreases HOXB13 protein levels, an effect rescued by MG132 (20uM, 6h) in PC3 cells. **F,** SKP2 overexpression decreases HOXB13 stability in LNCaP cells. **G,** Genetic knockdown of SKP2 increases HOXB13 protein levels in PC3 cells. **H,** Treatment of LNCaP cells with 20μM of SKP2 inhibitor SZL P1-41 increases HOXB13 protein levels. **I,** Treatment of PC3 cells with 20μM of SKP2 inhibitor SZL P1-41 increases HOXB13 protein levels.

See also **Figure 4**.

Supplementary Figure 4.

Androgen response dependency on HOXB13 phosphorylation. **A,** RT-qPCR analysis of *NFKBIA* in HOXB13 KD LNCaP cells rescued with HOXB13 WT or mutants ± 10nM R1881 for 24h. Statistical significance was calculated by comparing HOXB13 mutants to empty vector (EV) in vehicle (EtOH) or R1881 conditions. **B,** Effect of mTOR inhibitor Torin 1 (100nM) or Rapamycin (40nM) for 24h on the expression of *NFKBIA* in LNCaP cells. Statistical significance was calculated by comparing Torin 1/Rapamycin with DMSO in either vehicle (EtOH) or R1881 conditions. **C,** HOXB13 phosphorylation promotes NF-κB (p65 and p50) nuclear translocation in the presence of R1881 (24h). **D,** Immunoblot analysis of mTOR rescue in mTOR KD LNCaP cells. **E,** Heatmaps showing the shared set of 106 DEGs ($p < 0.05$, $|Log2FC| > 0.5$) identified in Figure 5D found commonly and consistently regulated by phospho-HOXB13 and mTOR cells under vehicle (EtOH) and/or R1881 conditions. Heatmaps represent z-scaled Log2(FPKM+1) values. **F,** RT-qPCR analysis of *KLK3*, *FASN*, and *SREBF2* in LNCaP cells with shRNA-mediated HOXB13 knockdown and rescued with HOXB13 WT or mutants ± 10nM R1881 for 24h. Statistical significance was calculated by comparing HOXB13 mutants to empty vector (EV) in vehicle (EtOH) or R1881 conditions. Data in A, B, and F represent means ± SEM from four independent experiments. Statistics was calculated by one-way ANOVA test. *, $p < 0.05$. **, $p < 0.01$. ns, not significant.

See also **Figure 5**.

Figure 1

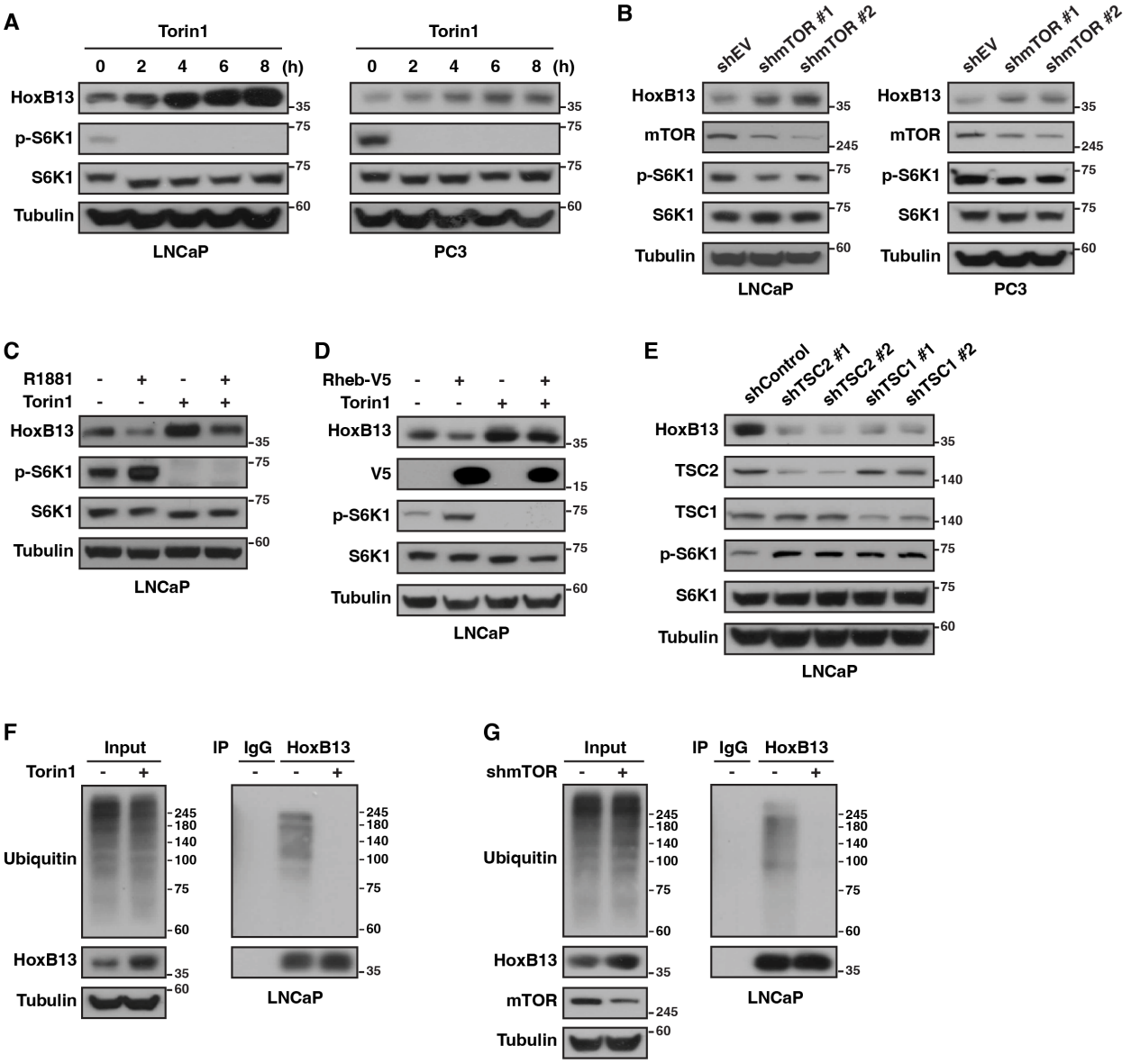
A
Torin1
0 2 4 6 8 (h)
HoxB13
p-S6K1
S6K1
Tubulin
LNCaP
PC3
B
shEV
shmTOR #1
shmTOR #2
HoxB13
mTOR
p-S6K1
S6K1
Tubulin
LNCaP
PC3
C
R1881
Torin1
HoxB13
p-S6K1
S6K1
Tubulin
LNCaP
D
Rheb-V5
Torin1
HoxB13
V5
p-S6K1
S6K1
Tubulin
LNCaP
E
shControl
shTSC2 #1
shTSC2 #2
shTSC1 #1
shTSC1 #2
HoxB13
TSC2
TSC1
p-S6K1
S6K1
Tubulin
LNCaP
F
Input
IP IgG HoxB13
Torin1
Ubiquitin
HoxB13
Tubulin
LNCaP
G
Input
IP IgG HoxB13
shmTOR
Ubiquitin
HoxB13
mTOR
Tubulin
LNCaP

Figure 2

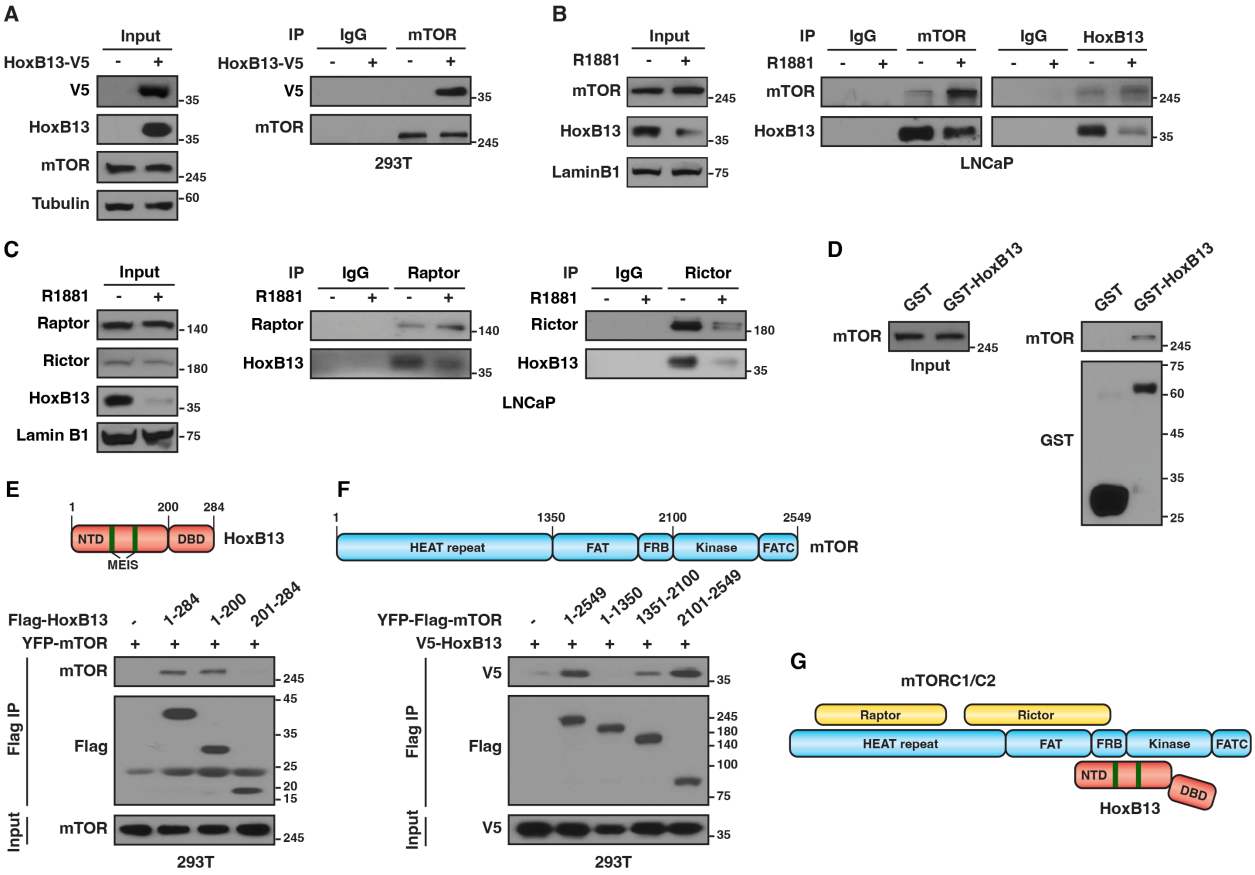
A
Input
IP
IgG
mTOR
HoxB13-V5
V5
HoxB13
mTOR
Tubulin
293T
B
Input
IP
IgG
mTOR
IgG
HoxB13
R1881
LaminB1
LNCaP
C
Input
IP
IgG
Raptor
IgG
Rictor
R1881
Raptor
Rictor
HoxB13
Lamin B1
LNCaP
D
GST
GST-HoxB13
mTOR
Input
GST
E
NTD
DBD
MEIS
HoxB13
Flag-HoxB13
YFP-mTOR
1-284
1-200
201-284
Flag IP
Input
Flag
F
HEAT repeat
FAT
FRB
Kinase
FATC
mTOR
YFP-Flag-mTOR
V5-HoxB13
1-2549
1-1350
1351-2100
2101-2549
G
mTORC1/C2
Raptor
Rictor
HEAT repeat
FAT
FRB
Kinase
FATC
NTD
DBD
HoxB13

Figure 3

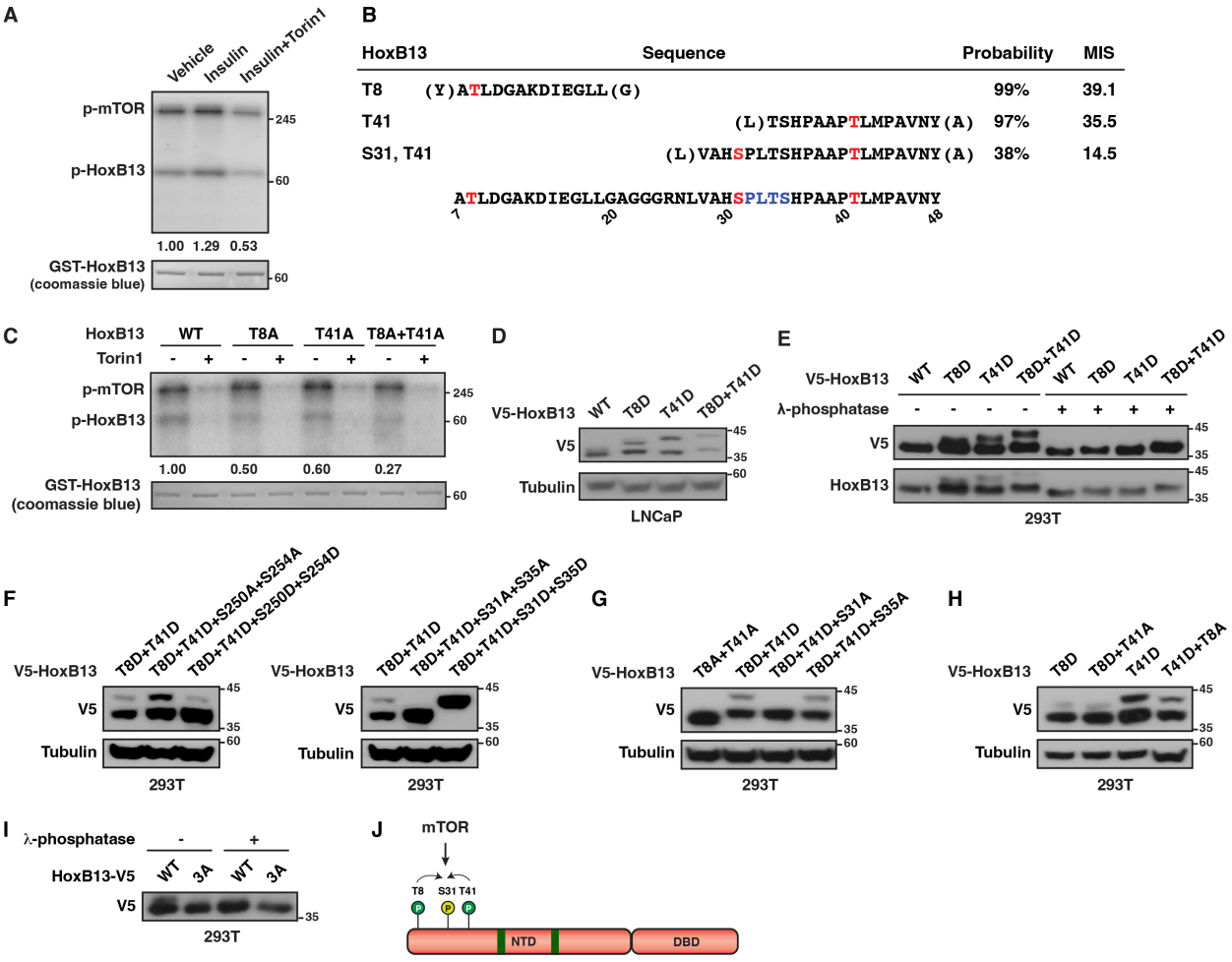
A
Vehicle
Insulin
Insulin+Torin1
p-mTOR
p-HoxB13
245
60
1.00 1.29 0.53
GST-HoxB13
(coomassie blue)
60
B
HoxB13 Sequence Probability MIS
T8 (Y)ATLDGAKDIEGLL(G) 99% 39.1
T41 (L)TSHPAAPTLMPAVNY(A) 97% 35.5
S31, T41 (L)VAHSPLTSHPAAPTLMPAVNY(A) 38% 14.5
ATLDGAKDIEGLLGAGGGRNLVAHSPLTSHPAAPTLMPAVNY
7 20 30 40 48
C
HoxB13 WT T8A T41A T8A+T41A
Torin1 - + - + - + - +
p-mTOR
p-HoxB13
245
60
1.00 0.50 0.60 0.27
GST-HoxB13
(coomassie blue)
60
D
V5-HoxB13 WT T8D T41D T8D+T41D
V5
Tubulin
45
35
60
LNCaP
E
V5-HoxB13 WT T8D T41D T8D+T41D WT T8D T41D T8D+T41D
λ-phosphatase - - - - + + + +
V5
HoxB13
45
35
293T
F
V5-HoxB13 T8D+T41D T8D+T41D+S250A+S254A T8D+T41D+S250D+S254D
V5
Tubulin
45
35
60
293T
V5-HoxB13 T8D+T41D T8D+T41D+S31A+S35A T8D+T41D+S31D+S35D
V5
Tubulin
293T
G
V5-HoxB13 T8A+T41A T8D+T41D T8D+T41D+S31A T8D+T41D+S35A
V5
Tubulin
293T
H
V5-HoxB13 T8D T8D+T41A T41D T41D+T8A
V5
Tubulin
293T
I
λ-phosphatase - +
HoxB13-V5 WT 3A WT 3A
V5
35
293T
J
mTOR
T8 S31 T41
P
NTD
DBD

Figure 4

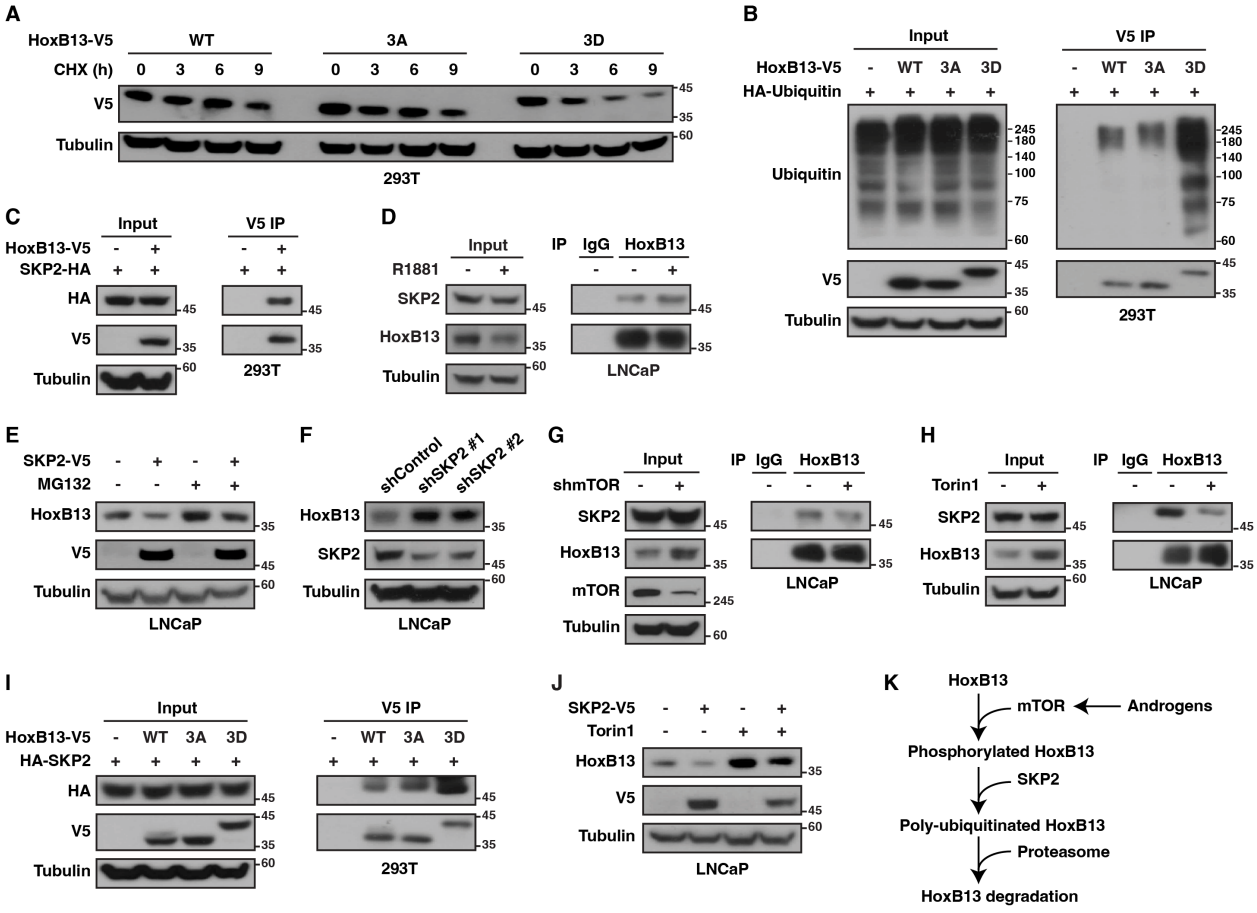
A
HoxB13-V5
WT
3A
3D
CHX (h)
0 3 6 9 0 3 6 9 0 3 6 9
V5
Tubulin
293T
B
Input
V5 IP
HoxB13-V5
HA-Ubiquitin
Ubiquitin
V5
Tubulin
293T
C
Input
V5 IP
HoxB13-V5
SKP2-HA
HA
V5
Tubulin
293T
D
Input
IP IgG HoxB13
R1881
SKP2
HoxB13
Tubulin
LNCaP
E
SKP2-V5
MG132
HoxB13
V5
Tubulin
LNCaP
F
shControl
shSKP2 #1
shSKP2 #2
HoxB13
SKP2
Tubulin
LNCaP
G
Input
IP IgG HoxB13
shmTOR
SKP2
HoxB13
mTOR
Tubulin
LNCaP
H
Input
IP IgG HoxB13
Torin1
SKP2
HoxB13
Tubulin
LNCaP
I
Input
V5 IP
HoxB13-V5
HA-SKP2
HA
V5
Tubulin
293T
J
SKP2-V5
Torin1
HoxB13
V5
Tubulin
LNCaP
K
HoxB13
mTOR
Androgens
Phosphorylated HoxB13
SKP2
Poly-ubiquitinated HoxB13
Proteasome
HoxB13 degradation

Figure 5

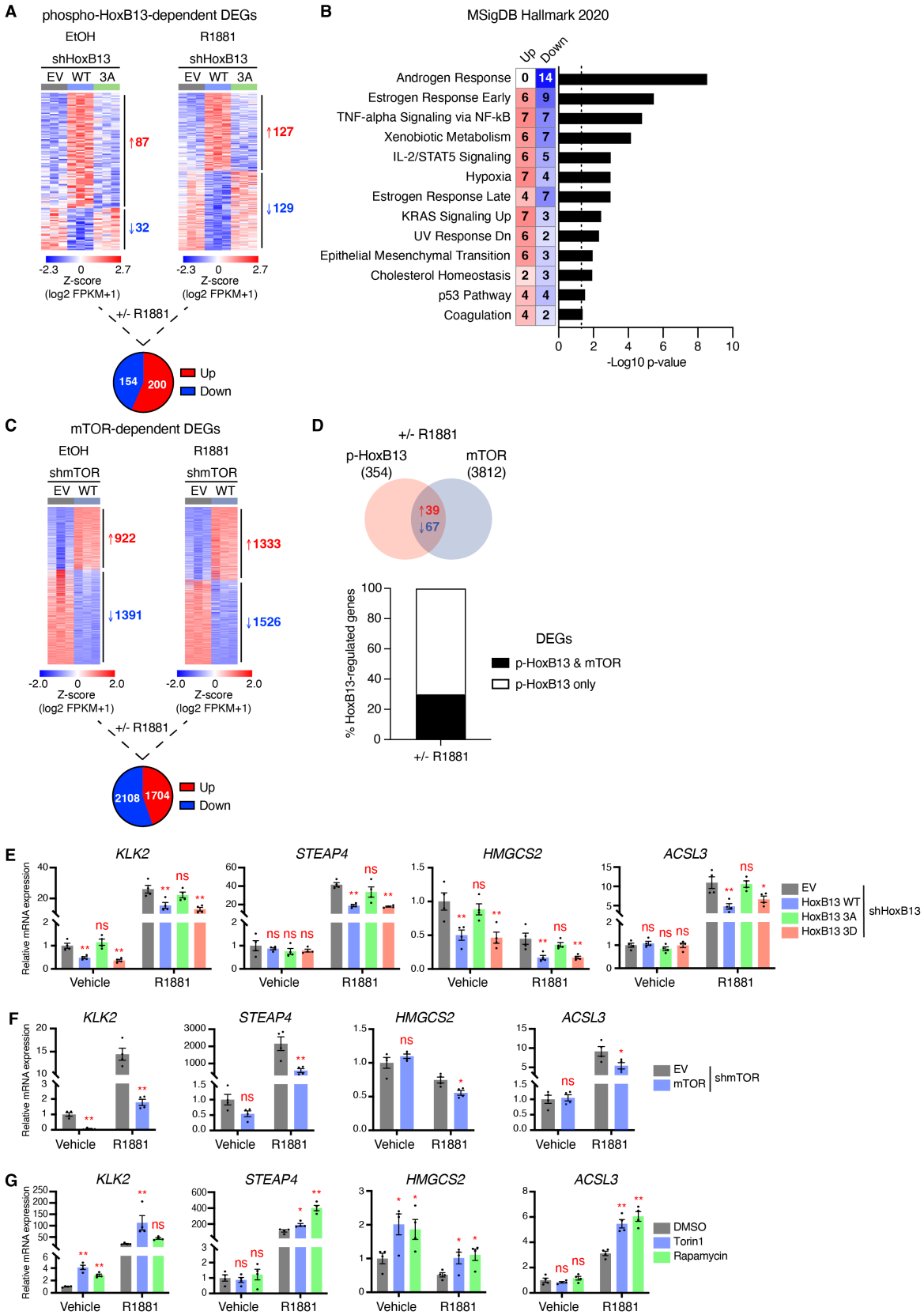
A
phospho-HoxB13-dependent DEGs
EtOH
R1881
shHoxB13
EV WT 3A
↑87
↓32
↑127
↓129
-2.3 0 2.7
Z-score
(log2 FPKM+1)
+/- R1881
154
200
Up
Down
B
MSigDB Hallmark 2020
Up Down
Androgen Response 0 14
Estrogen Response Early 6 9
TNF-alpha Signaling via NF-kB 7 7
Xenobiotic Metabolism 6 7
IL-2/STAT5 Signaling 6 5
Hypoxia 7 4
Estrogen Response Late 4 7
KRAS Signaling Up 7 3
UV Response Dn 6 2
Epithelial Mesenchymal Transition 6 3
Cholesterol Homeostasis 2 3
p53 Pathway 4 4
Coagulation 4 2
0 2 4 6 8 10
-Log10 p-value
C
mTOR-dependent DEGs
EtOH
R1881
shmTOR
EV WT
↑922
↓1391
↑1333
↓1526
-2.0 0 2.0
Z-score
(log2 FPKM+1)
+/- R1881
2108
1704
Up
Down
D
+/- R1881
p-HoxB13
(354)
mTOR
(3812)
↑39
↓67
% HoxB13-regulated genes
DEGs
p-HoxB13 & mTOR
p-HoxB13 only
+/- R1881
E
KLK2
STEAP4
HMGCS2
ACSL3
Relative mRNA expression
Vehicle
R1881
EV
HoxB13 WT
HoxB13 3A
HoxB13 3D
shHoxB13
F
KLK2
STEAP4
HMGCS2
ACSL3
Relative mRNA expression
Vehicle
R1881
EV
mTOR
shmTOR
G
KLK2
STEAP4
HMGCS2
ACSL3
Relative mRNA expression
Vehicle
R1881
DMSO
Torin1
Rapamycin

Figure 6

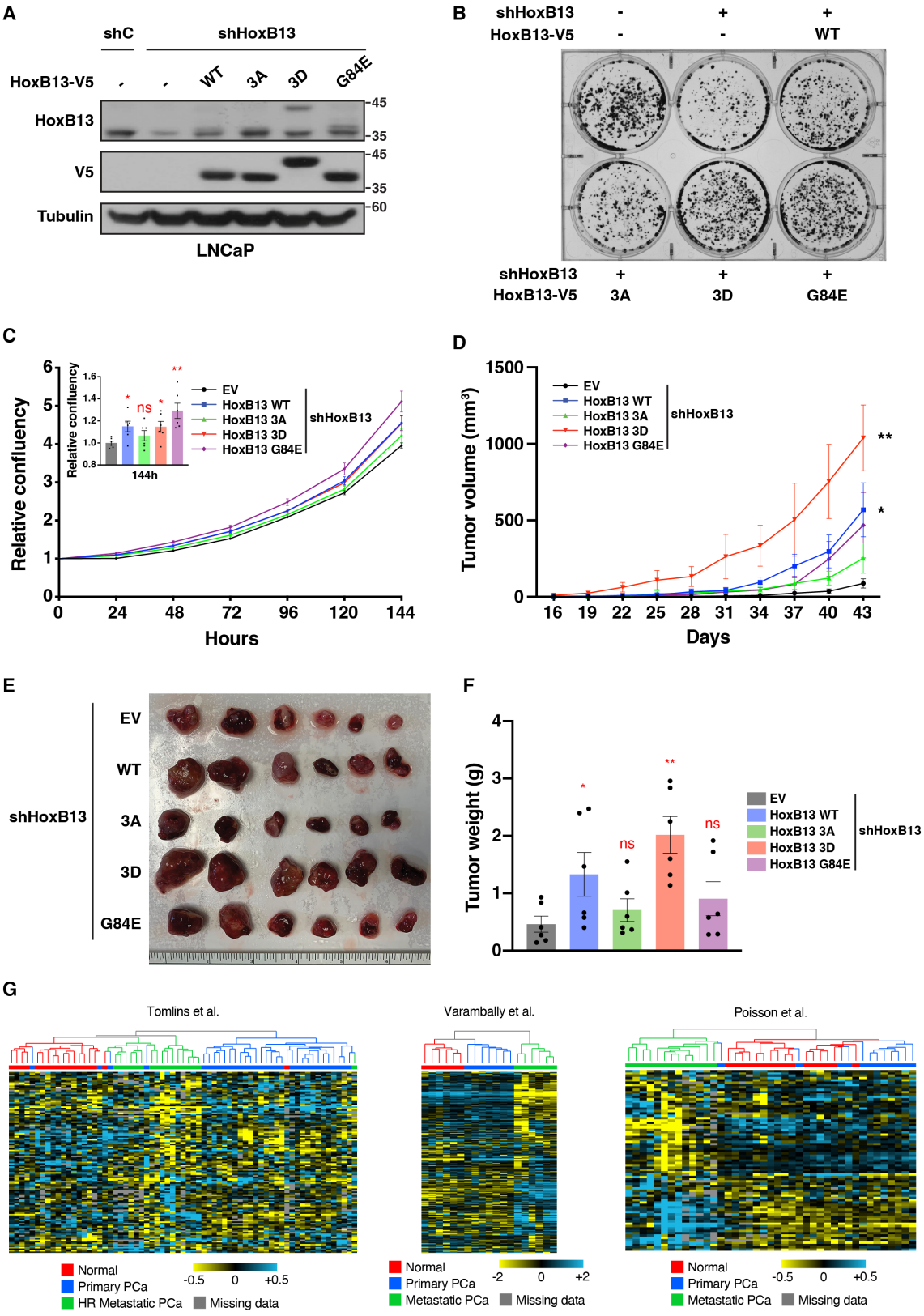
A
shC
shHoxB13
HoxB13-V5
WT
3A
3D
G84E
HoxB13
V5
Tubulin
45
35
60
LNCaP
B
shHoxB13
HoxB13-V5
WT
3A
3D
G84E
C
Relative confluency
Hours
144h
EV
HoxB13 WT
HoxB13 3A
HoxB13 3D
HoxB13 G84E
shHoxB13
ns
D
Tumor volume (mm³)
Days
E
shHoxB13
EV
WT
3A
3D
G84E
F
Tumor weight (g)
G
Tomlins et al.
Varambally et al.
Poisson et al.
Normal
Primary PCa
HR Metastatic PCa
Metastatic PCa
Missing data

Supplementary Figure 1

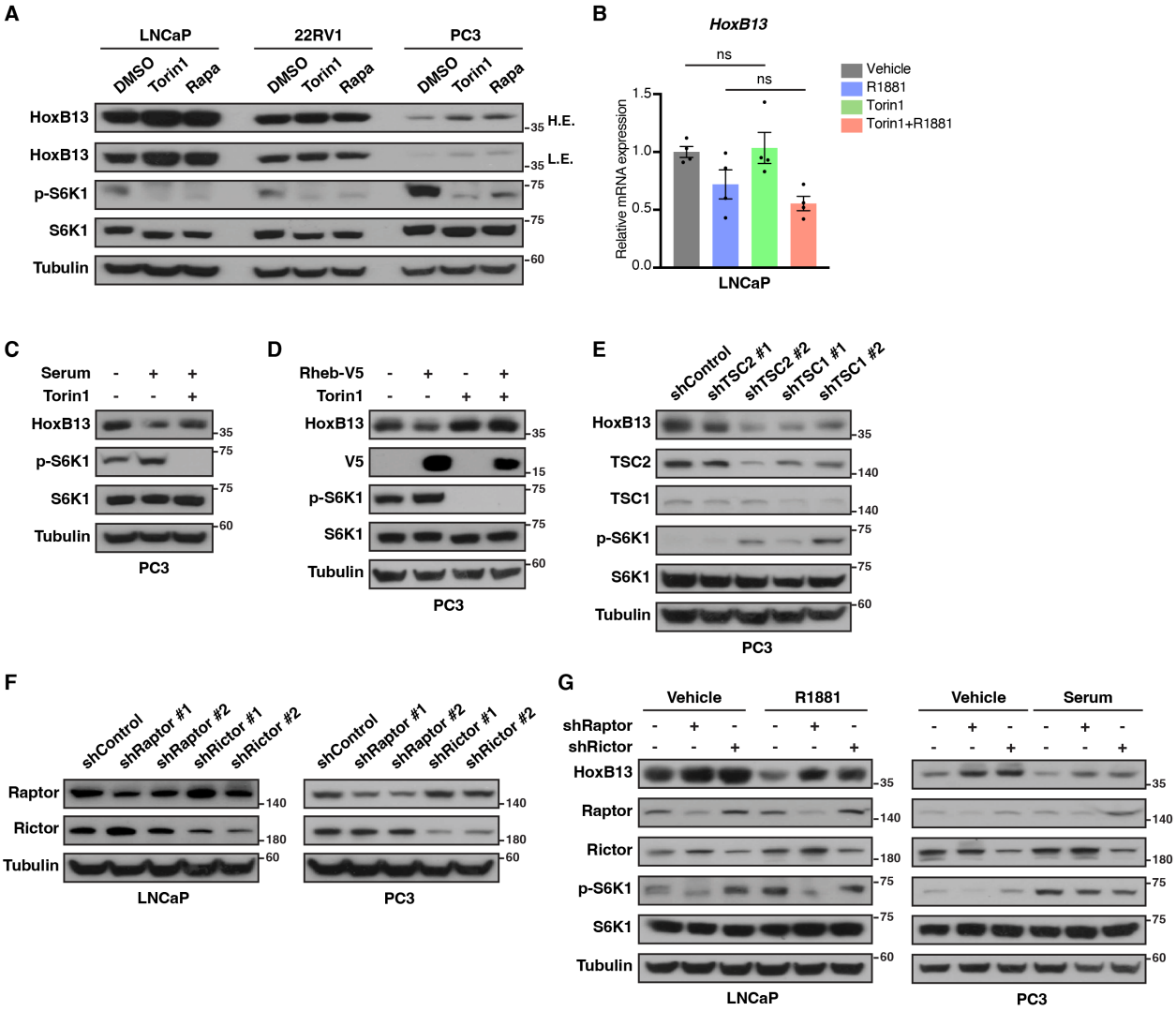

Supplementary Figure 2

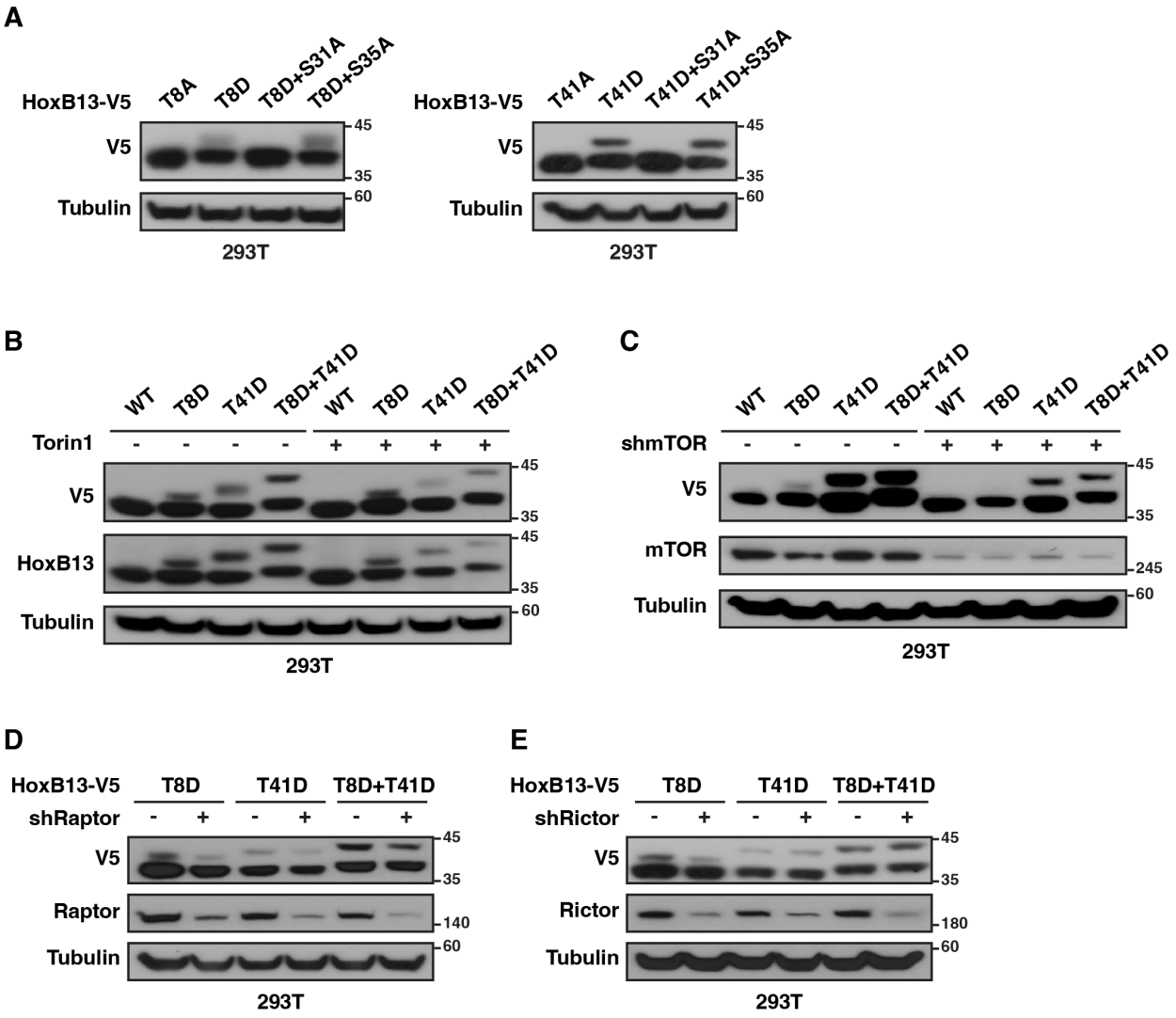

Supplementary Figure 3

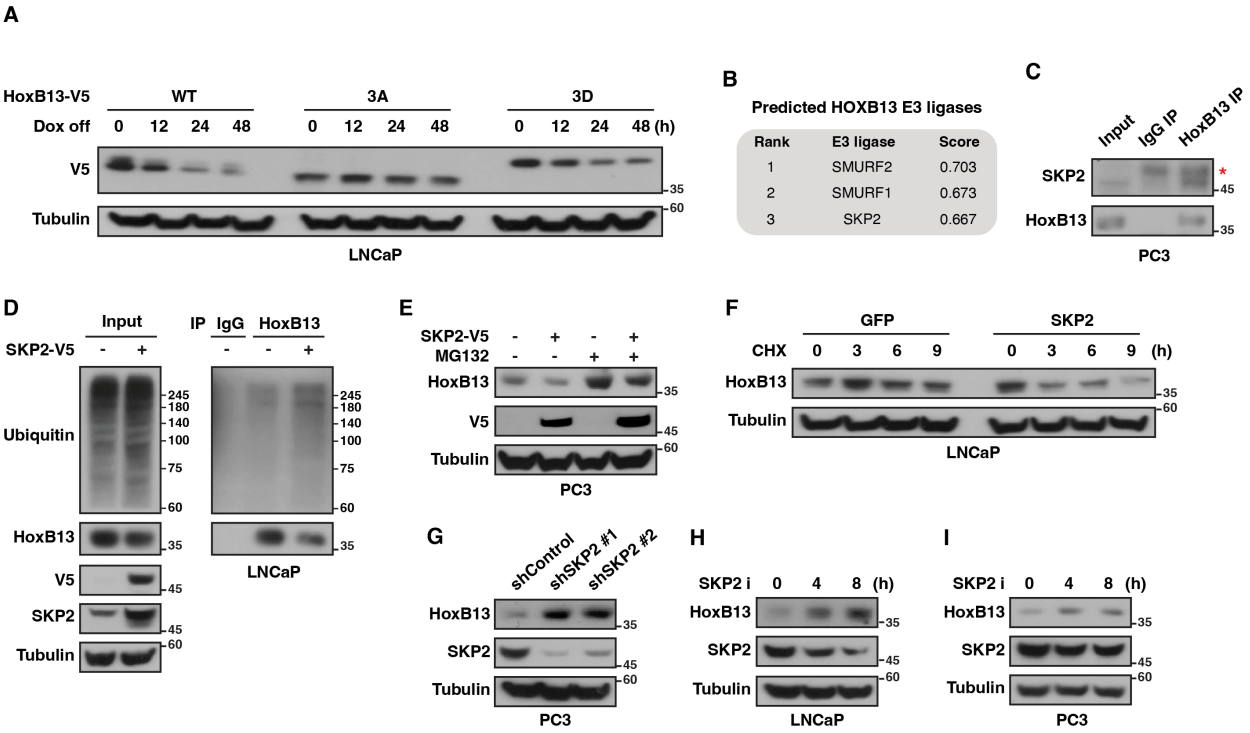

Supplementary Figure 4

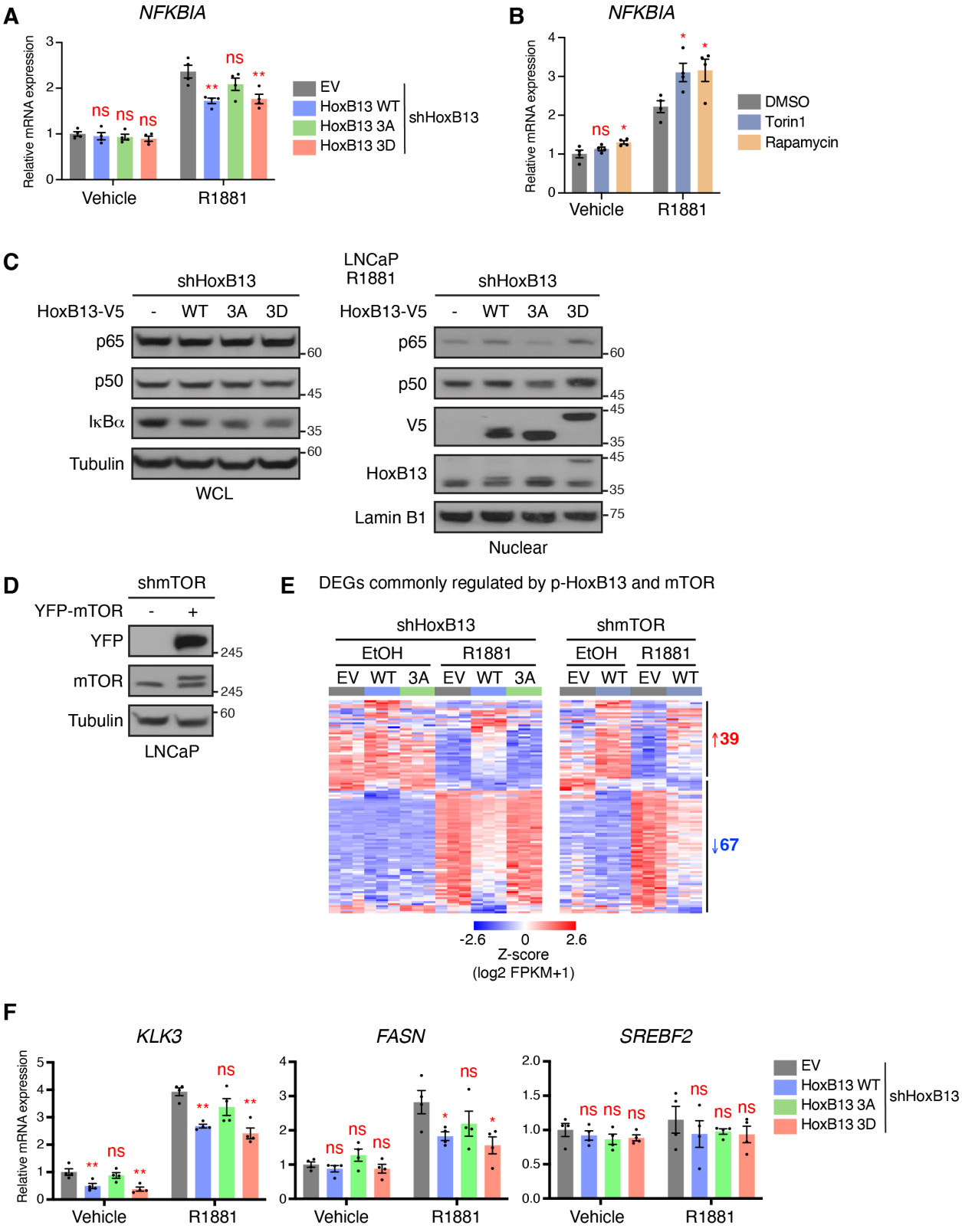

Bridge between Chapter 2 and Chapter 3

It is now known that mTOR can regulate gene transcription in both indirect and direct ways. In Chapter 2, I uncover that mTOR phosphorylates the transcription factor HOXB13 to modulate its transcriptional activity and impact HOXB13/AR target genes expression. It is an indirect mechanism for mTOR to control gene transcription, which requires the kinase activity of mTOR. This novel mechanism is similar to the action of mTOR phosphorylating transcription factors in the cytoplasm leading to their translocation to the nucleus in response to the upstream signals.

Furthermore, I am questioning whether there is a closer and more direct mechanism for mTOR to mediate transcriptional regulation. Due to the previous evidence that mTOR can be induced by AR activation to enter the nucleus and nuclear mTOR is proposed to coordinate with AR for controlling energy metabolism transcriptionally, it is reasonable to explore in more details the nuclear functions of mTOR. Therefore, in chapter 3, I attempt to explore the mechanisms by which nuclear mTOR regulates gene transcription. Several important questions, such as what is the identity of nuclear mTOR-dependent target genes and whether some transcriptional functions of nuclear mTOR require its kinase activity, will be investigated in Chapter 3.

The overarching goal of my PhD study is to demonstrate two distinct but not mutually exclusive molecular mechanisms for mTOR to regulate gene transcription. Remarkably, the function of nuclear mTOR that has not been appreciated much before is being studied here, thus enhancing our understanding of mTOR biology.

Chapter 3.

Nuclear mTOR abrogates AR signaling and promotes

AR-independent prostate cancer progression

Yonghong Chen[1,2], Catherine Rosa Dufour[1], Lingwei Han[1,2], and Vincent Giguère[1,2,*]

[1]Goodman Cancer Institute, McGill University, Montreal, Québec, H3A 1A3, Canada.

[2]Department of Biochemistry, Faculty of Medicine, McGill University, Montréal, Québec, H3G 1Y6, Canada.

*Correspondence: vincent.giguere@mcgill.ca

Keywords: Androgen receptor; ChIP-seq; NEPC; nmTOR

Abstract

While nuclear mTOR (nmTOR) expression increases in advanced prostate cancer (PCa), the precise roles played by nmTOR remain elusive. Herein, we establish a biochemical system involving mTOR tagging with a nuclear localization or export signal that dictates mTOR localization to distinguish nmTOR from cytosolic mTOR (cmTOR) function. Transcriptome profiling in androgen receptor (AR) positive PCa cells revealed that nmTOR predominately downregulates androgen response genes independently of its kinase activity, while cmTOR upregulates a cell cycle-related E2F gene signature in a kinase-dependent manner. Co-immunoprecipitation and ChIP-seq analyses further showed that nmTOR suppresses AR signaling in a FOXA1-dependent manner. Furthermore, functional studies identified nmTOR as a promoter of androgen-independent PCa evolution by inducing expression of the neuroendocrine PCa marker ENO2, thus enhancing migration, invasion and proliferation of AR negative PCa cells. This work thus highlights the transcriptional function of nmTOR as an alternative therapeutic target to inhibit androgen independent PCa.

Introduction

Prostate cancer (PCa) is one of the most prevalent cancer types among men. Androgen and its receptor (AR) are critical in PCa development with androgen deprivation therapy (ADT) being the mainstay treatment (1). Initially the treatment works but eventually the disease progresses toward castration resistant PCa (CRPC). It has been reported that AR still remains hyperactive in CRPC by multiple mechanisms such as AR gene amplification, expression of AR splice variants and AR point mutations (2). Second-generation AR antagonists such as enzalutamide can inhibit AR transcriptional activity more efficiently (3), which unfortunately exerts a strong selective pressure leading PCa tumors to become AR-independent (4,5). Disease progression will then involve other oncogenic alterations such as *P53* mutations, *RB* deletion, *PTEN* loss, and *MYC* overexpression, leading PCa cell differentiation toward the neuroendocrine phenotype (NEPC) (1,6-8). In NEPC, targeting AR is no longer an option and thus discovery of novel therapeutic targets is necessary to improve the outcome of this aggressive form of PCa (9).

mTOR (mechanistic target of rapamycin), a serine/threonine kinase belonging to the PI3K related kinase family, is known to control cellular growth by promoting anabolism like protein synthesis, lipid synthesis and nucleotide synthesis, and also by inhibiting catabolism such as autophagy (10). Canonically, mTOR functions as two distinct complexes at different subcellular localizations, mTORC1 and mTORC2 defined by the presence of RAPTOR and RICTOR, respectively (11). mTORC1 is mainly locating on the surface of lysosomes where it is activated by upstream growth factors and amino acids stimulation, while mTORC2 primarily locates on mitochondria associated ER membranes to phosphorylate and activate AKT which positively regulates cell survival and proliferation (12). Still, other sites for mTOR localization have been reported (13,14). Notably, increasing evidences support that mTOR plays a key role in the nucleus

in the regulation of gene transcription (15-23). In PCa cells, nuclear mTOR (nmTOR) has been shown to act as a transcriptional integrator of the androgen signaling pathway in association with the chromatin remodeling machinery and the pioneer transcription factor FOXA1 (24-26). However, the exact contribution of nmTOR activity in the progression of PCa remains to be fully explored.

FOXA1, a critical cofactor of AR activity, has conflicting roles in PCa (27). FOXA1 increases cell proliferation through AR but inhibits cell invasion independently of AR (28,29). Opposing findings reported FOXA1 as an oncogene or tumor suppressor in PCa associated with either high or low levels of FOXA1 in metastatic and CRPC patient tumors (30-33). Also, FOXA1 was shown to inhibit PCa neuroendocrine differentiation (34), but was suggested to be an essential factor for NEPC (35) and potentiate lineage-specific enhancer activation (36). Moreover, FoxA2, as a closely related family member to FOXA1, was reported to drive lineage plasticity in NEPC (37), which may have competing or compensating effects with FOXA1 to regulate NEPC progression. In addition, FOXA1 is highly mutated in PCa, which can alter its pioneer activity and PCa development (38,39). The influence of FOXA1 on nmTOR transcriptional activity has yet to be explored.

Previous reports found that hyperactive PI3K/AKT/mTOR signaling caused by PTEN loss promotes PCa resistance to AR inhibition and that elevated levels of nmTOR are associated with advanced PCa (24,40), denoting that nmTOR may act as a direct nuclear effector of PI3K signaling to drive androgen-independent PCa progression. Here, we established a biochemical tool to study nmTOR function through the introduction of a nuclear localization signal (NLS) tag to mTOR (NLS-mTOR) acting to guide exogenous mTOR to the nucleus. In parallel, we engineered a nuclear export signal (NES)-tagged mTOR (NES-mTOR), allowing us to differentiate between

nmTOR from cytoplasmic mTOR (cmTOR) functions. RNA-seq analysis of androgen-dependent LNCaP cells revealed that cmTOR predominately upregulates E2F target gene expression to drive cell cycle progression while nmTOR has dominant negative impacts on androgen response genes conferring cellular androgen independency in a kinase-independent manner. Upon further investigation, nmTOR was found to require interaction with the pioneer factor FOXA1 to directly inhibit AR activity and transcription of its target genes. Functionally, we demonstrate that nmTOR upregulates the expression of the NEPC marker ENO2 and promotes migration, invasion, and proliferation of AR negative PCa cells, highlighting nmTOR as a potential drug target for AR negative PCa, including NEPC.

Results

An NLS-mTOR tool to study nuclear mTOR function

We have previously shown that androgens induce mTOR translocation into the nucleus of androgen-dependent PCa cells (24,25). To discern specific actions of nmTOR from cmTOR, we first established an inducible system to overexpress distinct mTOR constructs: 1) NES-mTOR as a control for cmTOR function; 2) NLS-mTOR to direct mTOR to the nucleus to study nmTOR function; and 3) NLS-mTOR^{D2357E}, a kinase dead mutant, to discern whether nmTOR function requires its kinase activity (Fig. 1A). Immunoblotting of nuclear extracts from LNCaP cells with inducible overexpression of these mTOR constructs confirmed that NLS-mTOR can robustly translocate into the nucleus compared to WT-mTOR and in a manner independent of its kinase activity (Fig. 1B). NES-mTOR was virtually undetectable in the nuclear lysates (Fig. 1B). Next, we paired this inducible mTOR overexpression system with inducible shRNA-mediated knockdown of mTOR to force LNCaP cells to rely on exogenous mTOR, thus minimizing effects of endogenous mTOR on downstream functional studies. Interestingly, both NES-mTOR and NLS-mTOR were able to activate the canonical mTOR downstream substrate S6K1 denoted by its increased phosphorylation status (Fig. 1C). S6K1 activation by NLS-mTOR was found disabled by the kinase dead mutant (Fig. 1C). As the mTOR constructs harbored a YFP tag, this enabled green fluorescence to visualize their localization directly in live cells. As shown in Fig. 1D, WT-mTOR and NES-mTOR formed green net-like structures around the cellular nucleus while NLS-mTOR and NLS-mTOR^{D2357E} were found highly concentrated in the nucleus appearing as green dot shapes (Fig 1D). These data validate the specific subcellular localization of NLS- and NES-tagged mTOR, supporting their effectiveness in facilitating the delineation of nmTOR and cmTOR functions.

Nuclear mTOR exerts distinct functions from cytosolic mTOR

We next sought to differentiate the actions of nmTOR from cmTOR on the transcriptome. To address this, RNA-seq analyses were performed on LNCaP cells in which endogenous mTOR was knocked down by inducible shRNA and rescued by inducible expression of either NES-mTOR (as cmTOR), NLS-mTOR (as nmTOR) or YFP as the empty vector (EV) control. As androgens significantly promote nmTOR levels, we focused our attention primarily on transcriptional changes in cells exposed to R1881. Our analysis uncovered 1,470 upregulated and 1,411 downregulated genes by cmTOR (NES-mTOR vs EV) and 898 upregulated and 930 downregulated genes by nmTOR (NLS-mTOR vs EV) (Fig. 2A and Supplementary Table 1). Intersection of cmTOR- and nmTOR-dependent differentially expressed genes (DEGs) revealed three gene clusters: NES-mTOR only, NLS-mTOR only and a set of commonly regulated genes (Fig. 2A). Functional enrichment analysis by Enrichr (https://maayanlab.cloud/Enrichr/) found the cell cycle-related E2F target gene signature and the androgen response signature as top mTOR-modulated gene sets (Fig 2A and Supplementary Table 2). While cmTOR was found largely responsible for the upregulation of E2F targets, the downregulation of androgen response signaling was more attributed to nmTOR (Fig. 2A). RT-qPCR experiments validated the transcriptional dependencies of several E2F targets and androgen response genes on cmTOR, nmTOR or both (Fig 2B, C). Consistent with previous reports demonstrating that inhibition of canonical mTOR activity causes cell cycle arrest and cell growth suppression (41), NES-mTOR-mediated upregulation of E2F target expression was found very sensitive to mTOR inhibitors Torin1 and Rapamycin (Supplementary Fig. 1A), indicating that cmTOR requires its kinase activity to control E2F targets transcriptionally. Consistently, NES-mTOR provoked a more pronounced increase in

retinoblastoma protein (RB) phosphorylation in parallel with a decrease in cell cycle inhibitor p27 compared to NLS-mTOR (Fig. 2D), opposite to that observed with Torin1 treatment (Fig. 2E), supporting that cmTOR promotes cell cycle progression in a kinase-dependent manner. In contrast, androgen response genes were downregulated similarly by both NLS-mTOR and its kinase dead mutant NLS-mTOR^{D2357E} (Fig 2C), underscoring a previously unrecognized kinase-independent property of nmTOR to control transcription. In fact, intersection of NLS-mTOR regulated genes with NLS-mTOR^{D2357E} regulated genes determined that about two thirds of nmTOR-regulated genes occur independently of its kinase activity in LNCaP cells (Fig. 2F and Supplementary Table 1). For this reason, androgen response genes (*KRT19*, *KRT8*) under the sole control of NLS-mTOR were found insensitive to mTOR inhibitors (Supplementary Fig. 1B). In contrast, the effect of mTOR inhibition on the expression of androgen response genes (*TMPRSS2*, *CAMKK2*) under the control of both NLS-mTOR and NES-mTOR was unpredictable (Supplementary Fig. 1B), likely dependent on which mTOR fraction, nmTOR or cmTOR, plays a dominant regulatory role. While mTOR inhibitors would anticipatingly result in a decrease in cmTOR activity, its effect on nmTOR action could instead be increased as Torin1 treatment promotes mTOR nuclear accumulation (Supplementary Fig. 1C) (24), whereby the final output would ultimately reflect the cooperation and coordination between nmTOR and cmTOR activities. As summarized in Supplementary Fig. 1D, our data reveal that cmTOR predominantly upregulates E2F target gene expression to promote cell cycle progression, whereas nmTOR mainly downregulates androgen response signaling independently of its kinase activity.

Nuclear mTOR complexes with AR and FOXA1

As mTOR does not harbor a DNA binding domain and consequently no consensus DNA binding motif, it must rely on the interaction and cooperation with other cofactors to control gene transcription. Interrogation of identified NLS-mTOR-dependent DEGs (1,828) by Enrichr revealed several top enriched candidate mTOR transcriptional coregulators (Supplementary Fig. 2A), including AR and FOXA1 in agreement with our previous studies of mTOR ChIP-seq in LNCaP cells and identification of the nmTOR chromatin interactome (24,26). Co-immunoprecipitation (co-IP) assays confirmed that both exogenous and endogenous AR and FOXA1 can interact with mTOR as determined using whole cell extracts from 293T cells and nuclear extracts from LNCaP cells, respectively (Fig. 3A-C). Domain mapping revealed that both AR and FOXA1 interact with the mTOR C-terminal half that includes the kinase domain (Fig. 3D). Conversely, mTOR was found to interact with the AR ligand binding domain (LBD) and FOXA1 DNA binding domain (DBD) (Fig. 3E, F). Intersection of available mTOR, AR, and FOXA1 ChIP-seq binding profiles in LNCaP cells (24,42,43) uncovered thousands of co-occupied loci in the absence of androgens, with androgen stimulation increasing the overlap by 2.5-fold (Supplementary Fig. 2B), thus further supporting the existence of a functional nmTOR-AR-FOXA1 chromatin complex.

Nuclear mTOR cooperates with FOXA1 to impair AR signaling

Given that nmTOR, AR and FOXA1 can interact together, we next investigated the extent to which the pioneer transcription factor FOXA1 participates in nmTOR-mediated transcriptional control, particularly in attenuation of AR signaling. First, ChIP-seq experiments in R1881-treated LNCaP cells revealed a drastic cistromic reprogramming of nmTOR upon shRNA-mediated knockdown

of FOXA1 (Fig. 4A and Supplementary Table 3). FOXA1 deficiency resulted in a gain of mTOR binding at >20,000 new sites and a concomitant loss of mTOR binding at ~10,000 regions, representing 65% of the total identified peaks, indicating that FOXA1 plays a vital, yet more restrictive role in governing nmTOR chromatin accessibility (Fig. 4A). These findings are similar to the effects shown for AR DNA binding upon FOXA1 modulation (44). Second, we defined androgen-regulated genes (ARGs) that were negatively impacted by nmTOR. Among the total 2,531 ARGs found in LNCaP cells following a 24h exposure to R1881, 591 (23%) were inversely regulated by nmTOR, whereby NLS-mTOR (nmTOR) reversed the upregulation and downregulation of 329 and 262 ARGs, respectively (Fig. 4B). Of note, this inhibitory action of nmTOR on AR signaling occurred independently of its kinase activity as the NLS-mTOR kinase dead mutant D2357E virtually mirrored the effects of NLS-mTOR (Fig. 4B). Third, we intersected the FOXA1 reprogrammed mTOR cistrome restricted to binding events ± 50kb of gene transcription start sites (TSSs) with the nmTOR-dependent ARGs (591), refining the list to 335 ARGs (Fig. 4C, D). This gene list was further filtered by cross comparison with microarray data from androgen-treated (DHT) LNCaP cells ± FOXA1 siRNA-mediated knockdown (GSE27682) (45), giving rise to 65 ARGs found negatively regulated by both nmTOR and FOXA1 (Fig. 4E). The effects of FOXA1 deficiency by shRNA-mediated knockdown or CRISPR engineered knockout on mTOR recruitment to a subset of these ARGs were validated by mTOR ChIP-qPCR analyses in LNCaP cells (Supplementary Fig. 3A, B). qRT-PCR analysis of several of these genes (*GRB10*, *UGT2B15*, *PIK3R1*, *PKNOX2*) confirmed their modulation by nmTOR independently of its kinase activity as well as their modulation by FOXA1 knockdown or its rescue in LNCaP cells (Fig. 4F and Supplementary Fig. 3C, D). FOXA1 knockdown also abrogated the increase in

GRB10 and UGT2B15 protein induced by NLS-mTOR (Fig. 4G), reinforcing the reliance on FOXA1 for nmTOR blockade of AR signaling.

Nuclear mTOR promotes androgen-independent PCa progression

Antagonizing AR signaling is known to drive AR-independent PCa progression to CRPC and NEPC. Consistent with our current findings demonstrating that nmTOR promotes AR signaling inhibition, NLS-mTOR decreased levels of AR itself concomitant with upregulation of the NEPC marker ENO2 on both mRNA and protein levels in LNCaP cells independently of its kinase activity (Supplementary Fig. 4A-D). In the AR negative PCa cell lines DU145 and PC3, where AR signaling is bypassed, NLS-mTOR also effectively drove augmentation of ENO2 levels similarly to that observed with the NLS-mTOR kinase dead mutant (Fig. 5A, B). The observed decreased expression of epithelial marker E-Cadherin by NLS-mTOR (Fig. 5A, B) suggests that nmTOR activates epithelial-mesenchymal transition (EMT). Transwell cell migration and invasion assays established that nmTOR can significantly promote cell migration and invasion in both DU145 and PC3 cells regardless of its kinase activity (Fig. 5C, D). In addition, nmTOR significantly increased cell colony formation independently of AR signaling (Fig. 5E), signifying its oncogenic potential for PCa androgen-independent progression. Taken together, the data show that nmTOR inhibits AR activity and promotes AR independent PCa progression, thus supporting its therapeutic targeting in advanced PCa especially those AR negative PCa.

Discussion

mTOR has been shown to localize in the nucleus of various tissues and cancer types (15,22,23,46,47) making it accessible to interact with a diverse repertoire of cofactors to control distinct gene programs. Herein, by tagging mTOR with an NLS or NES to modulate nmTOR or cmTOR abundance and activity, respectively, we were able to discriminate between nmTOR- and cmTOR-dependent transcriptional signatures. Although both nmTOR and cmTOR impacted the expression of androgen response genes and E2F targets, the downregulation of androgen response genes was largely tied to nmTOR regardless of its kinase activity. In contrast, cmTOR was chiefly responsible for the upregulation of E2F targets in a kinase-dependent manner. We also provide evidence for a functional nmTOR-AR-FOXA1 complex with structural domain mapping revealing that the C-terminal domain of nmTOR interacts with the LBD of AR and DBD of FOXA1. Indeed, functional genomics studies revealed a strong dependency on the pioneer factor FOXA1 for nmTOR-mediated suppression of AR signaling and further showed that nmTOR may promote androgen-independent PCa progression via control of cell lineage plasticity.

Several oncogenic alterations such as PTEN loss, PKC deficiency, TMPRSS2-ERG fusion, N-MYC overexpression and even AR itself can result in inhibition of AR signaling and promotion of CRPC to NEPC (8,40,48-51). It is well-known that hyperactivation of PI3K-AKT-mTOR signaling via mutations or PTEN loss is associated with CRPC progression (52). While most studies have focused on the dysfunction of cmTOR, which may plausibly also indirectly impact nmTOR function, this study demonstrates a potential role for nmTOR in regulating cell lineage plasticity. In agreement with our findings, a previous report showed that overexpression of a mTOR hyperactive mutant induced LNCaP cell neuroendocrine differentiation (53). Indeed, this report showed that hyperactive mTOR could downregulate AR signaling and promote cell growth

arrest of LNCaP cells. While we found that nmTOR drives AR independency and PCa evolution, it also was found to suppress LNCaP cell growth (data not shown). Accordingly, nmTOR displayed oncogenic activity and significantly promoted the migration, invasion, and proliferation of the AR negative DU145 and PC3 cells. Thus, the growth inhibitory effect of nmTOR could reflect the direct suppression of AR signaling required for androgen-dependent growth of LNCaP cells.

An unexpected but important finding of this study was the previously unrecognized kinase-independent transcriptional regulatory property of nmTOR. While mTOR inhibitors (Torin1 or Rapamycin) suppress cmTOR activity, they can paradoxically increase nmTOR function by inducing its nuclear abundance, a potential underlying cause for the unsatisfactory outcome of mTOR inhibitors in clinical trials (54-56). In a manner similar to AR PROTAC (proteolysis targeting chimera) (57), nmTOR-specific PROTAC could be designed to decrease the nuclear levels of mTOR, whereby combining nmTOR PROTAC with cmTOR-targeting inhibitors may be more efficacious to attenuate disease burden and tackle drug resistance.

In summary, our work revealed molecular mechanisms underlying mTOR regulation of transcription, either directly by nmTOR or via canonical signaling by cmTOR. In particular, nmTOR attenuates AR signaling, thus promoting androgen-independent PCa progression. As such, pharmacological interventions aimed at targeting the transcriptional activity of nmTOR may be a rational therapeutic strategy to manage advanced PCa.

Methods

Reagents

A complete list of reagents used in this study are presented in Supplementary Table 4.

DNA constructs

Plasmid YFP-mTOR (Cat#73384), pcDNA3-Flag-mTOR (Cat#26603), pCW57-blasticidine inducible backbone (Cat#80921), and inducible shRNA backbone (Cat#21915) were purchased from Addgene.

HA-NLS:

(TACCCATACGATGTTCCAGATTACGCTGGACCTAAGAAGAAGAGGAAGGTGGAGAGCGGT) or Myc-NES:

(GAACAAAAACTCATCTCAGAAGAGGATCTGTTGCAGTTGCCGCCATTGGAGAGATTGACGTTG) was inserted into YFP-mTOR plasmid at the HindIII site. Then, YFP-mTOR (no localization tag), YFP-HA-NLS-mTOR or YFP-Myc-NES-mTOR cDNA was sub-cloned into inducible pCW57-blasticidine backbone between the restriction sites of enzyme AvrII and MluI. As a control, YFP only cDNA was also inserted into pCW57-blasticidine backbone. CloneAmp HiFi DNA polymerase (Takara, Cat#639298) was used for mTOR cloning, while Q5 DNA polymerase (NEB, Cat#M0491S) was used for cloning other smaller genes. The mTOR kinase dead mutation D2357E was further introduced to pCW57-YFP-HA-NLS-mTOR using a Q5 site-directed mutagenesis kit (NEB, Cat#E0554S). Also, domain fragments of mTOR (N-terminal, Middle and C-terminal) were generated from YFP-mTOR plasmid by deletion strategy using a Q5 mutagenesis kit. Inducible mTOR and FOXA1 shRNAs were self-cloned by inserting the short hairpin sequence (see Supplementary Table 4) into the inducible shRNA backbone (Addgene,

Cat#21915). FOXA1 sgRNA was inserted into backbone LentiCRISPR-V2 (Addgene, Cat#52961) to generate CRISPR plasmid to knockout FOXA1. In addition, pLENTI-AR plasmid (Cat#85128) and pLX302-FOXA1 (Cat#70090) were purchased from Addgene. Domains of AR and FOXA1 were sub-cloned into pLPC-3xFlag backbone (Addgene, Cat#73560). All molecular cloning plasmids were sequence verified using the Sanger Sequencing service provided by Genome Quebec.

Cell Culture

PCa cell lines (LNCaP, DU145, PC3) were originally purchased from ATCC and kept in culture with phenol-red free RPMI medium (Wisent, Cat#350-046CL) supplemented with 10% FBS (Thermo Fisher Scientific, Cat#12483020). 293T cells were growing in DMEM medium (Wisent, Cat#319-005CL) supplemented with 10% FBS. The presence of mycoplasma was regularly monitored using a mycoplasma PCR detection kit (Applied Biological Materials, Cat#G238). No contamination was detected.

For treatments with the synthetic androgen R1881, LNCaP cells (after reaching 70% confluency) were first androgen deprived by culturing them in RPMI medium containing 2% charcoal-stripped serum (CSS) for 48h. Then, cells were treated with Vehicle (Ethanol, 0.1% final) or 10nM R1881 (Steraloids, Cat#E3164-000) in freshly added CSS medium for another 24h unless otherwise indicated. In addition, 100nM Torin1 (Toronto Research Chemicals, Cat#T548700) or 40nM Rapamycin (Millipore, Cat#553211) was used to treat cells with or without 10nM R1881 for 24h after androgen deprivation in CSS medium for 48h.

Stable LNCaP cell lines

Inducible pCW57-YFP-mTOR variants (WT without localization tag, NES-tagged, NLS-tagged) or pCW57-YFP as the empty vector (EV) control were transfected into 293T cells using the calcium-phosphate precipitation method to generate lentivirus. Two days following plasmid transfection, viral soup was collected from 293T cells and further filtered using a 0.45 μm filter before addition to LNCaP cells. Blasticidine (1μg/ml; Sigma, Cat#15205) was used to select LNCaP cells for stable cell line establishment. The selection did not end until the dead cell control had no remaining live cells. Generally, stable cell lines should be established after successful selection. However, this was not the case for mTOR overexpression in LNCaP cells. After using doxycycline (1μg/ml; Clontech, Cat#631311) to induce exogenous expression of the YFP-mTOR variants for three days, only a few LNCaP cells showed intense green fluorescence although they had already been resistant to blasticidine selection. Therefore, FACS (fluorescence activated cell sorting) was additionally applied to enrich the green fluorescent cells which had a relatively high expression level of exogenous mTOR. Following expansion of LNCaP cells displaying a good expression level of the YFP-mTOR variants, lentivirus (produced in 293T cells) containing mTOR inducible shRNAs were used to infect these cells to knockdown endogenous mTOR. Cells were further selected using puromycin (1μg/ml; Sigma, Cat#P8833). Eventually, LNCaP cells were sequentially sorted and selected to inducibly express YFP-mTOR variants and mTOR shRNAs simultaneously so that the stable cells were forced to rely on exogenous mTOR.

Fluorescence activated cell sorting (FACS)

LNCaP cells were induced using doxycycline (1μg/ml) for three days to express exogenous YFP-mTOR variants. For sorting, cells (one confluent 10 cm plate per condition) were first trypsinized for 10min and pipetted up and down in medium with 10% serum to obtain single cells. Then, cells were centrifuged down and resuspended in 0.5 ml cold 1x PBS (on ice). Cell sorting was performed in the McGill Flow Cytometry Core Facility for flow cytometry and single cell analysis within the Life Science Complex. In the end, cells with strong green fluorescence signal were collected in 1 ml FBS on ice and recovered to grow in RPMI medium with 10% serum at 37^{o} C in a 5% CO_2 incubator.

Immunoblotting

Following cell treatments (usually one 10 cm confluent plate per condition), medium was discarded and cold 1x PBS was used to wash the cells once. Then, cells were scraped in cell lysis Buffer K (20mM phosphate buffer pH 7.4, 150mM NaCl, 0.1% NP40, 5mM EDTA and Roche protease inhibitors) supplemented with 0.6% CHAPS (Sigma, Cat#C3023) and transferred to 1.5ml Eppendorf tubes. For complete cell lysis, tubes were incubated with rotation at 4^{o} C for at least 40 min followed by centrifugation at 12000 rpm, 4^{o} C for 15min and the supernatants (whole cell lysates) were collected.

For cytosolic and nuclear fractionation, cells from 15 cm confluent plates were lysed in Harvest Buffer (10mM Hepes, 50mM NaCl, 0.5M Sucrose, 10mM EDTA, 0.5% Triton X-100 and Roche protease inhibitors) for 8 min on ice. The mixture was centrifuged at 3000 rpm, 4^{o} C for another 8 min. The upper supernatant was collected and centrifuged further at 12000 rpm, 4^{o} C for 15 min to collect the cytosolic fraction, while the lower cell pellets were kept for nuclear protein lysis. Buffer A (10mM Hepes, 10mM KCl, 0.1mM EDTA and 0.1mM EGTA) was used to wash

the nuclear pellets twice and then Buffer K supplemented with 0.6% CHAPS was added to extract the nuclear proteins. To facilitate the nuclear lysis, samples were briefly sonicated, and nuclear extracts were collected after centrifugation at 12000rpm, 4° C for 15 min.

For immunoprecipitation of nuclear proteins, at least five confluent 15 cm plates per condition of LNCaP cells were lysed in Buffer K supplemented with 0.6% CHAPS. Antibody (2μg) was pre-bound with 1mg Protein G magnetic beads (Invitrogen, Cat#10009D) at RT for one hour and 300-1000μg nuclear proteins were added to the antibody-beads mix and left to rotate at 4° C overnight. The next day, the target protein-bound beads were washed three times with 1x PBS-T and heated with 1x Western loading buffer at 70° C for 5 min.

Protein concentration was measured using Bradford reagent (Bio-Rad, Cat#500-0006). Equal quantities of protein from each treatment condition were mixed with 1x Western loading buffer and heated at 95° C for 5 min. Denatured proteins (20-30μg) were run on 6-9% SDS-PAGE gels, transferred to PVDF membranes (Bio-Rad), blocked for 1h at RT in 1x PBS supplemented with 0.1% Tween 20 (PBS-T) and 5% milk (BIOSHOP, Cat#SK1400.500), and primary antibodies were incubated with membrane slices (cut around the corresponding molecular sizes of target proteins) overnight at 4° C. The next day, anti-rabbit or anti-mouse HRP-linked secondary antibody were added to incubate with the membrane slices for one hour at RT. After washing with PBS-T for at least three times (15 min each), membranes were ready for chemiluminescent detection by adding Clarity or Clarity Max Western ECL substrate mix (Bio-Rad, Cat#1705061 or Cat#1705062). Protein detections were acquired by film (Diamed, Cat# DIAFILM810) or a ChemiDoc MP imaging system (Bio-Rad). Antibodies used are found in Supplementary data 4. Portions of uncropped blots (indicated by red boxes) used to generate the figures are shown in Supplementary Figure 5.

RT-qPCR and RNA-seq

Total RNA was extracted from cells using a RNeasy Mini Kit (Qiagen, Cat#74106). RNA concentration was measured using a Nanodrop and 1μg RNA per condition was reverse-transcribed by ProtoScript II Reverse Transcriptase (NEB, Cat#M0368L). mRNA levels were quantified by RT-qPCR using SYBR Green Master Mix (Roche, Cat#4887352001) on a LightCycler 480 instrument (Roche). The relative expression levels of target genes were normalized to the average of two human housekeeping genes (*TBP* and *β-Actin*). Specific human primers used for RT-qPCR are listed in Supplementary Table 4.

For RNA-seq, RNA was prepared as described above and RNAse-free DNAse I (Qiagen, Cat#79254) digestion was performed during the RNA extraction to eliminate DNA contamination. Illumina RNA-seq and analysis were performed by Novogene Bioinformatics Technology Co.,Ltd. Sample libraries prepared using the NEBNext Ultra II RNA Library Prep kit according to manufacturer’s recommendations were sequenced on an Illumina platform (NovaSeq 6000) and 150bp paired-end reads were generated. Raw data (raw reads) of fastq format were processed through in-house perl scripts to remove reads containing adapter and poly-N sequences and reads with low quality. Hisat2 software (version 2.0.5) was used to align paired-end clean reads to the Homo Sapiens reference genome hg38 and Feature Counts software (version 1.5.0-p3) was used to count the number of reads mapped per gene. FPKM (Fragments per kilobase of transcript sequence per millions base pairs sequenced) of each gene was calculated based on the length of the gene and read counts mapped to this gene. Differential expression analysis between groups was performed using the DESeq2 R package (version 1.20.0). Significant DEGs between groups (n=3 per group) were determined using DESeq2 p-value < 0.05 and an absolute log2 fold-change

> 0.5 (Supplementary Table 1). Heatmaps of DEGs using z-scaled log2(FPKM+1) values were generated using Morpheus (https://software.broadinstitute.org/morpheus/). Functional enrichment analysis of DEGs was performed using Enrichr (https://maayanlab.cloud/Enrichr/) to identify enriched Molecular Signature Database (MSigDB) hallmark signatures (v 2020). Enriched gene signatures are shown in Supplementary Table 2.

ChIP-qPCR and ChIP-seq

Crosslinking was performed with 1% formaldehyde added directly to LNCaP cultured plates shaken in 20ml medium at RT for 10 min. Medium was then discarded and cold 1x PBS was used to wash the cells twice. Fixed cells were harvested in cold 1x PBS and centrifuged at 1400 rpm, 4 ^{o} C for 10 min. The cell pellets were incubated in Buffer A (0.25% Triton, 10mM pH8 Tris-HCl, 10mM EDTA, 0.5mM EGTA and Roche protease inhibitors; 1mL per 15 cm plate) on ice for 5 min before being centrifuged at 1400 rpm, 4^{o} C for 10 min. Next, the pellets were further incubated with Buffer B (200mM NaCl, 10mM pH8 Tris-HCl, 1mM EDTA, 0.5mM EGTA and Roche protease inhibitors; 1mL per 15 cm plate) on ice for 30 min and centrifuged at 1400 rpm, 4^{o} C for 10 min. At this point, the pellets (chromatin) could be stored at -80^{o} C until future use. The stored pellets were suspended in Buffer CD (0.5% SDS, 0.5% Triton, 10mM pH8 Tris-HCl, 140mM NaCl, 1mM EDTA, 0.5mM EGTA and Roche protease inhibitors; 0.5ml per 150 cm plate) and sonicated until DNA fragments were concentrated between 250-750bp. DNA concentrations were determined using a Nanodrop after rapid chromatin decrosslinking and subsequent purification with a QIAquick PCR purification kit (Qiagen, Cat#28106). Usually, 2mg magnetic protein G beads were pre-incubated with 4 μg antibody in ChIP Dilution Buffer (1% Triton, 10mM pH8 Tris-HCl, 150mM NaCl, 2mM EDTA) one night prior and then incubated with 100μg sonicated

chromatin overnight. Beads-chromatin complexes were sequentially washed once with Wash Buffer 1 (0.5% NP40, 150mM KCl, 10mM pH8 Tris-HCl, 1mM EDTA), Wash Buffer 2 (0.5% Triton, 100mM NaCl, 10mM pH8 Tris-HCl), and Wash Buffer 3A (0.5% Triton, 400mM NaCl, 10mM pH8 Tris-HCl), Wash Buffer 3B (0.5% Triton, 500mM NaCl, 10mM pH8 Tris-HCl), then twice with Wash Buffer 4 (0.5% NP40, 250mM LiCl, 10mM pH8 Tris-HCl, 1mM EDTA). Then, Buffer E (1% SDS, 50mM pH8 Tris-HCl, 10mM EDTA) was added to the beads to de-crosslink chromatin from proteins bound at 65^{o} C overnight. The next day, 3µl 10mg/ml RNAse A and 10µl 10mg/ml Protease K were used to digest the contaminated RNA and protein at 37 ^{o}C for 1h and 55^{o} C for 1h, respectively. ChIP DNA was purified using a Qiagen PCR purification kit (eluted in 90µl Elution Buffer 10mM pH8 Tris-HCl). Eluted DNA was measured by quantitative real-time PCR (ChIP-qPCR) using SYBR Green Master Mix (Roche, Cat#4887352001) on a LightCycler 480 instrument (Roche). The relative ChIP enrichment was normalized to corresponding input and the average of two negative controls. Specific human primers used for ChIP-qPCR are listed in Supplementary Table 4.

For mTOR ChIP-seq in LNCaP cells with or without shRNA-mediated FOXA1 knockdown ± 10nM R1881 (24h), ChIP DNA was prepared similarly to that described above. Briefly, for each condition, two independent batches of crosslinked cells (7 x 15 cm plates per batch) were pooled together prior to sonication and ChIP DNA prepared from a total mix of 3600µg chromatin and 72µg antibody was eluted in a final volume of 45µl. ChIP DNA was provided to Novogene Bioinformatics Technology Co., Ltd for library preparation using the NEBNext Ultra II DNA Library Prep kit according to manufacturer’s recommendations and sequenced using a NovaSeq 6000 platform (Illumina) as 150bp paired-end reads. ChIP-seq reads were first trimmed for adapter sequences and low-quality score bases using Trimmomatic v0.36

(58). The resulting reads were mapped to the human reference genome (hg38) using BWA-MEM v0.7.12 (59) in paired-end mode at default parameters. Only reads that had a unique alignment (mapping quality > 20) were retained and PCR duplicates were removed using Picard tools v2.0.1 (https://broadinstitute.github.io/picard/). Peaks (summit ± 150 bp) were called using MACS2 software suite v2.1.1.20160309 (60) at an FDR < 0.05 using sequenced libraries of input DNA as control. Peaks in mitochondrial chromosome and scaffold regions were removed. Peak annotation analysis was performed using the *annotatePeaks* command from HOMER software suite v4.11.1 (61). Peak intersections were performed using HOMER's *mergePeaks* command with parameter -d 300 or dgiven. Genome browser tracks were created with the HOMER *makeUCSCfile* command and *bedGraphToBigWig* v4 utility from UCSC. Tracks were normalized so that each value represents the read count per base pair per 10 million reads. mTOR ChIP-seq tracks were visualized using IGV (version v2.8.6) (62). For heatmap generation, once output bed files containing merged (overlapping) and unique peaks from HOMER's *mergePeaks* (-d 300) command were obtained, we used *computeMatrix* followed by *plotHeatmap* from deepTools v3.5.0 (63) to formulate the figure. *ComputeMatrix* utilizes normalized (RPKM) bigwig track information combined with the locations identified by the merged or unique bed files to create intensity comparisons. mTOR ChIP-seq datasets generated in this study using LNCaP cells with or without shRNA-mediated FOXA1 knockdown ± 10nM R1881 (24h) are presented in Supplementary Table 3.

ChIP-seq peak intersections involving publicly available mTOR, AR and FOXA1 datasets in LNCaP cells were performed with HOMER v4.11 using the script *mergePeaks -d 300* and overlapping peaks were annotated using *annotatePeaks.pl*. Uniformly processed ChIP-seq peak lists annotated to the hg38 genome assembly (q < 1E-05) were downloaded from the ChIP-seq

repository ChIP-Atlas web tool (https://chip-atlas.org). Prior to ChIP-seq peak intersections, for any treatment group with available replicates, the datasets were compiled. The following datasets were used: mTOR (EtOH, SRX2505193; R1881, SRX2505194), AR (EtOH, SRX2545037/SRX2545039/SRX736053; R1881, SRX2545038/SRX2545040/SRX736054), and FOXA1 (EtOH, SRX2545049/ SRX2545051; R1881, SRX2545050/ SRX2545052).

Cell Migration and Invasion Assays

NLS-mTOR, NLS-mTOR^{D2357E}, or empty vector (EV) control were pre-induced in DU145 and PC3 cells using 2μg/ml doxycycline (Wisent, Cat#450-185-QG) for seven days. For migration assays, cells were trypsinized, counted, re-suspended in serum-free medium and 50,000 cells (200μl) were added per upper Transwell chamber (Fisher, Cat#07-200-174) in a 24-well plate. 750μl 30% FBS medium was added into the lower chambers and the plates were incubated in a 37 ^{o}C, 5% CO_2 incubator for two days. Then, medium was discarded from the upper and lower chambers and cold 1x PBS was used to wash the cells twice. Cells were fixed with 1ml formaldehyde (3.7% in PBS) per Transwell chamber at RT for 2 min. The formaldehyde was removed and 1x PBS was used to wash the cells twice. Next, cells were permeabilized by 1ml 100% methanol per chamber at RT for 20 min. Methanol was removed and 1x PBS was used to wash twice. Subsequently, 1ml Crystal Violet (Sigma, Cat#V5365) was added to stain cells at RT for 15min. Crystal Violet was removed and 1x PBS was used to wash sufficiently until no free Crystal Violet was left. Non-migrated cells were scraped away by cotton swabs. The Transwells were air-dried and cell images were taken under microscope (bright field, 10x). For each Transwell, images from five random visual fields were taken and Image J software was used to quantify and analyze for statistical significance.

For invasion assays, Matrigel (VWR, Cat#354262) was diluted by cold serum-free medium (1:8) and 70µl diluted Matrigel was added to each upper Transwell chamber and put in a 37° C incubator to solidify for at least 30min. Then, 50,000 cells (200µl) suspended in serum-free medium were added on top of the solidified Matrigel and allowed to invade towards the lower chamber filled with 750µl 30% FBS medium in a 37° C incubator for three days. The rest of the process including fixing and staining was conducted as described for the migration assay above. Image J software was used to quantify and analyze images taken from the five random visual fields per chamber.

Colony Formation Assay

DU145 or PC3 cells (2,000 cells) were added to each well in 6-well plates and incubated in a 37° C, 5% CO_2 incubator for 2-3 weeks. Doxycycline (2µg/ml) was constantly used to induce NLS-mTOR expression. RPMI medium containing 10% FBS and doxycycline (2µg/ml) was refreshed every five days. Then, medium was discarded and cold 1x PBS was used to wash the cells twice. 1ml 100% methanol was added per well to fix the cell colonies in the 6-well plates at RT for 20 min. Cold 1x PBS was used to wash twice before staining cells with Crystal Violet (Sigma, Cat#V5365) at RT for 15 min. Next, Crystal Violet was removed and cold 1x PBS was used to wash sufficiently to get a clear background. The plates were air-dried at RT and pictures of the colonies were taken. Image J software was used to quantify and analyze the four replicates for statistical significance.

Statistical analysis

GraphPad Prism 9 software was used to draw graphs and for statistical analysis. All experiments were performed at least three times. Unless otherwise specified, differences were considered significant when p-value calculated by One-way ANOVA analysis was less than 0.05.

Data availability

RNA-seq data of mTOR shRNA-mediated knockdown in LNCaP cells rescued with either WT-mTOR, NES-mTOR, NLS-mTOR, NLS-mTOR^{D2357E} or empty vector (EV) control ± 10nM R1881 for 24h as well as mTOR ChIP-seq data in LNCaP cells ± shRNA-mediated FOXA1 knockdown ± 10nM R1881 for 24h have been deposited in NCBI's Gene Expression Omnibus (GEO) and are accessible through GEO SuperSeries accession number GSE225207 encompassing SubSeries GSE225205 (RNA-seq) and GSE225196 (ChIP-seq). Public microarray data from LNCaP cells ± FOXA1 siRNA-mediated knockdown ± DHT treatment are available from the GEO database under accession number GSE27682 (45). Public ChIP-seq data from LNCaP cells ± R1881 treatment used in this study are available from the GEO database: mTOR (GSM2463796, GSM2463797), AR (GSM2480800-GSM2480803, GSM1527822, GSM1527823), and FOXA1 (GSM2480812-GSM2480815).

Source data underlying the graphs are presented in Supplementary Table 5. Uncropped immunoblots are shown in Supplementary Figure 5.

Author Contributions

Y.C. and V.G. conceived the study. Y.C. designed the experiments and organized the data with the help of C.R.D. and V.G. Y.C. established the NLS-mTOR tool and performed most of the experimental work. C.R.D. helped with RNA-seq and ChIP-seq data analysis and L.H. helped run ChIP-qPCRs. Y.C. wrote the original draft of the manuscript with editing from C.R.D. and V.G. All authors commented on the manuscript.

Acknowledgments

We thank all members of Dr. Giguère's laboratory for daily support, Dr. Michel Tremblay and Dr. Jose Teodoro for advice as well as Dr. Mathieu Vernier and Dr. Ming Yan for the help with mTOR molecular cloning. The McGill Flow Cytometry Core Facility for flow cytometry and single cell analysis within the Life Science Complex was supported by funding from the Canadian Foundation for Innovation (CFI). This work was supported by a Foundation grant from the Canadian Institutes of Health Research (CIHR) to V.G. (FDT-156254).

Declaration of Interests

The authors declare no conflict of interests.

References

1. Watson PA, Arora VK, Sawyers CL. Emerging mechanisms of resistance to androgen receptor inhibitors in prostate cancer. Nat Rev Cancer **2015**;15:701-11
2. Shafi AA, Yen AE, Weigel NL. Androgen receptors in hormone-dependent and castration-resistant prostate cancer. Pharmacol Ther **2013**;140:223-38
3. Scher HI, Fizazi K, Saad F, Taplin ME, Sternberg CN, Miller K*, et al.* Increased survival with enzalutamide in prostate cancer after chemotherapy. N Engl J Med **2012**;367:1187-97
4. Zong Y, Goldstein AS. Adaptation or selection--mechanisms of castration-resistant prostate cancer. Nat Rev Urol **2013**;10:90-8
5. Formaggio N, Rubin MA, Theurillat JP. Loss and revival of androgen receptor signaling in advanced prostate cancer. Oncogene **2021**;40:1205-16
6. Mills IG. Maintaining and reprogramming genomic androgen receptor activity in prostate cancer. Nat Rev Cancer **2014**;14:187-98
7. Ku SY, Gleave ME, Beltran H. Towards precision oncology in advanced prostate cancer. Nat Rev Urol **2019**;16:645-54
8. Dardenne E, Beltran H, Benelli M, Gayvert K, Berger A, Puca L*, et al.* N-Myc Induces an EZH2-Mediated Transcriptional Program Driving Neuroendocrine Prostate Cancer. Cancer Cell **2016**;30:563-77
9. Beltran H, Demichelis F. Therapy considerations in neuroendocrine prostate cancer: what next? Endocr Relat Cancer **2021**;28:T67-T78
10. Kim J, Guan KL. mTOR as a central hub of nutrient signalling and cell growth. Nat Cell Biol **2019**;21:63-71

11. Szwed A, Kim E, Jacinto E. Regulation and metabolic functions of mTORC1 and mTORC2. Physiol Rev **2021**;101:1371-426
12. Betz C, Hall MN. Where is mTOR and what is it doing there? J Cell Biol **2013**;203:563-74
13. Drenan RM, Liu X, Bertram PG, Zheng XF. FKBP12-rapamycin-associated protein or mammalian target of rapamycin (FRAP/mTOR) localization in the endoplasmic reticulum and the Golgi apparatus. J Biol Chem **2004**;279:772-8
14. Rosner M, Hengstschlager M. Detection of cytoplasmic and nuclear functions of mTOR by fractionation. Methods Mol Biol **2012**;821:105-24
15. Li H, Tsang CK, Watkins M, Bertram PG, Zheng XF. Nutrient regulates Tor1 nuclear localization and association with rDNA promoter. Nature **2006**;442:1058-61
16. Bernardi R, Guernah I, Jin D, Grisendi S, Alimonti A, Teruya-Feldstein J*, et al.* PML inhibits HIF-1α translation and neoangiogenesis through repression of mTOR. Nature **2006**;442:779-85
17. Zhou X, Zhong Y, Molinar-Inglis O, Kunkel MT, Chen M, Sun T*, et al.* Location-specific inhibition of Akt reveals regulation of mTORC1 activity in the nucleus. Nat Commun **2020**;11:6088
18. Bachmann RA, Kim JH, Wu AL, Park IH, Chen J. A nuclear transport signal in mammalian target of rapamycin is critical for its cytoplasmic signaling to S6 kinase 1. J Biol Chem **2006**;281:7357-63
19. Tsang CK, Liu H, Zheng XF. mTOR binds to the promoters of RNA polymerase I- and III-transcribed genes. Cell Cycle **2010**;9:953-7

20. Kantidakis T, Ramsbottom BA, Birch JL, Dowding SN, White RJ. mTOR associates with TFIIIC, is found at tRNA and 5S rRNA genes, and targets their repressor Maf1. Proc Natl Acad Sci USA **2010**;107:11823-8
21. Giguère V. Canonical signaling and nuclear activity of mTOR-a teamwork effort to regulate metabolism and cell growth. Febs J **2018**;285:1572-88
22. Cunningham JT, Rodgers JT, Arlow DH, Vazquez F, Mootha VK, Puigserver P. mTOR controls mitochondrial oxidative function through a YY1-PGC-1α transcriptional complex. Nature **2007**;450:736-40
23. Wan W, You Z, Xu Y, Zhou L, Guan Z, Peng C*, et al.* mTORC1 Phosphorylates Acetyltransferase p300 to Regulate Autophagy and Lipogenesis. Mol Cell **2017**;68:323-35 e6
24. Audet-Walsh E, Dufour CR, Yee T, Zouanat FZ, Yan M, Kalloghlian G*, et al.* Nuclear mTOR acts as a transcriptional integrator of the androgen signaling pathway in prostate cancer. Genes Dev **2017**;31:1228-42
25. Audet-Walsh E, Vernier M, Yee T, Laflamme C, Li S, Chen Y*, et al.* SREBF1 activity Is regulated by an AR/mTOR nuclear axis in prostate cancer. Mol Cancer Res **2018**;16:1396-405
26. Dufour CR, Scholtes C, Yan M, Chen Y, Han L, Li T*, et al.* The mTOR chromatin-bound interactome in prostate cancer. Cell Rep **2022**;38:110534
27. Yang YA, Yu J. Current perspectives on FOXA1 regulation of androgen receptor signaling and prostate cancer. Genes Dis **2015**;2:144-51
28. Jin HJ, Zhao JC, Ogden I, Bergan RC, Yu J. Androgen receptor-independent function of FOXA1 in prostate cancer metastasis. Cancer Res **2013**;73:3725-36

29. Zhang C, Wang L, Wu D, Chen H, Chen Z, Thomas-Ahner JM*, et al.* Definition of a FOXA1 Cistrome that is crucial for G1 to S-phase cell-cycle transit in castration-resistant prostate cancer. Cancer Res **2011**;71:6738-48
30. Gerhardt J, Montani M, Wild P, Beer M, Huber F, Hermanns T*, et al.* FOXA1 promotes tumor progression in prostate cancer and represents a novel hallmark of castration-resistant prostate cancer. Am J Pathol **2012**;180:848-61
31. Sahu B, Laakso M, Ovaska K, Mirtti T, Lundin J, Rannikko A*, et al.* Dual role of FOXA1 in androgen receptor binding to chromatin, androgen signalling and prostate cancer. EMBO J **2011**;30:3962-76
32. Song B, Park SH, Zhao JC, Fong KW, Li S, Lee Y*, et al.* Targeting FOXA1-mediated repression of TGF-beta signaling suppresses castration-resistant prostate cancer progression. J Clin Invest **2019**;129:569-82
33. Wang X, Brea L, Lu X, Gritsina G, Park SH, Xie W*, et al.* FOXA1 inhibits hypoxia programs through transcriptional repression of HIF1A. Oncogene **2022**;41:4259-70
34. Kim J, Jin H, Zhao JC, Yang YA, Li Y, Yang X*, et al.* FOXA1 inhibits prostate cancer neuroendocrine differentiation. Oncogene **2017**;36:4072-80
35. Baca SC, Takeda DY, Seo JH, Hwang J, Ku SY, Arafeh R*, et al.* Reprogramming of the FOXA1 cistrome in treatment-emergent neuroendocrine prostate cancer. Nat Commun **2021**;12:1979
36. Yang YA, Zhao JC, Fong KW, Kim J, Li S, Song C*, et al.* FOXA1 potentiates lineage-specific enhancer activation through modulating TET1 expression and function. Nucleic Acids Res **2016**;44:8153-64

37. Han M, Li F, Zhang Y, Dai P, He J, Li Y*, et al.* FOXA2 drives lineage plasticity and KIT pathway activation in neuroendocrine prostate cancer. Cancer Cell **2022**;40:1306-23 e8
38. Adams EJ, Karthaus WR, Hoover E, Liu D, Gruet A, Zhang Z*, et al.* FOXA1 mutations alter pioneering activity, differentiation and prostate cancer phenotypes. Nature **2019**;571:408-12
39. Parolia A, Cieslik M, Chu SC, Xiao L, Ouchi T, Zhang Y*, et al.* Distinct structural classes of activating FOXA1 alterations in advanced prostate cancer. Nature **2019**;571:413-8
40. Mulholland DJ, Tran LM, Li Y, Cai H, Morim A, Wang S*, et al.* Cell autonomous role of PTEN in regulating castration-resistant prostate cancer growth. Cancer Cell **2011**;19:792-804
41. Thoreen CC, Kang SA, Chang JW, Liu Q, Zhang J, Gao Y*, et al.* An ATP-competitive mammalian target of rapamycin inhibitor reveals rapamycin-resistant functions of mTORC1. J Biol Chem **2009**;284:8023-32
42. Stelloo S, Nevedomskaya E, Kim Y, Hoekman L, Bleijerveld OB, Mirza T*, et al.* Endogenous androgen receptor proteomic profiling reveals genomic subcomplex involved in prostate tumorigenesis. Oncogene **2018**;37:313-22
43. Takayama K, Suzuki T, Tsutsumi S, Fujimura T, Urano T, Takahashi S*, et al.* RUNX1, an androgen- and EZH2-regulated gene, has differential roles in AR-dependent and -independent prostate cancer. Oncotarget **2015**;6:2263-76
44. Jin HJ, Zhao JC, Wu L, Kim J, Yu J. Cooperativity and equilibrium with FOXA1 define the androgen receptor transcriptional program. Nat Commun **2014**;5:3972
45. Wang D, Garcia-Bassets I, Benner C, Li W, Su X, Zhou Y*, et al.* Reprogramming transcription by distinct classes of enhancers functionally defined by eRNA. Nature **2011**;474:390-4

46. Alayev A, Salamon RS, Berger SM, Schwartz NS, Cuesta R, Snyder RB*, et al.* mTORC1 directly phosphorylates and activates ERalpha upon estrogen stimulation. Oncogene **2016**;35:3535-43
47. Torres AS, Holz MK. Unraveling the multifaceted nature of the nuclear function of mTOR. Biochim Biophys Acta Mol Cell Res **2021**;1868:118907
48. Labbe DP, Brown M. Transcriptional Regulation in Prostate Cancer. Cold Spring Harb Perspect Med **2018**;8
49. Yu J, Yu J, Mani RS, Cao Q, Brenner CJ, Cao X*, et al.* An integrated network of androgen receptor, polycomb, and TMPRSS2-ERG gene fusions in prostate cancer progression. Cancer Cell **2010**;17:443-54
50. Reina-Campos M, Linares JF, Duran A, Cordes T, L'Hermitte A, Badur MG*, et al.* Increased serine and one-carbon pathway metabolism by PKClambda/iota deficiency promotes neuroendocrine prostate cancer. Cancer Cell **2019**;35:385-400 e9
51. Cai C, He HH, Chen S, Coleman I, Wang H, Fang Z*, et al.* Androgen receptor gene expression in prostate cancer is directly suppressed by the androgen receptor through recruitment of lysine-specific demethylase 1. Cancer Cell **2011**;20:457-71
52. Shen MM, Abate-Shen C. Molecular genetics of prostate cancer: new prospects for old challenges. Genes Dev **2010**;24:1967-2000
53. Kanayama M, Hayano T, Koebis M, Maeda T, Tabe Y, Horie S*, et al.* Hyperactive mTOR induces neuroendocrine differentiation in prostate cancer cell with concurrent up-regulation of IRF1. Prostate **2017**;77:1489-98
54. Crumbaker M, Khoja L, Joshua AM. AR signaling and the PI3K pathway inprostate cancer. Cancers (Basel) **2017**;9

55. Statz CM, Patterson SE, Mockus SM. mTOR inhibitors in castration-resistant prostate cancer: a systematic review. Target Oncol **2017**;12:47-59
56. Fruman DA, Rommel C. PI3K and cancer: lessons, challenges and opportunities. Nat Rev Drug Discov **2014**;13:140-56
57. Han X, Wang C, Qin C, Xiang W, Fernandez-Salas E, Yang CY*, et al.* Discovery of ARD-69 as a highly potent proteolysis targeting chimera (PROTAC) degrader of androgen receptor (AR) for the treatment of prostate cancer. J Med Chem **2019**;62:941-64
58. Bolger AM, Lohse M, Usadel B. Trimmomatic: a flexible trimmer for Illumina sequence data. Bioinformatics **2014**;30:2114-20
59. Li H, Durbin R. Fast and accurate short read alignment with Burrows-Wheeler transform. Bioinformatics **2009**;25:1754-60
60. Zhang Y, Liu T, Meyer CA, Eeckhoute J, Johnson DS, Bernstein BE*, et al.* Model-based analysis of ChIP-Seq (MACS). Genome Biol **2008**;9:R137
61. Heinz S, Benner C, Spann N, Bertolino E, Lin YC, Laslo P*, et al.* Simple combinations of lineage-determining transcription factors prime cis-regulatory elements required for macrophage and B cell identities. Mol Cell **2010**;38:576-89
62. Robinson JT, Thorvaldsdóttir H, Winckler W, Guttman M, Lander ES, Getz G, Mesirov JP. Integrative genomics viewer. Nature Biotechnology **2011**;29:24-6
63. Ramirez F, Ryan DP, Gruning B, Bhardwaj V, Kilpert F, Richter AS*, et al.* deepTools2: a next generation web server for deep-sequencing data analysis. Nucleic Acids Res **2016**;44:W160-5

Figure Legends

Figure 1.

NLS-mTOR tool is established for nmTOR functional studies. **A,** Schematic showing the molecular cloning strategy to tag mTOR with an NLS or NES. NLS-mTOR with a kinase dead mutation (D2357E) was also established. **B,** Immunoblotting of LNCaP nuclear extracts overexpressing the mTOR constructs in (**A**). **C,** Immunoblotting of LNCaP whole cell extracts showing the exogenous expression of the mTOR variants in (**A**) whereby endogenous mTOR was knocked down by shRNA. **D,** Representative fluorescent images showing the distribution of NLS or NES-tagged mTOR in LNCaP cells.

Figure 2.

nmTOR has distinct function with cmTOR on transcription. **A,** RNA-seq analysis was performed (p-value < 0.05, |Log2FC|> 0.5) on LNCaP cells in which endogenous mTOR was knocked down by inducible shRNA and rescued by inducible expression NES-mTOR (as cmTOR), NLS-mTOR (as nmTOR), and YFP as empty vector (EV) control. NES-mTOR or NLS-mTOR was compared to EV in cells treated with R1881 (24h) to identify gene signatures dependent on cmTOR or nmTOR, respectively. Venn diagrams showing the upregulated and downregulated genes by NES-mTOR, NLS-mTOR or both along with their associated enriched MSigDB Hallmark gene signatures using EnrichR. Heatmaps illustrating the upregulation of E2F targets signature genes predominantly by cmTOR and the downregulation of androgen response signature genes mainly by nmTOR. **B, C,** RT-qPCR analysis of selected E2F targets (**B**) and androgen response genes (**C**) identified in (**A**) validating their transcriptional control by cmTOR, nmTOR or both. Statistics were calculated by comparing the mTOR variants with EV in either vehicle or R1881-treated (24h)

conditions. *p < 0.05, **p < 0.01; ns, not significant. **D,** Immunoblots supporting NES-mTOR promotion of cell cycle progression via induction of RB phosphorylation and reduction in cell cycle inhibitor p27. **E,** Immunoblots showing reduced RB phosphorylation and increased expression of cell cycle inhibitor p27 following mTOR inhibition with Torin1. **F,** Pie Charts illustrating that ~2/3 of nmTOR-regulated genes are independent of its kinase activity under either vehicle or R1881-treated (24h) conditions.

See also **Supplementary Figure 1**.

Figure 3.

mTOR complexes with AR and FOXA1. **A, B,** Co-IP experiments in whole cell extracts from 293T cells showing that exogenous AR and FOXA1 can interact with exogenous mTOR. **C,** Co-IP experiments in nuclear extracts of LNCaP cells treated with or without R1881 (48h) showing that endogenous AR, FOXA1, and nmTOR all interact together. **D,** Schematic of mTOR structural domains and construction of N-terminal, Middle and C-terminal kinase domain constructs for interaction studies. Both AR and FOXA1 interacted with the C-terminal half of mTOR (including Middle and C-terminal kinase domain) in 293T cells. **E,** Schematic of AR structural domains and construction of N-terminal, DNA binding domain (DBD) and ligand binding domain (LBD) constructs for interaction studies in 293T cells which showed that mTOR interacts with the AR LBD. **F,** Schematic of FOXA1 structural domains and construction of N-terminal, DBD and C-terminal domain constructs for interaction studies in 293T cells which showed that mTOR interacts with the FOXA1 DBD.

See also **Supplementary Figure 2**.

Figure 4.

nmTOR cooperates with FOXA1 to impair AR signaling. **A,** Heatmap showing the impact of FOXA1 knockdown on global mTOR ChIP-seq binding profiles. **B,** RNA-seq analysis identified 591 of 2,531 ARGs in R1881-treated (24h) LNCaP cells (p-value< 0.05, |Log2FC|> 0.5) to be inversely regulated by NLS-mTOR (nmTOR). Pie Chart shows that around one quarter of Androgen Regulated Genes (ARGs) are reversed by nmTOR. **C,** Genomic annotation of mTOR ChIP-seq peaks in LNCaP cells ± FOXA1 knockdown found ± 50kb of gene TSSs (transcription start sites). **D,** Among the 591 ARGs identified in (B) to be inversely regulated by nmTOR, 335 (57%) were also found to exhibit nmTOR genomic reprogramming elicited by FOXA1 knockdown. **E,** Heatmap showing 39 upregulated and 26 downregulated ARGs showing inverse regulation by both nmTOR and FOXA1. **F,** RT-qPCR analysis showing the effects of FOXA1 knockdown or its rescue on ARG expression in LNCaP cells. *p< 0.05, **p< 0.01; ns, not significant. **G,** Immunoblot analysis showing that loss of FOXA1 blocks the increase in GRB10 and UGT2B15 proteins by NLS-mTOR (nmTOR).

See also **Supplementary Figure 3**.

Figure 5.

nmTOR promotes androgen independent prostate cancer progression. **A, B,** NLS-mTOR or NLS^{D2357E}-mTOR (kinase dead mutant) was inducibly expressed into AR negative PCa cell lines DU145 (**A**) and PC3 (**B**). Immunoblots show that nmTOR drives increased expression of NEPC marker ENO2 and upregulation of EMT as indicated by decreased levels of E-Cadherin following doxycycline induction for seven days. **C, D,** Transwell cell migration (**C**) and invasion (**D**) assays demonstrating that nmTOR significantly promotes DU145 and PC3 cell migration and invasion

independently of its kinase activity. **E,** Colony formation assay showing that nmTOR significantly promotes colony formation of both DU145 and PC3 cells in a kinase-independent manner.

See also **Supplementary Figure 4**.

Supplemental Information

Supplementary Tables 1-5 (excel files)

Supplementary Figures 1-5

Supplementary Table 1. RNA-seq analysis of LNCaP mTOR knockdown cells rescued with either WT-mTOR, NES-mTOR, NLS-mTOR, NLS-mTOR^{D2357E} or empty vector (EV) control ± 10nM R1881 for 24h.

Supplementary Table 2. Enrichr MSigDB hallmark gene signatures enriched in genes regulated by NES-mTOR, NLS-mTOR or both in 10nM R1881-treated LNCaP cells for 24h.

Supplementary Table 3. mTOR ChIP-seq analysis in LNCaP cells ± FOXA1 knockdown in the presence or absence of 10nM R1881 for 24h.

Supplementary Table 4. List of reagents, plasmids, antibodies, and human RT-qPCR and ChIP-qPCR primers used in this study.

Supplementary Table 5. Source data.

Supplementary Figure Legends

Supplementary Figure 1.

nmTOR transcriptional activity is primarily kinase-independent. **A,** mTOR inhibition by Torin1 or Rapamycin treatment (24h) robustly decreased the gene expression of E2F targets found regulated specifically by NES-mTOR or commonly regulated by NES-mTOR and NLS-mTOR. **B,** mTOR inhibition by Torin1 or Rapamycin treatment (24h) resulted in either no effect or a variable effect on the expression of androgen response genes specifically downregulated by NLS-mTOR or those commonly regulated by NES-mTOR and NLS-mTOR, respectively. **C,** Immunoblots showing that Torin1 treatment (24h) increases mTOR nuclear abundance. **D,** Schematic summarizing distinct functional actions of nmTOR and cmTOR.

See also **Figure 2**.

Supplementary Figure 2.

mTOR colocalizes with AR and FOXA1 on chromatin. **A,** Top candidate nmTOR transcriptional coregulators identified by EnrichR (ChEA_2022) using the total list of DEGs found modulated by NLS-mTOR (1828 genes) in Figure 2A. Hits for AR and FOXA1 are shown in red. **B,** Intersection of public mTOR, AR, and FOXA1 ChIP-seq data shows that androgen stimulation (R1881) induces their genomic colocalization.

See also **Figure 3**.

Supplementary Figure 3.

FOXA1 participates in nmTOR-dependent hindrance of AR signaling. **A,** IGV genome browser views of mTOR DNA binding at several ARGs by ChIP-seq analyses in LNCaP cells ± FOXA1

knockdown. **B,** mTOR ChIP-qPCR validation of the ARGs in (**A**) in LNCaP cells with or without FOXA1 knockdown or CRISPR knockout. Immunoblots confirming the loss of FOXA1 upon shRNA-mediated knockdown or CRISPR knockout. **C,** RT-qPCR analysis shows that both nmTOR and its kinase dead mutant can reverse the gene expression of the ARGs shown. *p< 0.05, **p< 0.01; ns, not significant. **D,** RT-qPCR analysis shows that mTOR inhibition by Torin1 or Rapamycin for 24h either has no effect or a stimulatory effect on the expression of the ARGs shown.

See also **Figure 4**.

Supplementary Figure 4.

nmTOR up-regulates NEPC marker ENO2 in LNCaP cells. **A,** RT-qPCR analysis of NEPC marker *ENO2* shows its transcriptional control by nmTOR independently of its kinase activity in LNCaP cells. Statistics were calculated by comparing the mTOR variants with empty vector (EV) control in either vehicle or R1881-treated (24h) conditions. *p< 0.05, **p< 0.01; ns, not significant. **B,** Immunoblot analysis showing decreased AR and increased levels of NEPC marker ENO2 by nmTOR in LNCaP cells in the absence of androgen stimulation. **C,** RT-qPCR analysis shows that mTOR inhibition by Torin1 or Rapamycin for 24h has no effect on *ENO2* expression. **D,** Immunoblot analysis confirms that mTOR inhibition by Torin1 or Rapamycin for 24h has no effect on ENO2 expression.

See also **Figure 5**.

Supplementary Figure 5.

Source images. For immunoblotting, membranes were sliced to maximize sample use to increase the number of protein detections per gel. Portions of uncropped blots used to generate the figures are indicated by red boxes.

Figure 1

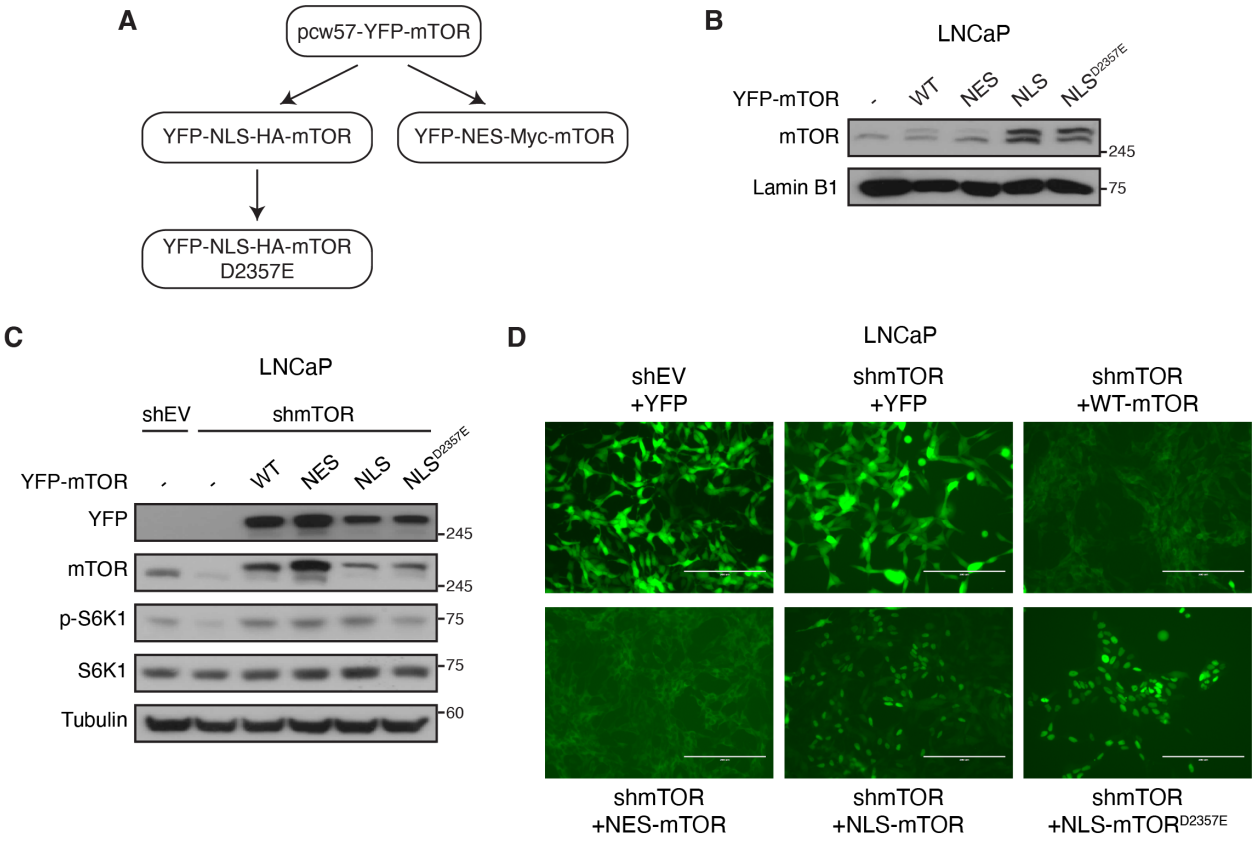
A
pcw57-YFP-mTOR
YFP-NLS-HA-mTOR
YFP-NES-Myc-mTOR
YFP-NLS-HA-mTOR D2357E
B
LNCaP
YFP-mTOR
WT
NES
NLS
NLS D2357E
mTOR
Lamin B1
245
75
C
LNCaP
shEV
shmTOR
YFP-mTOR
WT
NES
NLS
NLS D2357E
YFP
mTOR
p-S6K1
S6K1
Tubulin
245
245
75
75
60
D
LNCaP
shEV +YFP
shmTOR +YFP
shmTOR +WT-mTOR
shmTOR +NES-mTOR
shmTOR +NLS-mTOR
shmTOR +NLS-mTOR D2357E

Figure 2

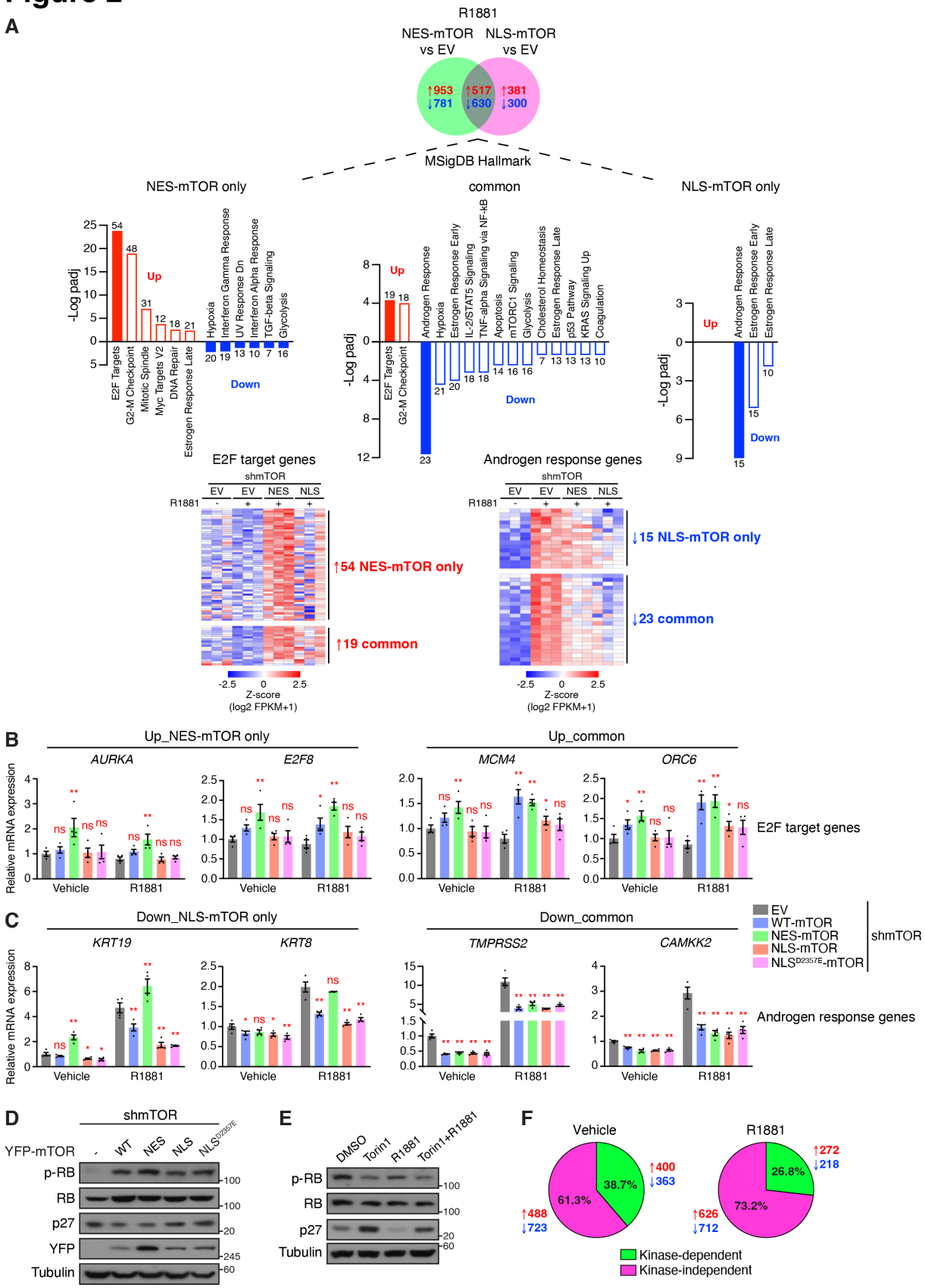
A
R1881
NES-mTOR vs EV
NLS-mTOR vs EV
↑953 ↓781
↑517 ↓630
↑381 ↓300
MSigDB Hallmark
NES-mTOR only
common
NLS-mTOR only
-Log padj
Up
Down
E2F Targets
G2-M Checkpoint
Mitotic Spindle
Myc Targets V2
DNA Repair
Estrogen Response Late
Hypoxia
Interferon Gamma Response
UV Response Dn
Interferon Alpha Response
TGF-beta Signaling
Glycolysis
Androgen Response
Estrogen Response Early
IL-2/STAT5 Signaling
TNF-alpha Signaling via NF-kB
Apoptosis
mTORC1 Signaling
Cholesterol Homeostasis
Estrogen Response Late
p53 Pathway
KRAS Signaling Up
Coagulation
E2F target genes
Androgen response genes
shmTOR
EV
NES
NLS
R1881
↑54 NES-mTOR only
↑19 common
↓15 NLS-mTOR only
↓23 common
Z-score
(log2 FPKM+1)
B
Up_NES-mTOR only
Up_common
AURKA
E2F8
MCM4
ORC6
Relative mRNA expression
Vehicle
R1881
E2F target genes
C
Down_NLS-mTOR only
Down_common
KRT19
KRT8
TMPRSS2
CAMKK2
EV
WT-mTOR
NES-mTOR
NLS-mTOR
NLSD2357E-mTOR
shmTOR
Androgen response genes
D
shmTOR
YFP-mTOR
WT
NES
NLS
NLSD2357E
p-RB
RB
p27
YFP
Tubulin
E
DMSO
Torin1
R1881
Torin1+R1881
F
Vehicle
R1881
38.7%
61.3%
↑400
↓363
↑488
↓723
26.8%
73.2%
↑272
↓218
↑626
↓712
Kinase-dependent
Kinase-independent

Figure 3

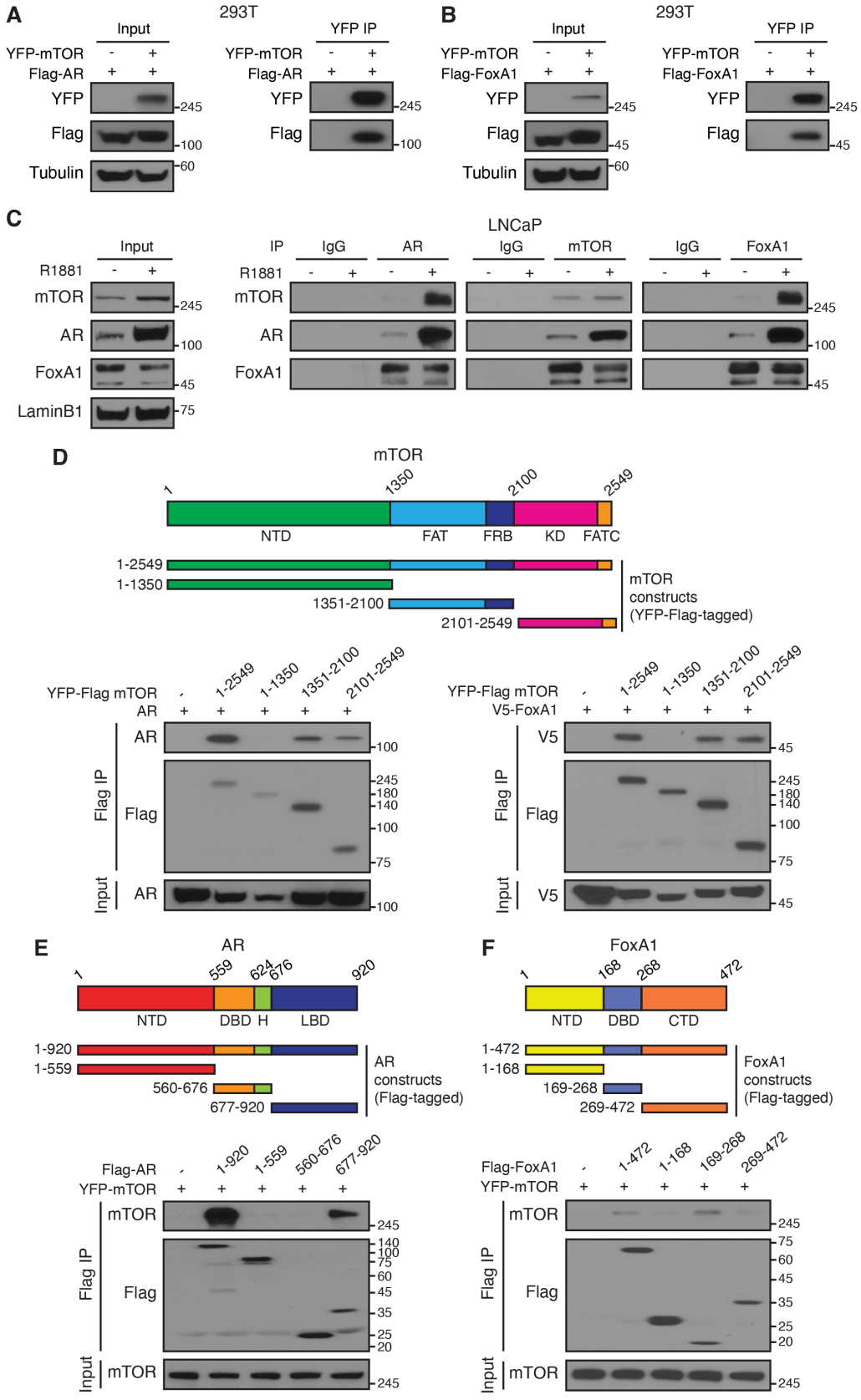
A
Input
293T
YFP IP
YFP-mTOR
Flag-AR
YFP
Flag
Tubulin
245
100
60
B
Input
293T
YFP IP
YFP-mTOR
Flag-FoxA1
YFP
Flag
Tubulin
245
45
60
C
LNCaP
Input
IP
IgG
AR
IgG
mTOR
IgG
FoxA1
R1881
mTOR
AR
FoxA1
LaminB1
245
100
45
75
D
mTOR
1
1350
2100
2549
NTD
FAT
FRB
KD
FATC
1-2549
1-1350
1351-2100
2101-2549
mTOR constructs (YFP-Flag-tagged)
YFP-Flag mTOR
AR
V5-FoxA1
Flag IP
Input
E
AR
1
559
624
676
920
NTD
DBD
H
LBD
1-920
1-559
560-676
677-920
AR constructs (Flag-tagged)
Flag-AR
YFP-mTOR
F
FoxA1
1
168
268
472
NTD
DBD
CTD
1-472
1-168
169-268
269-472
FoxA1 constructs (Flag-tagged)
Flag-FoxA1

Figure 4

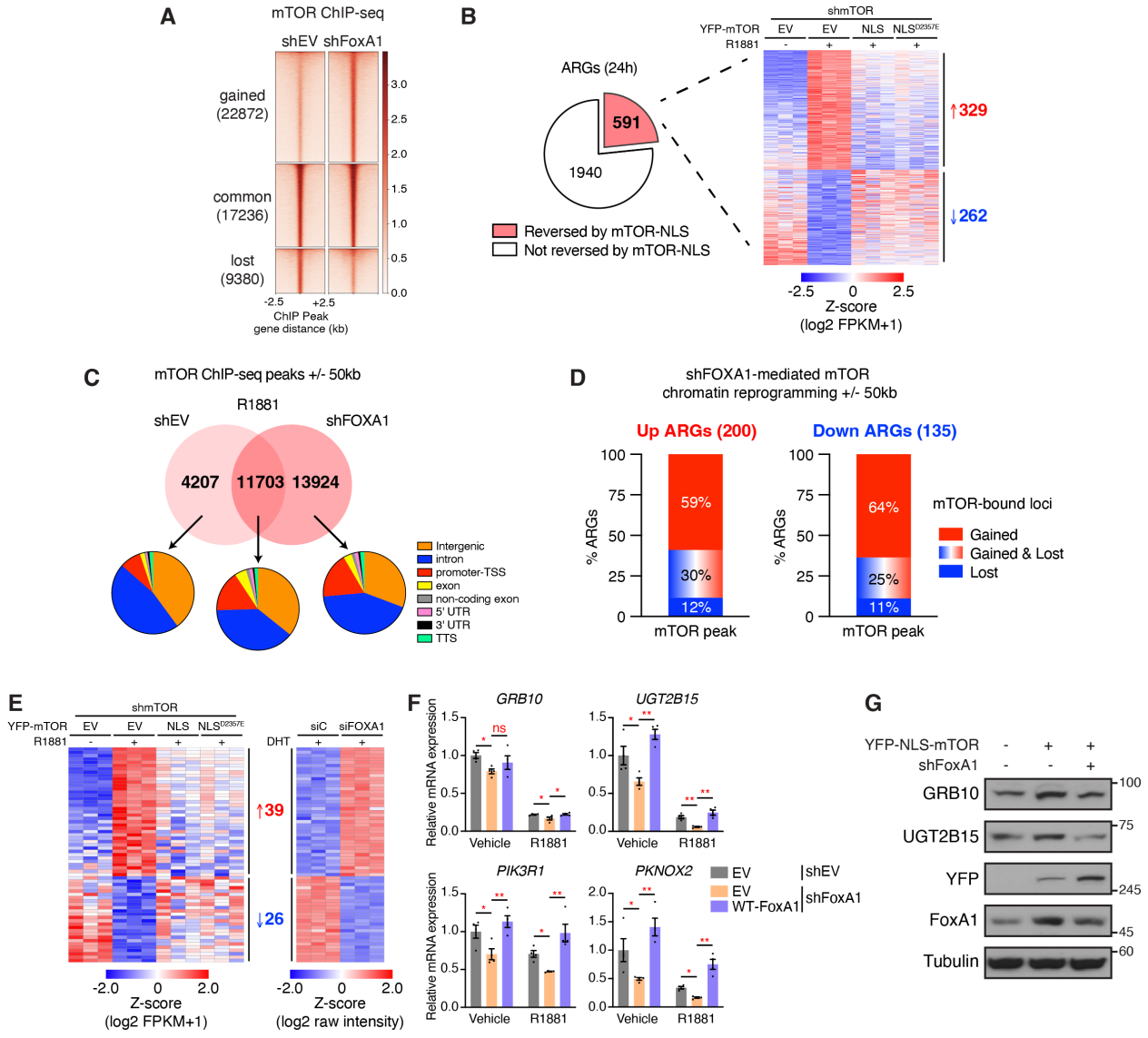
A
mTOR ChIP-seq
shEV shFoxA1
gained (22872)
common (17236)
lost (9380)
ChIP Peak gene distance (kb)
B
shmTOR
YFP-mTOR EV EV NLS NLS
R1881
ARGs (24h)
591
1940
Reversed by mTOR-NLS
Not reversed by mTOR-NLS
↑329
↓262
Z-score (log2 FPKM+1)
C
mTOR ChIP-seq peaks +/- 50kb
R1881
shEV
shFOXA1
4207
11703
13924
Intergenic
intron
promoter-TSS
exon
non-coding exon
5' UTR
3' UTR
TTS
D
shFOXA1-mediated mTOR chromatin reprogramming +/- 50kb
Up ARGs (200)
Down ARGs (135)
% ARGs
59%
30%
12%
64%
25%
11%
mTOR peak
mTOR-bound loci
Gained
Gained & Lost
Lost
E
shmTOR
YFP-mTOR EV EV NLS NLS
R1881
DHT
siC siFOXA1
↑39
↓26
Z-score (log2 FPKM+1)
Z-score (log2 raw intensity)
F
GRB10
UGT2B15
PIK3R1
PKNOX2
Relative mRNA expression
Vehicle
R1881
EV
EV
WT-FoxA1
shEV
shFoxA1
G
YFP-NLS-mTOR - + +
shFoxA1 - - +
GRB10
UGT2B15
YFP
FoxA1
Tubulin
100
75
245
45
60

Figure 5

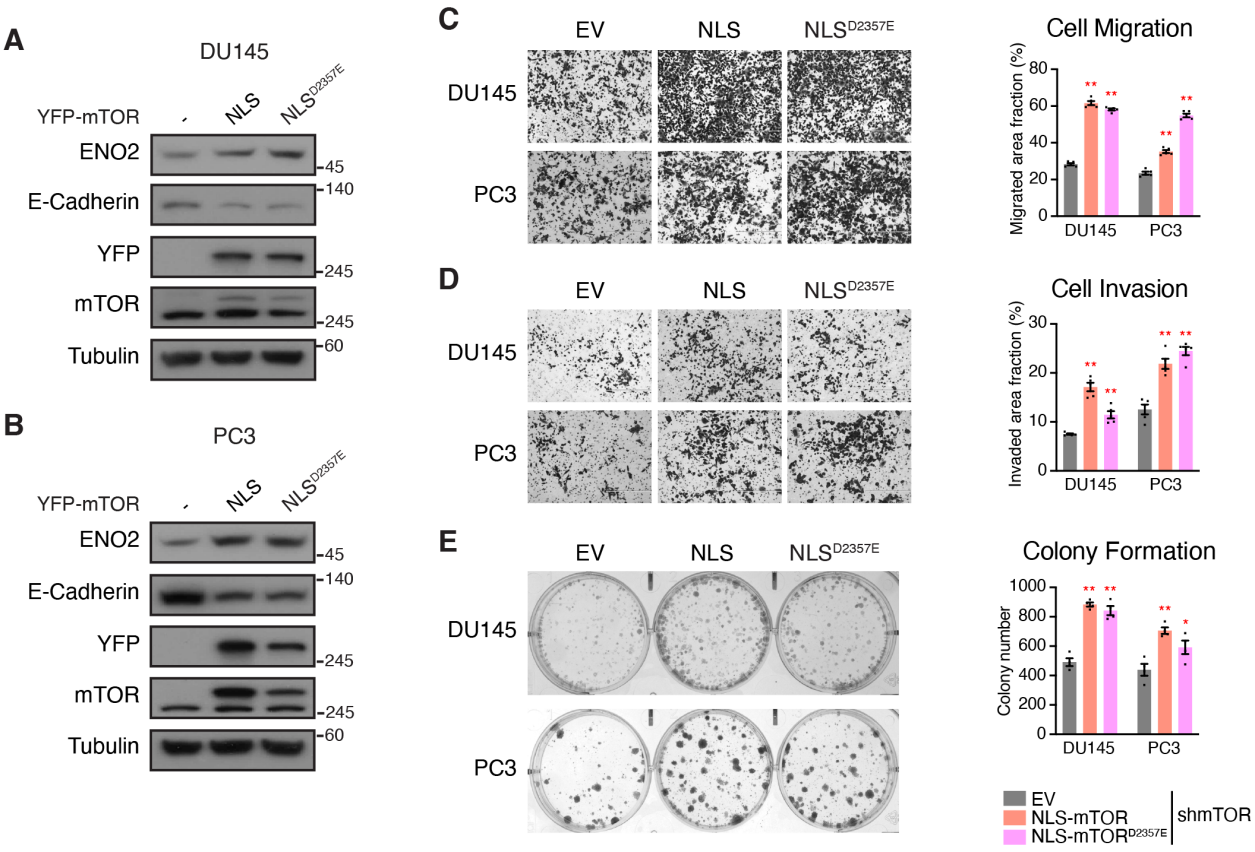
A
DU145
YFP-mTOR
-
NLS
NLS^D2357E
ENO2
E-Cadherin
YFP
mTOR
Tubulin
45
140
245
245
60
B
PC3
YFP-mTOR
-
NLS
NLS^D2357E
ENO2
E-Cadherin
YFP
mTOR
Tubulin
45
140
245
245
60
C
EV
NLS
NLS^D2357E
DU145
PC3
Cell Migration
Migrated area fraction (%)
80
60
40
20
0
DU145
PC3
D
EV
NLS
NLS^D2357E
DU145
PC3
Cell Invasion
Invaded area fraction (%)
30
20
10
0
DU145
PC3
E
EV
NLS
NLS^D2357E
DU145
PC3
Colony Formation
Colony number
1000
800
600
400
200
0
DU145
PC3
EV
NLS-mTOR
NLS-mTOR^D2357E
shmTOR

Supplementary Figure 1

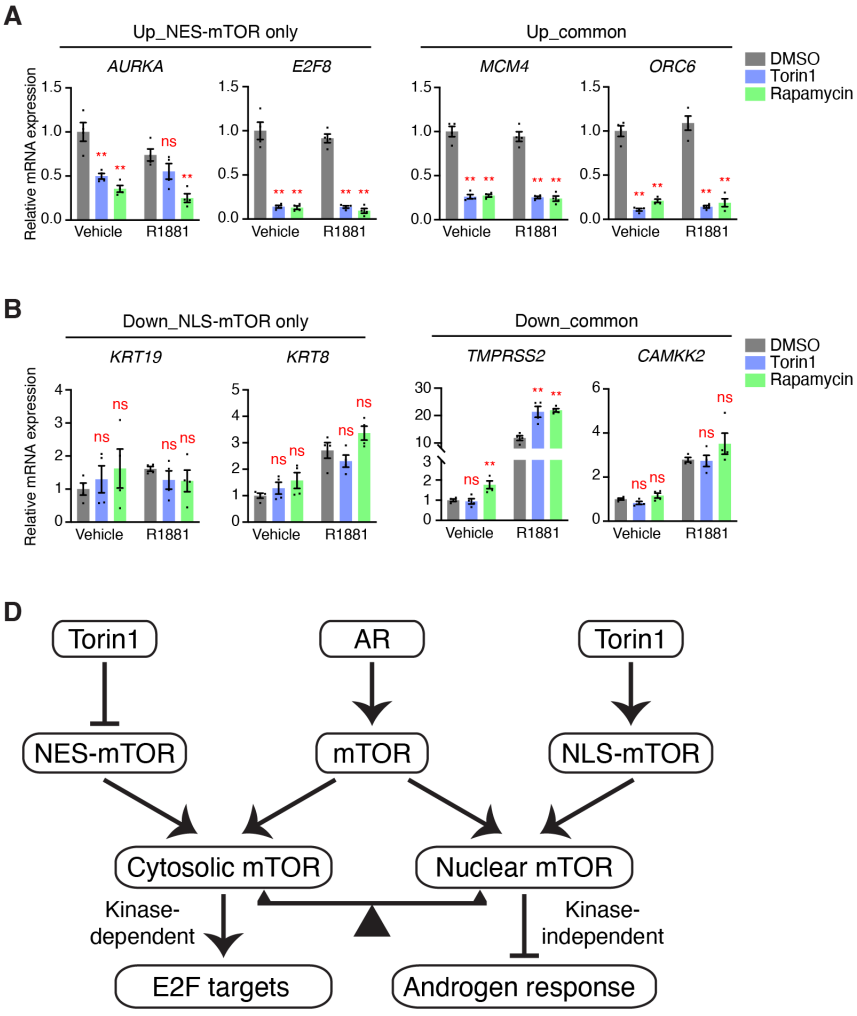

Supplementary Figure 2

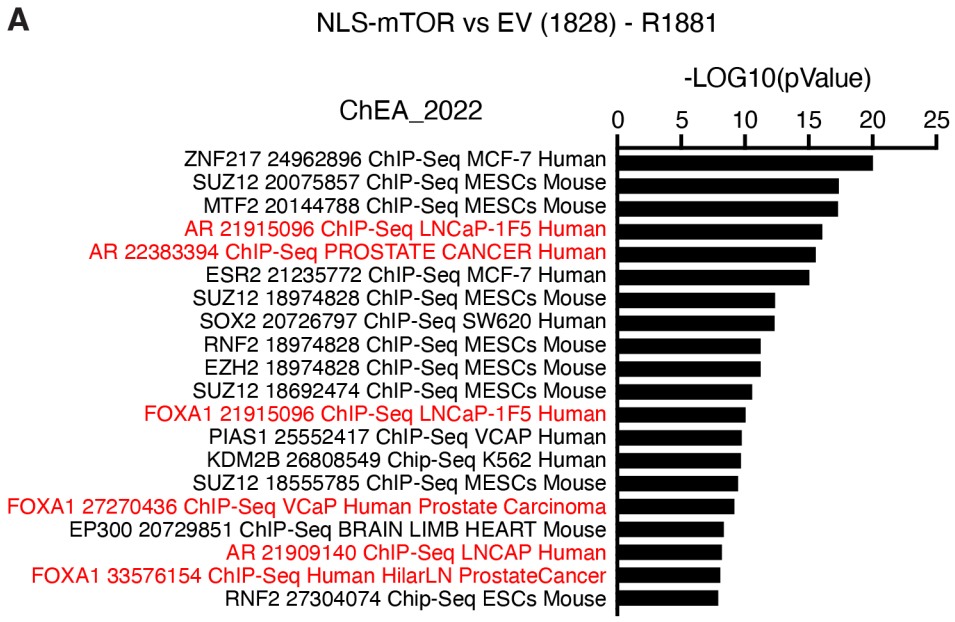

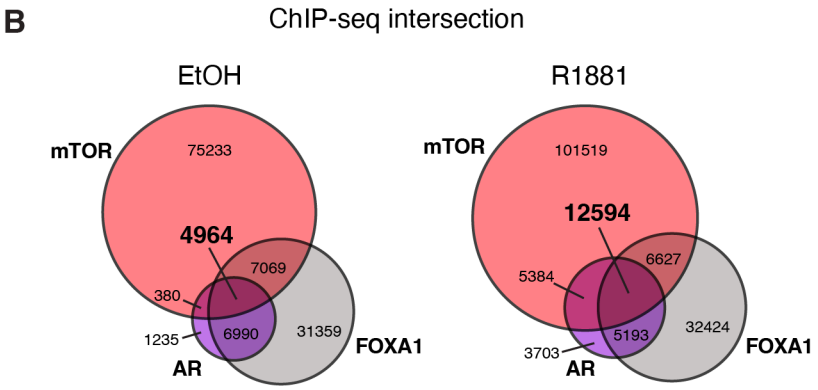

Supplementary Figure 3

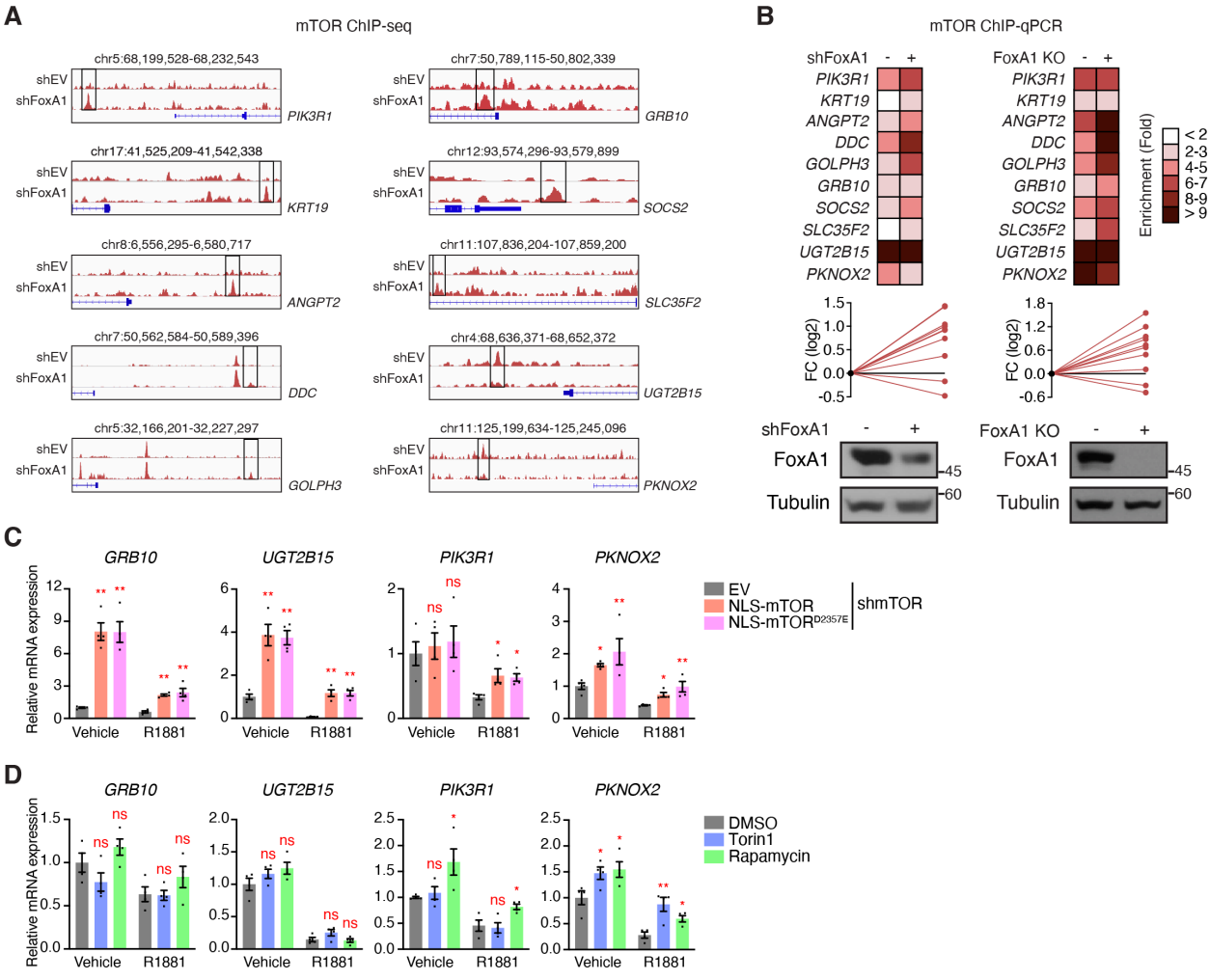

Supplementary Figure 4

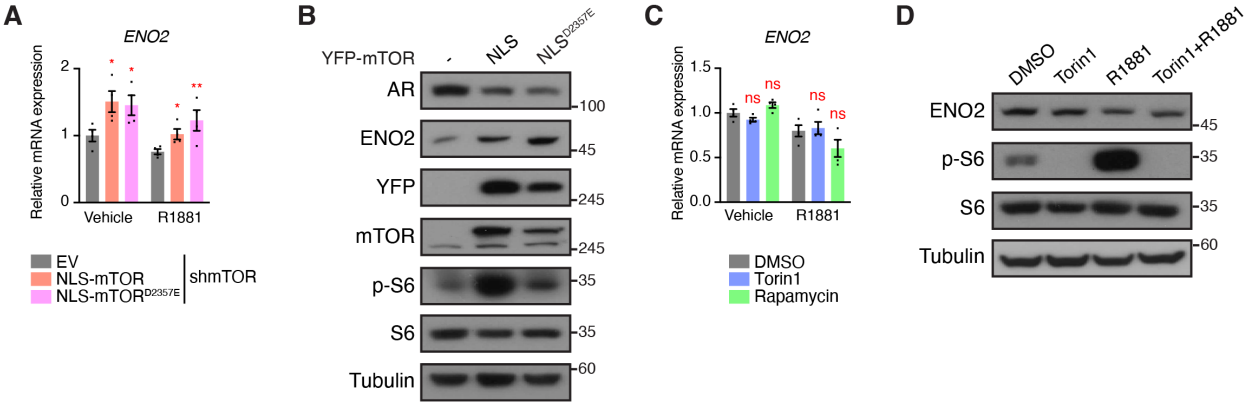

Chapter 4. Conclusion and Discussion

Conclusion

My PhD project has investigated the mechanisms by which mTOR regulates gene transcription in prostate cancer cells to impact AR signaling and PCa progression. It comprised two research sections. In the first section (Chapter 2), mTOR is found to indirectly control gene transcription by phosphorylating transcription factor HOXB13. HOXB13 phosphorylation by mTOR at Thr8 and Thr41 primes its further phosphorylation at Ser31. Functionally, phosphorylation of HOXB13 promotes its destabilization by E3-ligase SKP2 but enhances its transcriptional regulation on AR-HOXB13 co-target genes. Expression of HOXB13 phosphomimicking mutant (T8D+T41D+S31D) stimulates LNCaP PCa cells growth both in vitro and in murine xenografts. Transcriptional profiling study reveals that a phospho-HOXB13-dependent gene signature is capable of robustly discriminating between normal prostate tissues, primary and metastatic PCa samples. Altogether, mTOR phosphorylates HOXB13 to indirectly dictate a specific transcriptional program to promote PCa growth. In the second section (Chapter 3), mTOR is shown to directly control gene transcription by complexing with AR and FOXA1 on chromatin. Tagging mTOR with a NLS specifically guides mTOR translocation into the nucleus and thereby modulates nuclear mTOR (nmTOR) transcriptional activity. Transcriptomic analysis uncovers that nmTOR majorly down-regulates androgen response genes independent of its kinase activity. Mechanistically, nmTOR interacts with AR and FOXA1, and co-recruits them to the same genomic sites for transcriptional regulation, exerting inhibitory effects on a set of AR regulated genes. In addition, nmTOR induces the expression of the NEPC marker gene ENO2 and stimulates migration, invasion and proliferation of AR negative PCa cells. Taken together, I showed that mTOR complexes with AR and FOXA1 in the nucleus to directly abolish AR function and promote PCa androgen-independent progression.

In summary of the two research sections, mTOR not only indirectly regulates gene transcription which is dependent on its kinase activity, but also directly controls gene expression which is independent on its kinase activity. The kinase activity and transcriptional activity are two critical features required for mTOR function. Since the mTOR kinase inhibitor Torin1 could unexpectedly induce more mTOR nuclear translocation and higher transcription activity, combining therapy targeting both kinase and transcriptional activity will certainly help improve the efficiency to suppress mTOR action.

Discussion

mTOR mediated HOXB13 phosphorylation is a previously unrecognized regulation mechanism for HOXB13, which will help reconcile the current conflicts about HOXB13 roles in PCa (oncogene or tumor suppressor). Phosphorylated HOXB13 is oncogenic but also unstable, leading to confusion and contradicting conclusion when just detecting HOXB13 expression level in PCa patient tumors. Instead of the protein total abundance, HOXB13 phosphorylation level may be a promising marker for PCa diagnosis. Lacking commercial antibody specifically for phosphor-HOXB13, we are unable to verify the correlation between HOXB13 phosphorylation and PCa aggressiveness in clinical samples. Thus, it is necessarily important to develop phosphor-HOXB13 specific antibody in near future.

HOXB13 phosphor-mimic 3D significantly promotes prostate cancer cell growth in vitro and in vivo. Whether HOXB13 phosphorylation could also promote cancer metastasis is unknown. It is an intriguing question to study. Genetically Engineered Mouse model could be established by mutating HOXB13 phosphorylation sites to be phosphor-disabled or phosphor-mimicking particularly in prostate epithelial cells. It will definitely be one invariable tool to observe the impacts of HOXB13 phosphorylation in PCa initiation and progression. Since HOXB13 G84E as a phosphor-mimic mutant was shown before to maintain lipogenesis and stimulate prostate cancer metastasis [169], HOXB13 3D may be possibly involved in regulating metastasis. Also, HOXB13 phosphorylation at T8 and T41 primes its further phosphorylation at S31, thus whether G84E mutation can also trigger S31 phosphorylation is unknown. Although there is no one obviously additional upper band for HOXB13 G84E according to the immunoblot result, it is still likely that G84E could trigger small amount of S31 phosphorylation which is degraded

rapidly and not easy to be detected. In this case, it could help explain why G84E as the germline mutation just increases the risk of prostate cancer but does not have very prominent oncogenic effects. HOXB13 G84E may modestly promote S31 phosphorylation and consequently impact prostate tumorigenesis. In addition, HOXB13 phosphorylation certainly has changed its interactome which leads to differential effects on its target gene expression. Some target genes are really phosphor-HOXB13 dependent but others are not. Previous paper reported that WT HOXB13 but not G84E HOXB13 could interact with HDAC3 to inhibit the expression of FASN (Fatty Acid Synthase) [169]. Therefore, it is interesting to identify specific interactors for phosphorylated HOXB13, which will definitely help explain phosphor-HOXB13 dependent gene expression and growth advantage. HOXB13 phosphorylation is found to down-regulate Androgen Response genes, thus whether this regulation is mediated by disrupting or enhancing the interaction between phosphor-HOXB13 and AR requires further investigation. Lastly, the mechanisms for phosphor-HOXB13 to augment cell growth remain elusive. Several important pathways such as NF-KB signaling, IL2/STAT5 signaling and EMT process are revealed to be phosphor-HOXB13 dependent, which can contribute to the oncogenic function of phosphor-HOXB13. Some individual and critical effectors such as JAG1 and ACKR3 upregulated by phosphor-HOXB13 could be examined as well. Altogether, it is the phosphorylation level but not the total abundance of HOXB13 that determines its oncogenic property in prostate cancer, of which the mechanisms are required for deeper investigation.

One limitation of the study in Chapter 2 is that we did not verify HOXB13 physiological phosphorylation in vivo. Since HOXB13 phosphor-mimics could trigger S31 phosphorylation in cells which result in one additional upper band, S31 phosphorylation is highly likely to exist in

vivo. However, for in vivo validation of T8 and T41 phosphorylation, further investigation and more evidences are needed. Both sites were identified from mTOR in vitro kinase assay, which does not necessarily mean their phosphorylation can exist in vivo. Several approaches can be used to validate their physiological existence. One is to design and generate phosphorylation specific antibodies targeting HOXB13 T8, T41 and S31 phosphorylation individually. Certainly, those high-quality antibodies could enable us to detect those phosphorylation events in cells by immunoblotting and in tissues by immunohistochemistry. As positive and negative control, mTOR activation and inhibition should increase and decrease HOXB13 phosphorylation at three sites, respectively. Another approach is to immunoprecipitate endogenous HOXB13 and send for mass spectrometry to identify potential phosphorylation sites. Since endogenous HOXB13 is not very abundant, larger number of cells should be cultured and more amount of proteins should be used for HOXB13 immunoprecipitation in order to get better peptide coverage and quantity for HOXB13 in mass spectrometry detection.

HOXB13 is capable of interacting with both RAPTOR and RICTOR, suggesting its interaction with mTOR is independent of which canonic complex to be involved. Knockdown of both RAPTOR and RICTOR could increase HOXB13 protein level possibly by decreasing mTOR mediated phosphorylation. It implies both mTORC1 and mTORC2 could phosphorylate HOXB13. It is an interesting observation since very few proteins can be substrates for both complexes. Still, it can happen inside cells. One example is P53 which was reported to be bound and phosphorylated by both mTORC1 and mTORC2, leading to P53 stabilization and cell senescence induction [318]. Cell lysates were immunoprecipitated with anti-RAPTOR and anti-RICTOR antibody and then used for mTOR in vitro kinase assay in the addition of recombinant

P53 protein as the substrate. The results found both complexes can directly phosphorylate P53 at S15. Also, DEPTOR (DEP domain-containing mTOR interacting protein) was found to interact with mTOR, RAPTOR and RICTOR [190], indicating DEPTOR is a common factor shared by both complexes. Both mTORC1 and mTORC2 negatively regulate DEPTOR expression at the transcriptional and post-translational levels. Importantly, DEPTOR is phosphorylated at 13 serine/threonine sites in an mTOR dependent fashion. Back to our protein HOXB13, current data revealed that mTORC1 is responsible for S31 phosphorylation, but whether both mTORC1 and mTORC2 could phosphorylate T8 and T41 requires further study. In vitro kinase assay specific for mTORC1 or mTORC2 (using anti-RAPTOR or anti-RICTOR antibody to pull down their corresponding complex) could be conducted to test which site of HOXB13 is phosphorylated. Phosphor-HOXB13 specific antibodies targeting T8, T41 and S31 individually could help check whether disruption of each mTOR complex (shRNA mediated RAPTOR or RICTOR knockdown) could affect HOXB13 phosphorylation at these sites.

Post-translational modification is one important aspect to regulate the function of target proteins. It is an enzymatically covalent processing event by adding a modifying group to the side chain of amino acid residue, which is usually dynamically and reversibly regulated in cells. Phosphorylation by kinase and de-phosphorylation by phosphatase are two reversible modifications in cells to ensure protein function in a precise and sensitive way. Since my thesis here has demonstrated that mTOR as the kinase could phosphorylate HOXB13 at T8, T41 and S31, certain phosphatase is possibly existent to remove the phosphate group from these phosphorylation sites. There are around 200 phosphatases in human genome [319], and CRISPR screening or shRNA library screening by targeting these phosphatases could be practical to

uncover HOXB13 phosphatase. The readout needs HOXB13 phosphorylation specific antibodies to detect. Theoretically, site specific phosphorylation of HOXB13 will be increased after its phosphatase knockout or knockdown. In addition, the interaction between HOXB13 and its phosphatase may not necessarily be the determinant to confirm the phosphatase, because their interaction could be too transient and weak to detect. One way to validate the phosphatase candidate is to test whether the phosphatase could de-phosphorylate HOXB13 in vitro. Also, genetic knockdown or pharmacological inhibition of the phosphatase and overexpression of the phosphatase should significantly change the phosphorylation status of HOXB13 as expected in cells.

What is more, E3-ligase and De-ubiquitinase are two classes of enzymes to modify the ubiquitination level of target proteins. Since proteins such as PTEN have been reported to have more than two E3-ligase [320, 321], it is likely for HOXB13 to have multiple E3-ligases which can coordinate and cooperate together to regulate HOXB13 stability. My thesis here has proven SKP2 as one possible E3-ligase for HOXB13 which was originally predicted from a bioinformatics program, thus it may not be the strongest or the most dominant E3-ligase for HOXB13. Learning from one previous paper to find out the potential E3-ligase for SNAI2 [322], genome-wide E3-ligase siRNA library screening could be conducted. A dual-luciferase system needs to be generated by fusing HOXB13 coding sequence in frame with Firefly Luciferase coding sequence as the reporter and then co-transfecting with Renilla Luciferase as the internal control. Those E3-ligases whose knockdown resulted in more than two-fold increase of Firefly Luciferase/Renilla Luciferase ratio could be identified as the E3-ligase candidates for HOXB13. Then, the interaction between HOXB13 and those candidates should be tested experimentally by

co-immunoprecipitation assay. Functional validation by overexpressing or knocking down the E3-ligases should cause shorter or longer half-life of HOXB13 during the cycloheximide chase assay. The E3-ligase with strongest effects on HOXB13 protein stability could be chosen and focused for further investigation. Also, there are around 100 de-ubiquitinases in human genome [323], thus the same dual-luciferase reporter system could be easily used to screen out the possible de-ubiquitinase for HOXB13. All in all, with the identification of kinase and phosphatase, E3-ligase and De-ubiquitinase for HOXB13 could it enhance our understanding of the regulatory mechanisms for HOXB13 function and implicate possible drug targets for prostate cancer treatment.

Nuclear mTOR in Chapter 3 is shown to downregulate Androgen Response Genes regardless of its kinase activity. This previously unappreciated kinase independent function has certainly enhanced our understanding of mTOR biology. It is not surprising that many proteins used to be only regarded as cytoplasmic proteins could exert their non-canonical function in the nucleus and also independent of its intrinsic enzymatic activity. For example, PTEN could go into the nucleus to interact with APC (Anaphase Promoting Complex) to increase the tumor suppressive activity of APC-CDH complex and this function is PTEN phosphatase independent [324]. Mitochondrial kinase HK2 could localize in the nucleus of leukemic cells to maintain stemness and confer chemoresistance independently of its kinase activity [325].

The mechanisms for nuclear mTOR to regulate transcription are not well characterized. Similar to canonical mTOR to form two distinct complexes with diverse cofactors, nuclear mTOR is also assumed to interact and cooperate with many nuclear co-regulators such as these chromatin

remodelers, histone modifiers and transcription factors. Indeed, one recent proteomic study for nuclear mTOR identifies NuRD (Nucleosome Remodeling and Deacetylase) complex and SUMO epigenetic enzymes as the top two enriched classes of proteins [317], which may facilitate mTOR mediated transcriptional regulation. In addition, my data showed that transcription factor HOXB13, FOXA1 and AR all can interact with mTOR independently of each other. Domain interaction revealed that mTOR differentially interacts with HOXB13 N-terminal domain, FOXA1 DNA binding domain and AR ligand binding domain. It is interesting to check whether these four factors can exist in the same complex and whether the interaction between two factors could change the conformation and affect the interactions with other two factors. Also, in clinic FOXA1 has many hot-spot mutations in its DNA binding domain and AR has various mutations in its ligand binding domain as well, thus whether these mutations (locating at mTOR interacting regions) have increased or decreased affinity with mTOR remains elusive. It may need to investigate case by case. Certainly, it will result in dysregulated nuclear mTOR function since nuclear mTOR requires these factors for DNA binding and transcriptional regulation on target genes. In addition, whether mTOR as a kinase could phosphorylate AR and FOXA1 too? My thesis here failed to answer this question because recombinant GST-AR and GST-FOXA1 were not successfully expressed in bacteria and then cannot be used for mTOR in vitro kinase assay. GST-HOXB13 is a little small protein and thus can be easily expressed in bacteria. Further efforts are needed to solve this technical problem. Even though AR was reported before to be phosphorylated by mTOR at S96 (not in the ligand binding domain) in HCC (Hepatocellular Carcinoma) cells [310], it is still possible for mTOR to have unique phosphorylation sites for AR in prostate cancer cells. Also, if FOXA1 can also be

phosphorylated by mTOR, it will definitely enhance our understanding of the regulatory mechanism for this important pioneer factor.

Canonical mTORC1 activation requires amino acids stimulated mTOR recruitment to the lysosome surface where it meets growth factors activated RHEB. Canonical mTORC2 activation needs its cofactor mSIN1 binding to PIP3 generated by PI3K which releases the intrinsic inhibition of mSIN1 on mTOR kinase domain. However, the mechanisms for nuclear mTOR activation are not well studied. There may be two ways to activate nuclear mTOR. One is that mTOR could be activated via the canonical mechanisms in the cytoplasm first and then translocate into the nucleus [289, 326], and the other is that mTOR could translocate into the nucleus first and then be activated there by its unique nuclear activators. For the latter one, one paper reported that a small pool of active RHEB is present in the nucleus and required for nuclear mTORC1 activity [327]. The two ways here are not mutually exclusive but may work together for elaborate regulation of nuclear mTOR activity.

As for mTOR nuclear translocation, two possible mechanisms are proposed below. The first one is that mTOR may undergo certain post-translational modification which could facilitate mTOR to enter the nucleus. It is well known that post-translational modifications such as phosphorylation could affect protein subcellular localization by either sequestering the target proteins in the cytoplasm or promoting their shuttling into the nucleus. PTEN as one example that was regarded as pure cytosolic protein before can be still found in the nucleus. Mechanistically, PTEN is ubiquitinated by NEDD4-1 for nuclear trafficking but de-ubiquitinated by HAUSP for nuclear exclusion [328, 329], highlighting the ubiquitination to regulate PTEN

localization. As for mTOR, one previous mTOR proteomics study showed nuclear mTOR can strongly interact with SUMO (Small Ubiquitin-like Modifier) factors [317], implying SUMOylation to regulate mTOR localization. If true, several important aspects are needed to study. Which lysine residues of mTOR are SUMOylated? Considering that mTOR is a very large protein, it may be quite challenging to use mass spectrometry to identify the SUMOylation sites. Some bioinformatics program may help predict these possible sites, and mutating these sites should be additionally done to confirm the SUMOylation. Also, as a proof of concept, the SUMOylation defective mutant of mTOR should have difficulty to translocate into the nucleus. In addition, possible SUMO enzymes such as UBC9 should be uncovered for more detailed mechanisms to illustrate mTOR nuclear trafficking. Still, SUMOylation is one possibility, and other types of modification cannot be excluded currently.

The second possible mechanism is that mTOR may have certain chaperone protein to assist its nuclear translocation. Canonical theory for protein nuclear translocation is that NLS (Nuclear Localization Signal) sequence can be found in the primary sequence of target proteins, leading to importins mediated nuclear trafficking. However, none classic NLS is found in mTOR amino acid sequences. Therefore, mTOR has to go into the nucleus via a non-traditional way. One paper using biochemical methods successfully identified Hikeshi as a nuclear import carrier to transport HSP70 (Heat Shock Protein 70) into the nucleus independently of importin system [330]. it is possible for mTOR to have its unique chaperone for nuclear translocation too. Since this chaperone may have transient interaction with mTOR, mTOR immunoprecipitation coupled with mass spectrometry may have technical issues to identify it. In this case, BioID technique could be alternatively used [331]. First, a prokaryotic biotin ligase called BirA should be fused

with mTOR by molecular cloning. Second, stable cells with the expression of BirA-mTOR fusion protein should be established. Third, culturing cells in the presence of biotin could allow BirA to biotinylate mTOR interacting proteins. Lastly, streptavidin beads mediated affinity binding could pull down all the biotinylated proteins possibly interacting with mTOR, and mass spectrometry could help identify the potential interactors especially those weakly binding with mTOR. The chaperone for mTOR nuclear translocation may be likely uncovered in this way. With genetic knockdown or overexpression of this chaperone could we validate its effect on mTOR nuclear translocation. Taken together, the mechanism for mTOR to enter the nucleus is one important aspect to study nuclear mTOR function, of which the understanding may help us design drugs to prevent nuclear mTOR driven prostate cancer progression.

mTOR has two fractions, cytosolic mTOR and nuclear mTOR, which cooperate and coordinate together to contribute to cancer progression. Cytosolic mTOR functions via the canonical signaling by activating anabolism (such as protein synthesis, lipid synthesis and nucleotide synthesis) and inhibiting catabolism (such as autophagy). Protein synthesis is important for enzymes function and organelles biogenesis; lipid synthesis is required for membrane formation; nucleotide synthesis is sufficient for DNA replication. These processes work together to promote cell growth and proliferation. Nuclear mTOR I think may have cell-type specific function by accessing to different nuclear cofactors and effectors in different cells. For prostate cancer cells in my study, nuclear mTOR is found to majorly down-regulate Androgen Response genes, leading to AR independent prostate cancer progression. This is critical in clinic because it may contribute to drug resistance to AR pathway inhibition and drive AR negative prostate cancer development. Nuclear mTOR may be explored as a drug target for AR negative prostate cancer

treatment. Therefore, cytosolic mTOR generally promotes prostate cancer cell growth by activating these anabolic processes, while nuclear mTOR mainly promotes advance prostate cancer progression and confers drug resistance. Cytosolic mTOR function requires its kinase activity and nuclear mTOR function depends on its transcriptional activity, which suggests that targeting both kinase activity and transcriptional activity of mTOR could maximize the inhibitory effects on mTOR function and improve the outcome for prostate cancer treatment.

Nuclear mTOR function is independent of its kinase activity, and classical kinase inhibitors such as Torin1 have no inhibitory effects on the transcriptional activity of nuclear mTOR. Thus, other alternative approaches could be explored. ASO (Antisense Oligonucleotide) or CRISPR-Cas9 system targeting mTOR is possible to specifically reduce mTOR expression level and inhibit its function regardless of which mTOR fraction (cytosolic mTOR and nuclear mTOR). Also, learning from AR PROTAC (Proteolysis Targeting Chimera), nuclear mTOR specific PROTAC is rational to be designed and tested. PROTAC is consisted of two ligands connected by a linker that bind to a target protein and an E3-ligase, which can hijack the intracellular protein destruction machine (26S proteasome) to remove target proteins from cells [332]. PROTACs have the ability to target previously undruggable proteins [333], as they do not need to target the catalytic pockets. mTOR specific PROTAC can degrade both cytosolic and nuclear form of mTOR, while nuclear mTOR specific PROTAC is able to degrade the nuclear form only. One paper reported novel electrophilic PROTACs to only degrade nuclear FKBP12 by engaging DCAF16 (a substrate recognition component of CUL4-DDB1 E3-ligase complex) [334]. Nuclear protein specific PROTAC could be achieved by designing the ligand to specifically bind with a nuclear E3-ligase. Nuclear mTOR specific PROTAC helps to lower the dose used to degrade and

inhibit nuclear mTOR, while cytosolic mTOR function can be simply inhibited by classical kinase inhibitors. In summary, combining mTOR protein reduction with kinase activity inhibition could greatly improve the efficiency to suppress mTOR function.

Final Conclusion

mTOR regulates gene transcription in both indirect and direct ways. On one hand, mTOR phosphorylates HOXB13 to indirectly modulate gene expression, thereby promoting prostate cancer cell growth. It is dependent on the kinase activity of mTOR. On the other hand, mTOR complexes with AR and FOXA1 on chromatin to directly abrogate AR signaling, resulting in androgen independent prostate cancer progression. It is independent of mTOR kinase activity. In summary, mTOR requires its kinase activity and transcriptional activity to sufficiently regulate transcription in prostate cancer, which could be a promising drug target by inhibiting both activities.

References

1 Huggins C, Hodges CV. Studies on prostatic cancer I the effect of castration, of estrogen and androgen injection on serum phosphatases in metastatic carcinoma of the prostate. *CA Cancer J Clin* 1941; 22: 232-240.

2 Huggins C, Stevens RE, Hodges CV. Studies on prostate cancer II the effect of castration on advanced carcinoma of the prostate gland. *Arch Surg* 1941; 43: 209–223.

3 Chandrasekar T, Yang JC, Gao AC, Evans CP. Mechanisms of resistance in castration-resistant prostate cancer (CRPC). *Transl Androl Urol* 2015; 4: 365-380.

4 Watson PA, Arora VK, Sawyers CL. Emerging mechanisms of resistance to androgen receptor inhibitors in prostate cancer. *Nat Rev Cancer* 2015; 15: 701-711.

5 Hellerstedt BA, Pienta KJ. The current state of hormonal therapy for prostate cancer. *CA Cancer J Clin* 2002; 52: 154-179.

6 Zong Y, Goldstein AS. Adaptation or selection--mechanisms of castration-resistant prostate cancer. *Nat Rev Urol* 2013; 10: 90-98.

7 Mizokami A.; Koh E.; Fujita H.; Maeda Y.; Egawa M. *et al*. The adrenal androgen androstenediol is present in prostate cancer tissue after androgen deprivation therapy and activates mutated androgen receptor. *Cancer Research* 2004; 64: 765–771.

8 Mostaghel EA, Page ST, Lin DW, Fazli L, Coleman IM, True LD *et al*. Intraprostatic androgens and androgen-regulated gene expression persist after testosterone suppression: therapeutic implications for castration-resistant prostate cancer. *Cancer Res* 2007; 67: 5033-5041.

9 Visakorpi T.; Hyytinen E.; Koivisto P.; Tanner M.; Keinanen R. *et al*. In vivo amplification of the androgen receptor gene and progression of human prostate cancer. *Nature Genetics* 1995; 9: 401–406.

10 Gottlieb B, Beitel LK, Nadarajah A, Paliouras M, Trifiro M. The androgen receptor gene mutations database: 2012 update. *Hum Mutat* 2012; 33: 887-894.

11 Joseph JD, Lu N, Qian J, Sensintaffar J, Shao G, Brigham D *et al*. A clinically relevant androgen receptor mutation confers resistance to second-generation antiandrogens enzalutamide and ARN-509. *Cancer Discov* 2013; 3: 1020-1029.

12 Zhao XY. Malloy PJ. Aruna V. Krishnan. Swami S. *et al*. Glucocorticoids can promote androgen-independent growth of prostate cancer cells through a mutated androgen receptor. *Nature Medicine* 2000; 6: 703–706.

13 Hu R, Isaacs WB, Luo J. A snapshot of the expression signature of androgen receptor splicing variants and their distinctive transcriptional activities. *Prostate* 2011; 71: 1656-1667.

14 Hu R, Dunn TA, Wei S, Isharwal S, Veltri RW, Humphreys E *et al*. Ligand-independent androgen receptor variants derived from splicing of cryptic exons signify hormone-refractory prostate cancer. *Cancer Res* 2009; 69: 16-22.

15 Watson PA, Chen YF, Balbas MD, Wongvipat J, Socci ND, Viale A *et al*. Constitutively active androgen receptor splice variants expressed in castration-resistant prostate cancer require full-length androgen receptor. *Proc Natl Acad Sci U S A* 2010; 107: 16759-16765.

16 Arora VK, Schenkein E, Murali R, Subudhi SK, Wongvipat J, Balbas MD *et al*. Glucocorticoid receptor confers resistance to antiandrogens by bypassing androgen receptor blockade. *Cell* 2013; 155: 1309-1322.

17 Isikbay M, Otto K, Kregel S, Kach J, Cai Y, Vander Griend DJ *et al*. Glucocorticoid receptor activity contributes to resistance to androgen-targeted therapy in prostate cancer. *Horm Cancer* 2014; 5: 72-89.

18 Labbe DP, Brown M. Transcriptional Regulation in Prostate Cancer. *Cold Spring Harb Perspect Med* 2018; 8.

19 Tan HL, Sood A, Rahimi HA, Wang W, Gupta N, Hicks J *et al*. Rb loss is characteristic of prostatic small cell neuroendocrine carcinoma. *Clin Cancer Res* 2014; 20: 890-903.

20 Zhou Z, Flesken-Nikitin A, Corney DC, Wang W, Goodrich DW, Roy-Burman P *et al*. Synergy of p53 and Rb deficiency in a conditional mouse model for metastatic prostate cancer. *Cancer Res* 2006; 66: 7889-7898.

21 Mosquera JM, Beltran H, Park K, MacDonald TY, Robinson BD, Tagawa ST *et al*. Concurrent AURKA and MYCN gene amplifications are harbingers of lethal treatment-related neuroendocrine prostate cancer. *Neoplasia* 2013; 15: 1-10.

22 Lee JK, Phillips JW, Smith BA, Park JW, Stoyanova T, McCaffrey EF *et al*. N-Myc Drives Neuroendocrine Prostate Cancer Initiated from Human Prostate Epithelial Cells. *Cancer Cell* 2016; 29: 536-547.

23 Dardenne E, Beltran H, Benelli M, Gayvert K, Berger A, Puca L *et al*. N-Myc Induces an EZH2-Mediated Transcriptional Program Driving Neuroendocrine Prostate Cancer. *Cancer Cell* 2016; 30: 563-577.

24 Craft N. Chhor C. Tran C. Belldegrun A. DeKernion J. *et al*. Evidence for Clonal Outgrowth of Androgen-independent Prostate Cancer Cells from Androgen-dependent Tumors through a Two-Step Process. *Cancer Research* 1999; 59: 5030–5036.

25 Germann M, Wetterwald A, Guzman-Ramirez N, van der Pluijm G, Culig Z, Cecchini MG *et al*. Stem-like cells with luminal progenitor phenotype survive castration in human prostate cancer. *Stem Cells* 2012; 30: 1076-1086.

26 Magee JA, Piskounova E, Morrison SJ. Cancer stem cells: impact, heterogeneity, and uncertainty. *Cancer Cell* 2012; 21: 283-296.

27 Zhou BB, Zhang H, Damelin M, Geles KG, Grindley JC, Dirks PB. Tumour-initiating cells: challenges and opportunities for anticancer drug discovery. *Nat Rev Drug Discov* 2009; 8: 806-823.

28 Goldstein AS, Stoyanova T, Witte ON. Primitive origins of prostate cancer: in vivo evidence for prostate-regenerating cells and prostate cancer-initiating cells. *Mol Oncol* 2010; 4: 385-396.

29 Wang X, Kruithof-de Julio M, Economides KD, Walker D, Yu H, Halili MV *et al*. A luminal epithelial stem cell that is a cell of origin for prostate cancer. *Nature* 2009; 461: 495-500.

30 Lawson DA, Zong Y, Memarzadeh S, Xin L, Huang J, Witte ON. Basal epithelial stem cells are efficient targets for prostate cancer initiation. *Proc Natl Acad Sci U S A* 2010; 107: 2610-2615.

31 Huang J, Yao JL, di Sant'Agnese PA, Yang Q, Bourne PA, Na Y. Immunohistochemical characterization of neuroendocrine cells in prostate cancer. *Prostate* 2006; 66: 1399-1406.

32 Choi N, Zhang B, Zhang L, Ittmann M, Xin L. Adult murine prostate basal and luminal cells are self-sustained lineages that can both serve as targets for prostate cancer initiation. *Cancer Cell* 2012; 21: 253-265.

33 Goldstein AS. Huang J. Guo C. Garraway IP. Witte ON. Identification of a Cell of Origin for Human Prostate Cancer. *Science* 2010; 329: 568–571.

34 Formaggio N, Rubin MA, Theurillat JP. Loss and revival of androgen receptor signaling in advanced prostate cancer. *Oncogene* 2021; 40: 1205-1216.

35 Mu P. Zhang Z. Benelli M. Karthaus WR. Hoover E *et al*. SOX2 promotes lineage plasticity and antiandrogen resistance in TP53- and RB1-deficient prostate cancer. *Science* 2017; 355: 84–88.

36 Qiu X, Boufaied N, Hallal T, Feit A, de Polo A, Luoma AM *et al*. MYC drives aggressive prostate cancer by disrupting transcriptional pause release at androgen receptor targets. *Nat Commun* 2022; 13: 2559.

37 Bishop JL, Thaper D, Vahid S, Davies A, Ketola K, Kuruma H *et al*. The Master Neural Transcription Factor BRN2 Is an Androgen Receptor-Suppressed Driver of Neuroendocrine Differentiation in Prostate Cancer. *Cancer Discov* 2017; 7: 54-71.

38 Rotinen M, You S, Yang J, Coetzee SG, Reis-Sobreiro M, Huang WC *et al*. ONECUT2 is a targetable master regulator of lethal prostate cancer that suppresses the androgen axis. *Nat Med* 2018; 24: 1887-1898.

39 Nakayama T, Watanabe M, Suzuki H, Toyota M, Sekita N, Hirokawa Y *et al*. Epigenetic regulation of androgen receptor gene expression in human prostate cancers. *Lab Invest* 2000; 80: 1789-1796.

40 Kleb B, Estecio MR, Zhang J, Tzelepi V, Chung W, Jelinek J *et al*. Differentially methylated genes and androgen receptor re-expression in small cell prostate carcinomas. *Epigenetics* 2016; 11: 184-193.

41 Ku SY. Rosario S. Wang Y. Mu P. Seshadri M *et al*. Rb1 and Trp53 cooperate to suppress prostate cancer lineage plasticity,metastasis, and antiandrogen resistance. *Science* 2017; 355: 78–83.

42 Lilja H, Ulmert D, Vickers AJ. Prostate-specific antigen and prostate cancer: prediction, detection and monitoring. *Nat Rev Cancer* 2008; 8: 268-278.

43 Telesca D, Etzioni R, Gulati R. Estimating lead time and overdiagnosis associated with PSA screening from prostate cancer incidence trends. *Biometrics* 2008; 64: 10-19.

44 Ulmert D, Becker C, Nilsson JA, Piironen T, Bjork T, Hugosson J *et al*. Reproducibility and accuracy of measurements of free and total prostate-specific antigen in serum vs plasma after long-term storage at -20 degrees C. *Clin Chem* 2006; 52: 235-239.

45 D'Amico A. V. Renshaw A. A. Sussman B. Chen M. H. Pretreatment PSA Velocity and Risk of Death From Prostate Cancer Following External Beam Radiation Therapy. *JAMA* 2005; 294: 440–447.

46 D'Amico A. V. Chen M. H. Roehl K. A. Catalona W. J. Preoperative PSA Velocity and the Risk of Death from Prostate Cancer after Radical Prostatectomy. *NEJM* 2004; 351: 125–135.

47 Steuber T, Vickers AJ, Serio AM, Vaisanen V, Haese A, Pettersson K *et al*. Comparison of free and total forms of serum human kallikrein 2 and prostate-specific antigen for

prediction of locally advanced and recurrent prostate cancer. *Clin Chem* 2007; 53: 233-240.

48 Shafi AA, Yen AE, Weigel NL. Androgen receptors in hormone-dependent and castration-resistant prostate cancer. *Pharmacol Ther* 2013; 140: 223-238.

49 He B, Lee LW, Minges JT, Wilson EM. Dependence of selective gene activation on the androgen receptor NH2- and COOH-terminal interaction. *J Biol Chem* 2002; 277: 25631-25639.

50 Heery DM. Kalkhoven E. Hoare S. Parker MG. A signature motif in transcriptional co-activators mediates binding to nuclear receptors. *Nature* 1997; 387: 733–736.

51 Verrijdt G. Tanner T. Moehren U. Callewaert L. Haelens A. Claessens F. The androgen receptor DNA-binding domain determines androgen selectivity of transcriptional response. *Biochem Soc Trans* 2006; 34: 1089–1094.

52 Haelens A, Tanner T, Denayer S, Callewaert L, Claessens F. The hinge region regulates DNA binding, nuclear translocation, and transactivation of the androgen receptor. *Cancer Res* 2007; 67: 4514-4523.

53 van Royen ME, van Cappellen WA, de Vos C, Houtsmuller AB, Trapman J. Stepwise androgen receptor dimerization. *J Cell Sci* 2012; 125: 1970-1979.

54 Heemers HV, Tindall DJ. Androgen receptor (AR) coregulators: a diversity of functions converging on and regulating the AR transcriptional complex. *Endocr Rev* 2007; 28: 778-808.

55 McEwan IJ. Gustafsson J. Interaction of the human androgen receptor transactivation function with the general transcription factor TFIIF. *PNAS* 1997; 94: 8485–8490.

56 Lee DK, Duan HO, Chang C. From androgen receptor to the general transcription factor TFIIH. Identification of cdk activating kinase (CAK) as an androgen receptor NH(2)-terminal associated coactivator. *J Biol Chem* 2000; 275: 9308-9313.

57 Lee DK, Duan HO, Chang C. Androgen receptor interacts with the positive elongation factor P-TEFb and enhances the efficiency of transcriptional elongation. *J Biol Chem* 2001; 276: 9978-9984.

58 Wang Q, Li W, Liu XS, Carroll JS, Janne OA, Keeton EK *et al*. A hierarchical network of transcription factors governs androgen receptor-dependent prostate cancer growth. *Mol Cell* 2007; 27: 380-392.

59 Zhao JC, Fong KW, Jin HJ, Yang YA, Kim J, Yu J. FOXA1 acts upstream of GATA2 and AR in hormonal regulation of gene expression. *Oncogene* 2016; 35: 4335-4344.

60 Mills IG. Maintaining and reprogramming genomic androgen receptor activity in prostate cancer. *Nat Rev Cancer* 2014; 14: 187-198.

61 Pomerantz MM, Li F, Takeda DY, Lenci R, Chonkar A, Chabot M *et al*. The androgen receptor cistrome is extensively reprogrammed in human prostate tumorigenesis. *Nat Genet* 2015; 47: 1346-1351.

62 Li B, Carey M, Workman JL. The role of chromatin during transcription. *Cell* 2007; 128: 707-719.

63 Rouleau N. Domanskyi A. Reeben M. Moilanen AM. Havas K *et al*. Novel ATPase of SNF2-like Protein Family Interacts with Androgen Receptor and Modulates Androgen-dependent Transcription. *Biochem J* 2006; 393: 789–795.

64 Domanskyi A, Virtanen KT, Palvimo JJ, Janne OA. Biochemical characterization of androgen receptor-interacting protein 4. *Biochem J* 2006; 393: 789-795.

65 Marshall TW. Link KA. Petre-Draviam CE. Knudsen KE. Differential requirement of SWI/SNF for androgen receptor activity. *J Biol Chem* 2003; 278: 30605–30613.

66 Link KA. Burd CJ. Williams E. Marshall T. Rosson G. *et al*. BAF57 governs androgen receptor action and androgen-dependent proliferation through SWI/SNF. *Mol Cell Biol* 2005; 25: 2200–2215.

67 Hong CY, Suh JH, Kim K, Gong EY, Jeon SH, Ko M *et al*. Modulation of androgen receptor transactivation by the SWI3-related gene product (SRG3) in multiple ways. *Mol Cell Biol* 2005; 25: 4841-4852.

68 Shen M, Demers LK, Bailey SD, Labbe DP. To bind or not to bind: Cistromic reprogramming in prostate cancer. *Front Oncol* 2022; 12: 963007.

69 Fu M. Wang C. Reutens AT. Wang J. Angeletti RH *et al*. P300 and cAMP-response Element-binding Protein-associated Factor Acetylate the Androgen Receptor at Sites Governing Hormone-dependent Transactivation. *The journal of biological chemistry* 2000; 275: 20853–20860.

70 Alen P. Claessens F. Verhoeven G. Rombauts W. Peeters B. The androgen receptor amino-terminal domain plays a key role in p160 coactivator-stimulated gene transcription. *Mol Cell Biol* 1999; 19: 6085–6097.

71 Bevan CL. Hoare S. Claessens F. Heery DM. Parker MG. The AF1 and AF2 domains of the androgen receptor interact with distinct regions of SRC1. *Mol Cell Biol* 1999; 19: 8383–8392.

72 Zhou HJ, Yan J, Luo W, Ayala G, Lin SH, Erdem H *et al*. SRC-3 is required for prostate cancer cell proliferation and survival. *Cancer Res* 2005; 65: 7976-7983.

73 Chng KR, Chang CW, Tan SK, Yang C, Hong SZ, Sng NY *et al*. A transcriptional repressor co-regulatory network governing androgen response in prostate cancers. *EMBO J* 2012; 31: 2810-2823.

74 Zhao JC, Yu J, Runkle C, Wu L, Hu M, Wu D *et al*. Cooperation between Polycomb and androgen receptor during oncogenic transformation. *Genome Res* 2012; 22: 322-331.

75 Chen D. Ma H. Hong H. Koh SS. Huang SM *et al*. Regulation of transcription by a protein methyltransferase. *Science* 1999; 284: 2174–2177.

76 Wang H. Huang ZQ. Xia L. Feng Q. Erdjument-Bromage H. *et al*. Methylation of histone H4 at arginine 3 facilitating transcriptional activation by nuclear hormone receptor. *Science* 2001; 293: 853–857.

77 Cai C, He HH, Chen S, Coleman I, Wang H, Fang Z *et al*. Androgen receptor gene expression in prostate cancer is directly suppressed by the androgen receptor through recruitment of lysine-specific demethylase 1. *Cancer Cell* 2011; 20: 457-471.

78 Comstock CE, Knudsen KE. The complex role of AR signaling after cytotoxic insult: implications for cell-cycle-based chemotherapeutics. *Cell Cycle* 2007; 6: 1307-1313.

79 Wang Q, Li W, Zhang Y, Yuan X, Xu K, Yu J *et al*. Androgen receptor regulates a distinct transcription program in androgen-independent prostate cancer. *Cell* 2009; 138: 245-256.

80 Tomlins SA. Rhodes DR. Perner S. Dhanasekaran SM. *et al*. Recurrent Fusion of TMPRSS2 and ETS Transcription Factor Genes in Prostate Cancer. *Science* 2005; 310: 644-648.

81 Yu J, Yu J, Mani RS, Cao Q, Brenner CJ, Cao X *et al*. An integrated network of androgen receptor, polycomb, and TMPRSS2-ERG gene fusions in prostate cancer progression. *Cancer Cell* 2010; 17: 443-454.

82 Culig Z. Hobisch A. Cronauer MV. Radmayr C *et al*. Androgen Receptor Activation in Prostatic Tumor Cell Lines by Insulin-like Growth Factor-I, Keratinocyte Growth Factor, and Epidermal Growth Factor. *Cancer Research* 1994; 54: 5474-5478, .

83 Chen T. Wang L. Farrar W. Interleukin 6 Activates Androgen Receptor-mediated Gene Expression through a Signal Transducer and Activator of Transcription 3-dependent Pathway in LNCaP Prostate Cancer Cells. *Cancer Research* 2000; 60: 2132–2135.

84 Cheung S, Jain P, So J, Shahidi S, Chung S, Koritzinsky M. p38 MAPK Inhibition Mitigates Hypoxia-Induced AR Signaling in Castration-Resistant Prostate Cancer. *Cancers (Basel)* 2021; 13.

85 Edlind MP, Hsieh AC. PI3K-AKT-mTOR signaling in prostate cancer progression and androgen deprivation therapy resistance. *Asian J Androl* 2014; 16: 378-386.

86 Gao S, Gao Y, He HH, Han D, Han W, Avery A *et al*. Androgen Receptor Tumor Suppressor Function Is Mediated by Recruitment of Retinoblastoma Protein. *Cell Rep* 2016; 17: 966-976.

87 Niu Y. Altuwaijri S. Lai K. Wu C. Ricke WA *et al*. Androgen receptor is a tumor suppressor and proliferator in prostate cancer. *PNAS* 2008; 105: 12182–12187.

88 Grasso CS, Wu YM, Robinson DR, Cao X, Dhanasekaran SM, Khan AP *et al*. The mutational landscape of lethal castration-resistant prostate cancer. *Nature* 2012; 487: 239-243.

89 Taylor BS, Schultz N, Hieronymus H, Gopalan A, Xiao Y, Carver BS *et al*. Integrative genomic profiling of human prostate cancer. *Cancer Cell* 2010; 18: 11-22.

90 Li Y, Chan SC, Brand LJ, Hwang TH, Silverstein KA, Dehm SM. Androgen receptor splice variants mediate enzalutamide resistance in castration-resistant prostate cancer cell lines. *Cancer Res* 2013; 73: 483-489.

91 Liu LL, Xie N, Sun S, Plymate S, Mostaghel E, Dong X. Mechanisms of the androgen receptor splicing in prostate cancer cells. *Oncogene* 2014; 33: 3140-3150.

92 van der Steen T, Tindall DJ, Huang H. Posttranslational modification of the androgen receptor in prostate cancer. *Int J Mol Sci* 2013; 14: 14833-14859.

93 Coffey K, Robson CN. Regulation of the androgen receptor by post-translational modifications. *J Endocrinol* 2012; 215: 221-237.

94 Chen S. Xu Y. Yuan X. Bubley G. Balk S. Androgen receptor phosphorylation and stabilization in prostate cancer by cyclin-dependent kinase 1. *PNAS* 2006; 103: 15969–15974.

95 Gaughan L, Stockley J, Wang N, McCracken SR, Treumann A, Armstrong K *et al*. Regulation of the androgen receptor by SET9-mediated methylation. *Nucleic Acids Res* 2011; 39: 1266-1279.

96 Xu K, Shimelis H, Linn DE, Jiang R, Yang X, Sun F *et al*. Regulation of androgen receptor transcriptional activity and specificity by RNF6-induced ubiquitination. *Cancer Cell* 2009; 15: 270-282.

97 Nishida T, Yasuda H. PIAS1 and PIASxalpha function as SUMO-E3 ligases toward androgen receptor and repress androgen receptor-dependent transcription. *J Biol Chem* 2002; 277: 41311-41317.

98 Bono JS LC, Molina A, , Fizazi K, North S, Chu L, Chi KN, Jones RJ GO *et al*. Abiraterone and increased survival in metastatic prostate cancer. *N Engl J Med* 2011; 364: 1995-2005.

99 Efstathiou E, Titus M, Tsavachidou D, Tzelepi V, Wen S, Hoang A *et al*. Effects of abiraterone acetate on androgen signaling in castrate-resistant prostate cancer in bone. *J Clin Oncol* 2012; 30: 637-643.

100 Masiello D, Cheng S, Bubley GJ, Lu ML, Balk SP. Bicalutamide functions as an androgen receptor antagonist by assembly of a transcriptionally inactive receptor. *J Biol Chem* 2002; 277: 26321-26326.

101 Wong YN, Ferraldeschi R, Attard G, de Bono J. Evolution of androgen receptor targeted therapy for advanced prostate cancer. *Nat Rev Clin Oncol* 2014; 11: 365-376.

102 Tran C. Ouk S. Clegg NJ. Chen Y. Watson PA. Arora V *et al*. Development of a second-generation antiandrogen for treatment of advanced prostate cancer. *Science* 2009; 324: 787-790.

103 Scher HI, Beer TM, Higano CS, Anand A, Taplin ME, Efstathiou E *et al*. Antitumour activity of MDV3100 in castration-resistant prostate cancer: a phase 1-2 study. *Lancet* 2010; 375: 1437-1446.

104 Banuelos CA, Tavakoli I, Tien AH, Caley DP, Mawji NR, Li Z *et al*. Sintokamide A Is a Novel Antagonist of Androgen Receptor That Uniquely Binds Activation Function-1 in Its Amino-terminal Domain. *J Biol Chem* 2016; 291: 22231-22243.

105 Dalal K, Roshan-Moniri M, Sharma A, Li H, Ban F, Hessein M *et al*. Selectively targeting the DNA-binding domain of the androgen receptor as a prospective therapy for prostate cancer. *J Biol Chem* 2014; 289: 26417-26429.

106 Dalal K, Ban F, Li H, Morin H, Roshan-Moniri M, Tam KJ *et al*. Selectively targeting the dimerization interface of human androgen receptor with small-molecules to treat castration-resistant prostate cancer. *Cancer Lett* 2018; 437: 35-43.

107 De Velasco MA, Kura Y, Sakai K, Hatanaka Y, Davies BR, Campbell H *et al*. Targeting castration-resistant prostate cancer with androgen receptor antisense oligonucleotide therapy. *JCI Insight* 2019; 4.

108 Salami J, Alabi S, Willard RR, Vitale NJ, Wang J, Dong H *et al*. Androgen receptor degradation by the proteolysis-targeting chimera ARCC-4 outperforms enzalutamide in cellular models of prostate cancer drug resistance. *Commun Biol* 2018; 1: 100.

109 Perry AS, Watson RW, Lawler M, Hollywood D. The epigenome as a therapeutic target in prostate cancer. *Nat Rev Urol* 2010; 7: 668-680.

110 Xiao L. Parolia A. Qiao Y. Bawa P. Eyunni S. Ramachandra M. Chinnaiyan AM. Targeting SWI/SNF ATPases in enhancer-addicted prostate cancer. *Nature* 2022; 601: 434-439.

111 Kim KH, Roberts CW. Targeting EZH2 in cancer. *Nat Med* 2016; 22: 128-134.

112 Welti J. Sharp A. Brooks N. Yuan W. McNair C. Chand SN. Pegg N. Bono JS. Targeting the p300/CBP Axis in Lethal Prostate Cancer. *Cancer Discov* 2021; 11: 1118–1137.

113 Sato S, Katsushima K, Shinjo K, Hatanaka A, Ohka F, Suzuki S *et al*. Histone Deacetylase Inhibition in Prostate Cancer Triggers miR-320-Mediated Suppression of the Androgen Receptor. *Cancer Res* 2016; 76: 4192-4204.

114 Castaneda M, Hollander PD, Mani SA. Forkhead Box Transcription Factors: Double-Edged Swords in Cancer. *Cancer Res* 2022; 82: 2057-2065.

115 KL. C, ED. H, E. L, SK B. Co-crystal structure of the HNF-3/Forkhead DNA-recognition motif resembles histone H5. *Nature* 1993; 364: 412-420.

116 Cirillo LA. McPherson CE. Bossard P. Stevens K *et al*. Binding of the winged-helix transcription factor HNF3 to a linker histone site on the nucleosome. *EMBO J* 1998; 17: 244-254.

117 Cirillo LA. Lin FR. Cuesta I. Friedman D. Jarnik M. Zaret KS. Opening of Compacted Chromatin by Early Developmental Transcription Factors HNF3 (FoxA) and GATA-4. *Mol Cell* 2002; 9: 279-289.

118 Lupien M, Eeckhoute J, Meyer CA, Wang Q, Zhang Y, Li W *et al*. FoxA1 translates epigenetic signatures into enhancer-driven lineage-specific transcription. *Cell* 2008; 132: 958-970.

119 Serandour AA, Avner S, Percevault F, Demay F, Bizot M, Lucchetti-Miganeh C *et al*. Epigenetic switch involved in activation of pioneer factor FOXA1-dependent enhancers. *Genome Res* 2011; 21: 555-565.

120 Carroll JS, Liu XS, Brodsky AS, Li W, Meyer CA, Szary AJ *et al*. Chromosome-wide mapping of estrogen receptor binding reveals long-range regulation requiring the forkhead protein FoxA1. *Cell* 2005; 122: 33-43.

121 Jin HJ, Zhao JC, Wu L, Kim J, Yu J. Cooperativity and equilibrium with FOXA1 define the androgen receptor transcriptional program. *Nat Commun* 2014; 5: 3972.

122 Hurtado A, Holmes KA, Ross-Innes CS, Schmidt D, Carroll JS. FOXA1 is a key determinant of estrogen receptor function and endocrine response. *Nat Genet* 2011; 43: 27-33.

123 Seachrist DD, Anstine LJ, Keri RA. FOXA1: A Pioneer of Nuclear Receptor Action in Breast Cancer. *Cancers (Basel)* 2021; 13.

124 Sahu B, Laakso M, Ovaska K, Mirtti T, Lundin J, Rannikko A *et al*. Dual role of FoxA1 in androgen receptor binding to chromatin, androgen signalling and prostate cancer. *EMBO J* 2011; 30: 3962-3976.

125 Yang YA, Yu J. Current perspectives on FOXA1 regulation of androgen receptor signaling and prostate cancer. *Genes Dis* 2015; 2: 144-151.

126 Dong HY, Ding L, Zhou TR, Yan T, Li J, Liang C. FOXA1 in prostate cancer. *Asian J Androl* 2022.

127 Imamura Y, Sakamoto S, Endo T, Utsumi T, Fuse M, Suyama T *et al*. FOXA1 promotes tumor progression in prostate cancer via the insulin-like growth factor binding protein 3 pathway. *PLoS One* 2012; 7: e42456.

128 Gerhardt J, Montani M, Wild P, Beer M, Huber F, Hermanns T *et al*. FOXA1 promotes tumor progression in prostate cancer and represents a novel hallmark of castration-resistant prostate cancer. *Am J Pathol* 2012; 180: 848-861.

129 Robinson JL, Hickey TE, Warren AY, Vowler SL, Carroll T, Lamb AD *et al*. Elevated levels of FOXA1 facilitate androgen receptor chromatin binding resulting in a CRPC-like phenotype. *Oncogene* 2014; 33: 5666-5674.

130 Jain RK, Mehta RJ, Nakshatri H, Idrees MT, Badve SS. High-level expression of forkhead-box protein A1 in metastatic prostate cancer. *Histopathology* 2011; 58: 766-772.

131 Wang X, Brea L, Lu X, Gritsina G, Park SH, Xie W *et al*. FOXA1 inhibits hypoxia programs through transcriptional repression of HIF1A. *Oncogene* 2022; 41: 4259-4270.

132 Wang D, Garcia-Bassets I, Benner C, Li W, Su X, Zhou Y *et al*. Reprogramming transcription by distinct classes of enhancers functionally defined by eRNA. *Nature* 2011; 474: 390-394.

133 Song B, Park SH, Zhao JC, Fong KW, Li S, Lee Y *et al*. Targeting FOXA1-mediated repression of TGF-beta signaling suppresses castration-resistant prostate cancer progression. *J Clin Invest* 2019; 129: 569-582.

134 Zhang C, Wang L, Wu D, Chen H, Chen Z, Thomas-Ahner JM *et al*. Definition of a FoxA1 Cistrome that is crucial for G1 to S-phase cell-cycle transit in castration-resistant prostate cancer. *Cancer Res* 2011; 71: 6738-6748.

135 Jin HJ, Zhao JC, Ogden I, Bergan RC, Yu J. Androgen receptor-independent function of FoxA1 in prostate cancer metastasis. *Cancer Res* 2013; 73: 3725-3736.

136 Kim J, Jin H, Zhao JC, Yang YA, Li Y, Yang X *et al*. FOXA1 inhibits prostate cancer neuroendocrine differentiation. *Oncogene* 2017; 36: 4072-4080.

137 Baca SC, Takeda DY, Seo JH, Hwang J, Ku SY, Arafeh R *et al*. Reprogramming of the FOXA1 cistrome in treatment-emergent neuroendocrine prostate cancer. *Nat Commun* 2021; 12: 1979.

138 Yang YA, Zhao JC, Fong KW, Kim J, Li S, Song C *et al*. FOXA1 potentiates lineage-specific enhancer activation through modulating TET1 expression and function. *Nucleic Acids Res* 2016; 44: 8153-8164.

139 Han M, Li F, Zhang Y, Dai P, He J, Li Y *et al*. FOXA2 drives lineage plasticity and KIT pathway activation in neuroendocrine prostate cancer. *Cancer Cell* 2022; 40: 1306-1323 e1308.

140 Teng M, Zhou S, Cai C, Lupien M, He HH. Pioneer of prostate cancer: past, present and the future of FOXA1. *Protein Cell* 2021; 12: 29-38.

141 Li J. Xu C. Lee HJ. Ren S. Zi X *et al*. A genomic and epigenomic atlas of prostate cancer in Asian populations. *Nature* 2020; 580: 93-99.

142 Barbieri CE. Baca SC. Lawrence MS. Demichelis F. Rubin MA. Garraway LA. Exome sequencing identifies recurrent SPOP, FOXA1 and MED12 mutations in prostate cancer. *Nature Genetics* 2012; 44: 685-689.

143 Parolia A, Cieslik M, Chu SC, Xiao L, Ouchi T, Zhang Y *et al*. Distinct structural classes of activating FOXA1 alterations in advanced prostate cancer. *Nature* 2019; 571: 413-418.

144 Adams EJ, Karthaus WR, Hoover E, Liu D, Gruet A, Zhang Z *et al*. FOXA1 mutations alter pioneering activity, differentiation and prostate cancer phenotypes. *Nature* 2019; 571: 408-412.

145 Gao S. Chen S. Han D. Barrett D. Han W *et al*. Forkhead domain mutations in FOXA1 drive prostate cancer progression. *Cell Res* 2019; 29: 770–772.

146 Zhou S. Hawley JR. Soares F. Grillo G. Teng M *et al*. Noncoding mutations target cis-regulatory elements of the FOXA1 plexus in prostate cancer. *Nature Communication* 2020; 441: 1-13.

147 Annala M. Taavitsainen S. Vandekerkhove G. Bacon JVW *et al*. Frequent mutation of the FOXA1 untranslated region in prostate cancer. *Commun Biol* 2018; 122: 1-8.

148 Kohler S, Cirillo LA. Stable chromatin binding prevents FoxA acetylation, preserving FoxA chromatin remodeling. *J Biol Chem* 2010; 285: 464-472.

149 Yamaguchi N, Shibazaki M, Yamada C, Anzai E, Morii M, Nakayama Y *et al*. Tyrosine Phosphorylation of the Pioneer Transcription Factor FoxA1 Promotes Activation of Estrogen Signaling. *J Cell Biochem* 2017; 118: 1453-1461.

150 Sutinen P, Rahkama V, Rytinki M, Palvimo JJ. Nuclear mobility and activity of FOXA1 with androgen receptor are regulated by SUMOylation. *Mol Endocrinol* 2014; 28: 1719-1728.

151 Park SH. Fong K. Kim J. Wang F. Lu X. Zhao JC. Yu J. Posttranslational regulation of FOXA1 by Polycomb and BUB3/USP7 deubiquitin complex in prostate cancer. *Sci Adv* 2021; 7: 1-16.

152 Gao S, Chen S, Han D, Wang Z, Li M, Han W *et al*. Chromatin binding of FOXA1 is promoted by LSD1-mediated demethylation in prostate cancer. *Nat Genet* 2020; 52: 1011-1017.

153 Yu M, Zhan J, Zhang H. HOX family transcription factors: Related signaling pathways and post-translational modifications in cancer. *Cell Signal* 2020; 66: 109469.

154 Bhatlekar S, Fields JZ, Boman BM. HOX genes and their role in the development of human cancers. *J Mol Med (Berl)* 2014; 92: 811-823.

155 Hankey W, Chen Z, Wang Q. Shaping Chromatin States in Prostate Cancer by Pioneer Transcription Factors. *Cancer Res* 2020; 80: 2427-2436.

156 Johng D, Torga G, Ewing CM, Jin K, Norris JD, McDonnell DP *et al*. HOXB13 interaction with MEIS1 modifies proliferation and gene expression in prostate cancer. *Prostate* 2019; 79: 414-424.

157 Economides KD, Capecchi MR. HoxB13 is required for normal differentiation and secretory function of the ventral prostate. *Development* 2003; 130: 2061-2069.

158 Stelloo S, Nevedomskaya E, Kim Y, Hoekman L, Bleijerveld OB, Mirza T *et al*. Endogenous androgen receptor proteomic profiling reveals genomic subcomplex involved in prostate tumorigenesis. *Oncogene* 2018; 37: 313-322.

159 Norris JD, Chang CY, Wittmann BM, Kunder RS, Cui H, Fan D *et al*. The homeodomain protein HOXB13 regulates the cellular response to androgens. *Mol Cell* 2009; 36: 405-416.

160 Yao J, Chen Y, Nguyen DT, Thompson ZJ, Eroshkin AM, Nerlakanti N *et al*. The Homeobox gene, HOXB13, Regulates a Mitotic Protein-Kinase Interaction Network in Metastatic Prostate Cancers. *Sci Rep* 2019; 9: 9715.

161 Huang Q, Whitington T, Gao P, Lindberg JF, Yang Y, Sun J *et al*. A prostate cancer susceptibility allele at 6q22 increases RFX6 expression by modulating HOXB13 chromatin binding. *Nat Genet* 2014; 46: 126-135.

162 Liu Z, Ren G, Shangguan C, Guo L, Dong Z, Li Y *et al*. ATRA inhibits the proliferation of DU145 prostate cancer cells through reducing the methylation level of HOXB13 gene. *PLoS One* 2012; 7: e40943.

163 Hamid SM. Cicek S. Karamil S. Ozturk MB. Butuner BD *et al*. HOXB13 contributes to G1/S and G2/M checkpoint controls in prostate. *Molecular and Cellular Endocrinology* 2014; 383: 38-47.

164 VanOpstall C, Perike S, Brechka H, Gillard M, Lamperis S, Zhu B *et al*. MEIS-mediated suppression of human prostate cancer growth and metastasis through HOXB13-dependent regulation of proteoglycans. *Elife* 2020; 9.

165 Jung C. Kim RS. Lee SJ. Wang C. Jeng MH. HOXB13 Homeodomain Protein Suppresses the Growth of Prostate Cancer Cells by the Negative Regulation of T-cell Factor 4. *Cancer Res* 2004; 64: 3046–3051.

166 Jung C. Kim RS. Zhang HJ. Lee SJ. Jeng MH. HOXB13 Induces Growth Suppression of Prostate Cancer Cells as a Repressor of Hormone-Activated Androgen Receptor Signaling. *Cancer Res* 2004; 64: 9185-9192.

167 Kim YR, Oh KJ, Park RY, Xuan NT, Kang TW, Kwon DD *et al*. HOXB13 promotes androgen independent growth of LNCaP prostate cancer cells by the activation of E2F signaling. *Mol Cancer* 2010; 9: 124.

168 Kim YR, Kim IJ, Kang TW, Choi C, Kim KK, Kim MS *et al*. HOXB13 downregulates intracellular zinc and increases NF-kappaB signaling to promote prostate cancer metastasis. *Oncogene* 2014; 33: 4558-4567.

169 Lu X, Fong KW, Gritsina G, Wang F, Baca SC, Brea LT *et al*. HOXB13 suppresses de novo lipogenesis through HDAC3-mediated epigenetic reprogramming in prostate cancer. *Nat Genet* 2022.

170 Chen Z, Wu D, Thomas-Ahner JM, Lu C, Zhao P, Zhang Q *et al*. Diverse AR-V7 cistromes in castration-resistant prostate cancer are governed by HoxB13. *Proc Natl Acad Sci U S A* 2018; 115: 6810-6815.

171 Ouhtit A. Al-Kindi MN. Kumar PR. Gupta I. Shanmuganathan S. Tamimi Y. HOXB13, a potential prognostic biomarker for prostate cancer. *Frontiers in Bioscience* 2016; 8: 40-45.

172 Brechka H, Bhanvadia RR, VanOpstall C, Vander Griend DJ. HOXB13 mutations and binding partners in prostate development and cancer: Function, clinical significance, and future directions. *Genes Dis* 2017; 4: 75-87.

173 Cardoso M. Maia S. Paulo P. Teixeira MR. Oncogenic mechanisms of HOXB13 missense mutations in prostate carcinogenesis. *oncoscience* 2016; 3: 288-296.

174 Ewing CM. Ray AM. Lange EM. Zuhlke KA *et al*. Germline Mutations in HOXB13 and Prostate-Cancer Risk. *NEJM* 2012; 366: 141-149.

175 Beebe-Dimmer JL, Hathcock M, Yee C, Okoth LA, Ewing CM, Isaacs WB *et al*. The HOXB13 G84E Mutation Is Associated with an Increased Risk for Prostate Cancer and Other Malignancies. *Cancer Epidemiol Biomarkers Prev* 2015; 24: 1366-1372.

176 Liu B, Wang T, Wang H, Zhang L, Xu F, Fang R *et al*. Oncoprotein HBXIP enhances HOXB13 acetylation and co-activates HOXB13 to confer tamoxifen resistance in breast cancer. *J Hematol Oncol* 2018; 11: 26.

177 Nguyen NUN, Canseco DC, Xiao F, Nakada Y, Li S, Lam NT *et al*. A calcineurin-Hoxb13 axis regulates growth mode of mammalian cardiomyocytes. *Nature* 2020; 582: 271-276.

178 Keith CT. Schreiber SL. PIK- related kinases DNA repair, recombination, and cell cycle checkpoints. *Science* 1995; 270: 50-51.

179 Heitman J. Movva NR. Hall MN. Targets for Cell Cycle Arrest by the Immunosuppressant Rapamycin in Yeast. *Science* 1991; 253: 905–909.

180 Liu GY, Sabatini DM. mTOR at the nexus of nutrition, growth, ageing and disease. *Nat Rev Mol Cell Biol* 2020; 21: 183-203.

181 Aylett C. Sauer E. Imseng S. Boehringer D. Hall MN. Ban N. Maier T. Architecture of human mTOR complex 1. *Science* 2016; 351: 48–52.

182 Chen X, Liu M, Tian Y, Li J, Qi Y, Zhao D *et al*. Cryo-EM structure of human mTOR complex 2. *Cell Res* 2018; 28: 518-528.

183 Yang H, Rudge DG, Koos JD, Vaidialingam B, Yang HJ, Pavletich NP. mTOR kinase structure, mechanism and regulation. *Nature* 2013; 497: 217-223.

184 Kim J, Guan KL. mTOR as a central hub of nutrient signalling and cell growth. *Nat Cell Biol* 2019; 21: 63-71.

185 Kim DH. Sarbassov DD. Ali SM. King JE. Latek RR *et al*. mTOR Interacts with Raptor to Form a Nutrient-Sensitive Complex that Signals to the Cell Growth Machinery. *Cell* 2002; 110: 163–175.

186 Hara K. Maruki Y. Long X. Yoshino K. Oshiro N *et al*. Raptor, a Binding Partner of Target of Rapamycin (TOR), Mediates TOR Action. *Cell* 2002; 110: 177–189.

187 Sarbassov DD, Ali SM, Kim DH, Guertin DA, Latek RR, Erdjument-Bromage H *et al*. Rictor, a novel binding partner of mTOR, defines a rapamycin-insensitive and raptor-independent pathway that regulates the cytoskeleton. *Curr Biol* 2004; 14: 1296-1302.

188 Jacinto E, Loewith R, Schmidt A, Lin S, Ruegg MA, Hall A *et al*. Mammalian TOR complex 2 controls the actin cytoskeleton and is rapamycin insensitive. *Nat Cell Biol* 2004; 6: 1122-1128.

189 Kim DH. Sarbassov DD. Ali SM. Latek RR. Guntur KVP *et al*. GβL, a positive regulator of the rapamycin- sensitive pathway required for the nutrient sensitive interaction between raptor and mTOR. *Mol Cell* 2003; 11: 895–904.

190 Peterson TR, Laplante M, Thoreen CC, Sancak Y, Kang SA, Kuehl WM *et al*. DEPTOR is an mTOR inhibitor frequently overexpressed in multiple myeloma cells and required for their survival. *Cell* 2009; 137: 873-886.

191 Vezina C. Kudelski A. Sehgal SN. RAPAMYCIN (AY-22,989), A NEW ANTIFUNGAL ANTIBIOTIC. *J Antibiot* 1975; 28: 721–726.

192 Sabatini DM. Twenty-five years of mTOR: Uncovering the link from nutrients to growth. *Proc Natl Acad Sci U S A* 2017; 114: 11818-11825.

193 Betz C, Hall MN. Where is mTOR and what is it doing there? *J Cell Biol* 2013; 203: 563-574.

194 Battaglioni S, Benjamin D, Walchli M, Maier T, Hall MN. mTOR substrate phosphorylation in growth control. *Cell* 2022; 185: 1814-1836.

195 Burnett PE. Barrow RK. Cohen NA. Snyder SH. Sabatini DM. RAFT1 phosphorylation of the translational regulators p70 S6kinase and 4E-BP1. *PNAS* 1998; 95: 1432–1437.

196 Gingras AC. Gygi SP. Raught B. Polakiewicz RD *et al*. Regulation of 4E- BP1 phosphorylation- a novel two- step mechanism. *Genes Dev* 1999; 13: 1422–1437.

197 Gingras AC, Raught B, Gygi SP, Niedzwiecka A, Miron M, Burley SK *et al*. Hierarchical phosphorylation of the translation inhibitor 4E-BP1. *Genes Dev* 2001; 15: 2852-2864.

198 Chauvin C, Koka V, Nouschi A, Mieulet V, Hoareau-Aveilla C, Dreazen A *et al*. Ribosomal protein S6 kinase activity controls the ribosome biogenesis transcriptional program. *Oncogene* 2014; 33: 474-483.

199 Hannan KM, Brandenburger Y, Jenkins A, Sharkey K, Cavanaugh A, Rothblum L *et al*. mTOR-dependent regulation of ribosomal gene transcription requires S6K1 and is mediated by phosphorylation of the carboxy-terminal activation domain of the nucleolar transcription factor UBF. *Mol Cell Biol* 2003; 23: 8862-8877.

200 Mayer C, Zhao J, Yuan X, Grummt I. mTOR-dependent activation of the transcription factor TIF-IA links rRNA synthesis to nutrient availability. *Genes Dev* 2004; 18: 423-434.

201 Michels AA, Robitaille AM, Buczynski-Ruchonnet D, Hodroj W, Reina JH, Hall MN *et al*. mTORC1 directly phosphorylates and regulates human MAF1. *Mol Cell Biol* 2010; 30: 3749-3757.

202 Shor B, Wu J, Shakey Q, Toral-Barza L, Shi C, Follettie M *et al*. Requirement of the mTOR kinase for the regulation of Maf1 phosphorylation and control of RNA polymerase III-dependent transcription in cancer cells. *J Biol Chem* 2010; 285: 15380-15392.

203 Thoreen CC, Chantranupong L, Keys HR, Wang T, Gray NS, Sabatini DM. A unifying model for mTORC1-mediated regulation of mRNA translation. *Nature* 2012; 485: 109-113.

204 Hsieh AC, Liu Y, Edlind MP, Ingolia NT, Janes MR, Sher A *et al*. The translational landscape of mTOR signalling steers cancer initiation and metastasis. *Nature* 2012; 485: 55-61.

205 Choo AY. Yoon SO. Kim SG. Roux PP. Blenis J. Rapamycin differentially inhibits S6Ks and 4E- BP1 to mediate cell- type-specific repression of mRNA translation. *PNAS* 2008; 105: 17414–17419.

206 Kang SA, Pacold ME, Cervantes CL, Lim D, Lou HJ, Ottina K *et al*. mTORC1 phosphorylation sites encode their sensitivity to starvation and rapamycin. *Science* 2013; 341: 1236566.

207 Dowling R. Topisirovic I. Alain T. Bidinosti M. Fonseca BD *et al*. mTORC1-Mediated Cell Proliferation,But Not Cell Growth, Controlledby the 4E-BPs. *Science* 2010; 328: 1172-1176.

208 Duvel K, Yecies JL, Menon S, Raman P, Lipovsky AI, Souza AL *et al*. Activation of a metabolic gene regulatory network downstream of mTOR complex 1. *Mol Cell* 2010; 39: 171-183.

209 Horton JD, Goldstein JL, Brown MS. SREBPs: activators of the complete program of cholesterol and fatty acid synthesis in the liver. *Journal of Clinical Investigation* 2002; 109: 1125-1131.

210 Peterson TR, Sengupta SS, Harris TE, Carmack AE, Kang SA, Balderas E *et al*. mTOR complex 1 regulates lipin 1 localization to control the SREBP pathway. *Cell* 2011; 146: 408-420.

211 Porstmann T, Santos CR, Griffiths B, Cully M, Wu M, Leevers S *et al*. SREBP activity is regulated by mTORC1 and contributes to Akt-dependent cell growth. *Cell Metab* 2008; 8: 224-236.

212 Audet-Walsh E, Vernier M, Yee T, Laflamme C, Li S, Chen Y *et al*. SREBF1 Activity Is Regulated by an AR/mTOR Nuclear Axis in Prostate Cancer. *Mol Cancer Res* 2018; 16: 1396-1405.

213 Kim JE. Chen J. Regulation of Peroxisome Proliferator Activated Receptor Activity by Mammalian Target of Rapamycin and Amino Acids in Adipogenesis. *Diabetes* 2004; 53: 2748–2756.

214 Le Bacquer O, Petroulakis E, Paglialunga S, Poulin F, Richard D, Cianflone K *et al*. Elevated sensitivity to diet-induced obesity and insulin resistance in mice lacking 4E-BP1 and 4E-BP2. *J Clin Invest* 2007; 117: 387-396.

215 Ben-Sahra I. Hoxhaj G. Ricoult SJH. Asara JM. Manning BD. mTORC1 induces purine synthesisthrough control of the mitochondrialtetrahydrofolate cycle. *Science* 2016; 351: 728–733.

216 Ben-Sahra I. Howell JJ. Asara JM. Manning BD. Stimulation of de Novo Pyrimidine Synthesis by Growth Signaling Through mTOR and S6K1. *Science* 2013; 339: 1323–1328.

217 Robitaille AM. Christen S. Shimobayashi M. Cornu M *et al*. Quantitative phosphoproteomics reveal mTORC1 activates de novo pyrimidine synthesis. *Science* 2013; 339: 1320–1323.

218 Dikic I, Elazar Z. Mechanism and medical implications of mammalian autophagy. *Nat Rev Mol Cell Biol* 2018; 19: 349-364.

219 Yu L, McPhee CK, Zheng L, Mardones GA, Rong Y, Peng J *et al*. Termination of autophagy and reformation of lysosomes regulated by mTOR. *Nature* 2010; 465: 942-946.

220 Kim J, Kundu M, Viollet B, Guan KL. AMPK and mTOR regulate autophagy through direct phosphorylation of Ulk1. *Nat Cell Biol* 2011; 13: 132-141.

221 Hosokawa N. Hara T. Kaizuka T. Kishi C. Takamura A *et al*. Nutrient-dependent mTORC1 Association with the ULK1–Atg13–FIP200 Complex Required for Autophagy. *Mol Biol Cell* 2009; 20: 1981–1991.

222 Kim YM, Jung CH, Seo M, Kim EK, Park JM, Bae SS *et al*. mTORC1 phosphorylates UVRAG to negatively regulate autophagosome and endosome maturation. *Mol Cell* 2015; 57: 207-218.

223 Martina JA, Chen Y, Gucek M, Puertollano R. mTORC1 functions as a transcriptional regulator of autophagy by preventing nuclear transport of TFEB. *Autophagy* 2012; 8: 903-914.

224 Martina JA. Diab HI. Lishu L. Jeong-A L. *et al*. The Nutrient-Responsive Transcription Factor TFE3 Promotes Autophagy, Lysosomal Biogenesis, and Clearance of Cellular Debris. *Science Signaling* 2014; 7: 1-15.

225 Larsson C. Protein kinase C and the regulation of the actin cytoskeleton. *Cell Signal* 2006; 18: 276-284.

226 Sarbassov DD. Guertin DA. Ali SM. Sabatini DM. Phosphorylation and regulation of Akt/PKB by the rictor–mTOR complex. *Science* 2005; 307: 1098–1101.

227 Webb AE, Brunet A. FOXO transcription factors: key regulators of cellular quality control. *Trends Biochem Sci* 2014; 39: 159-169.

228 Cross D. Alessi D. Cohen P. Andjelkovicht M. Hemmingst BA. Inhibition of glycogen synthase kinase-3 by insulin mediated by protein kinase B. *Nature* 1995; 378: 785-789.

229 Garcia-Martinez JM, Alessi DR. mTOR complex 2 (mTORC2) controls hydrophobic motif phosphorylation and activation of serum- and glucocorticoid-induced protein kinase 1 (SGK1). *Biochem J* 2008; 416: 375-385.

230 Inoki K, Li Y, Zhu T, Wu J, Guan KL. TSC2 is phosphorylated and inhibited by Akt and suppresses mTOR signalling. *Nat Cell Biol* 2002; 4: 648-657.

231 Vander HE. Lee SI. Bandhakavi S. Griffin TJ. Kim DH. Insulin signalling to mTOR mediated by the Akt/PKB substrate PRAS40. *Nat Cell Biol* 2007; 9: 316–323.

232 Sancak Y, Thoreen CC, Peterson TR, Lindquist RA, Kang SA, Spooner E *et al*. PRAS40 is an insulin-regulated inhibitor of the mTORC1 protein kinase. *Mol Cell* 2007; 25: 903-915.

233 Copp J, Manning G, Hunter T. TORC-specific phosphorylation of mammalian target of rapamycin (mTOR): phospho-Ser2481 is a marker for intact mTOR signaling complex 2. *Cancer Res* 2009; 69: 1821-1827.

234 Harrington LS, Findlay GM, Gray A, Tolkacheva T, Wigfield S, Rebholz H *et al*. The TSC1-2 tumor suppressor controls insulin-PI3K signaling via regulation of IRS proteins. *J Cell Biol* 2004; 166: 213-223.

235 Shah OJ. Wang Z. Hunter T. Inappropriate activation of the TSC/Rheb/mTOR/S6K cassette induces IRS1/2 depletion, insulin resistance, and cell survival deficiencies. *Curr Biol* 2004; 14: 1650–1656.

236 Yu Y. Yoon S. Poulogiannis G. Yang Q. Ma X. *et al*. Phosphoproteomic analysis identifies Grb10 as an mTORC1 substrate that negatively regulates insulin signaling. *Science* 2011; 332: 1322–1326.

237 Hsu PP. Kang SA. Rameseder J. Zhang Y. Ottina KA. *et al*. The mTOR regulated phosphoproteome reveals a mechanism of mTORC1-mediated inhibition of growth factor signaling. *Science* 2011; 332: 1317–1322.

238 Julien LA, Carriere A, Moreau J, Roux PP. mTORC1-activated S6K1 phosphorylates Rictor on threonine 1135 and regulates mTORC2 signaling. *Mol Cell Biol* 2010; 30: 908-921.

239 Liu P, Gan W, Inuzuka H, Lazorchak AS, Gao D, Arojo O *et al*. Sin1 phosphorylation impairs mTORC2 complex integrity and inhibits downstream Akt signalling to suppress tumorigenesis. *Nat Cell Biol* 2013; 15: 1340-1350.

240 Gonzalez A, Hall MN, Lin SC, Hardie DG. AMPK and TOR: The Yin and Yang of Cellular Nutrient Sensing and Growth Control. *Cell Metab* 2020; 31: 472-492.

241 Inoki K. Zhu T. Guan KL. TSC2 Mediates Cellular Energy Response to Control Cell Growth and Survival. *Cell* 2003; 115: 577–590.

242 Gwinn DM, Shackelford DB, Egan DF, Mihaylova MM, Mery A, Vasquez DS *et al*. AMPK phosphorylation of raptor mediates a metabolic checkpoint. *Mol Cell* 2008; 30: 214-226.

243 Kazyken D. Magnuson B. Bodur C. Acosta-Jaquez H. *et al*. AMPK directly activates mTORC2 to promote cell survival during acute energetic stress. *Science Signaling* 2019; 12: 1-16.

244 Ling NXY, Kaczmarek A, Hoque A, Davie E, Ngoei KRW, Morrison KR *et al*. mTORC1 directly inhibits AMPK to promote cell proliferation under nutrient stress. *Nat Metab* 2020; 2: 41-49.

245 Saxton RA, Sabatini DM. mTOR Signaling in Growth, Metabolism, and Disease. *Cell* 2017; 168: 960-976.

246 Dibble CC, Elis W, Menon S, Qin W, Klekota J, Asara JM *et al*. TBC1D7 is a third subunit of the TSC1-TSC2 complex upstream of mTORC1. *Mol Cell* 2012; 47: 535-546.

247 Yang H, Jiang X, Li B, Yang HJ, Miller M, Yang A *et al*. Mechanisms of mTORC1 activation by RHEB and inhibition by PRAS40. *Nature* 2017; 552: 368-373.

248 Inoki K, Li Y, Xu T, Guan KL. Rheb GTPase is a direct target of TSC2 GAP activity and regulates mTOR signaling. *Genes Dev* 2003; 17: 1829-1834.

249 Demetriades C, Doumpas N, Teleman AA. Regulation of TORC1 in response to amino acid starvation via lysosomal recruitment of TSC2. *Cell* 2014; 156: 786-799.

250 Menon S, Dibble CC, Talbott G, Hoxhaj G, Valvezan AJ, Takahashi H *et al*. Spatial control of the TSC complex integrates insulin and nutrient regulation of mTORC1 at the lysosome. *Cell* 2014; 156: 771-785.

251 Garami A. Zwartkruis F. Nobukuni T. Joaquin M. *et al*. Insulin Activation of Rheb, a Mediator of mTOR/S6K/4E-BP Signaling, Is Inhibited by TSC1 and 2. *Mol Cell* 2003; 11: 1457–1466.

252 Kim E, Goraksha-Hicks P, Li L, Neufeld TP, Guan KL. Regulation of TORC1 by Rag GTPases in nutrient response. *Nat Cell Biol* 2008; 10: 935-945.

253 Sancak Y. Peterson TR. Shaul YD. Lindquist RA. *et al*. The Rag GTPases Bind Raptor and Mediate Amino Acid Signaling to mTORC1. *Science* 2008; 320: 1496–1501.

254 Shen K, Choe A, Sabatini DM. Intersubunit Crosstalk in the Rag GTPase Heterodimer Enables mTORC1 to Respond Rapidly to Amino Acid Availability. *Mol Cell* 2017; 68: 552-565 e558.

255 Rogala KB. Gu X. Kedir JF. Abu-Remaileh M. Bianchi LF. Brignole EJ. Sabatini DM. Structural basis for the docking of mTORC1 on the lysosomal surface. *Science* 2019; 366: 468–475.

256 Long X, Lin Y, Ortiz-Vega S, Yonezawa K, Avruch J. Rheb binds and regulates the mTOR kinase. *Curr Biol* 2005; 15: 702-713.

257 Bar-Peled L, Schweitzer LD, Zoncu R, Sabatini DM. Ragulator is a GEF for the rag GTPases that signal amino acid levels to mTORC1. *Cell* 2012; 150: 1196-1208.

258 Sancak Y, Bar-Peled L, Zoncu R, Markhard AL, Nada S, Sabatini DM. Ragulator-Rag complex targets mTORC1 to the lysosomal surface and is necessary for its activation by amino acids. *Cell* 2010; 141: 290-303.

259 Bar-Peled L. Chantranupong L. Cherniack AD. Chen W. Ottina KA. *et al*. A Tumor Suppressor Complex with GAPA ctivity for the Rag GTPases That Signal Amino Acid Sufficiency to mTORC1. *Science* 2013; 340: 1100–1106.

260 Shen K, Huang RK, Brignole EJ, Condon KJ, Valenstein ML, Chantranupong L *et al*. Architecture of the human GATOR1 and GATOR1-Rag GTPases complexes. *Nature* 2018; 556: 64-69.

261 Wolfson RL, Chantranupong L, Wyant GA, Gu X, Orozco JM, Shen K *et al*. KICSTOR recruits GATOR1 to the lysosome and is necessary for nutrients to regulate mTORC1. *Nature* 2017; 543: 438-442.

262 Tsun ZY. Bar-Peled L. Chantranupong L. Zoncu R. Wang T. Kim C. Spooner E. Sabatini DM. The folliculin tumor suppressor is a GAP for the RagC/D GTPases that signal amino acid levels to mTORC1. *Mol Cell* 2013; 52: 495–505.

263 Han JM, Jeong SJ, Park MC, Kim G, Kwon NH, Kim HK *et al*. Leucyl-tRNA synthetase is an intracellular leucine sensor for the mTORC1-signaling pathway. *Cell* 2012; 149: 410-424.

264 Wolfson RL, Sabatini DM. The Dawn of the Age of Amino Acid Sensors for the mTORC1 Pathway. *Cell Metab* 2017; 26: 301-309.

265 Wang S. Tsun ZY. Wolfson RL. Shen K. Wyant GA. Sabatini BL. Sabatini DM. Lysosomal amino acid transporter SLC38A9 signals arginine sufficiency to mTORC1. *Science* 2015; 347: 188–194.

266 Rebsamen M, Pochini L, Stasyk T, de Araujo ME, Galluccio M, Kandasamy RK *et al*. SLC38A9 is a component of the lysosomal amino acid sensing machinery that controls mTORC1. *Nature* 2015; 519: 477-481.

267 Zoncu R. Bar-Peled L. Efeyan A. Wang S. Sancak Y. Sabatini DM. mTORC1 senses lysosomal amino acids through an inside- out mechanism that requires the vacuolar H+-ATPase. *Science* 2011; 334: 678–683.

268 Wolfson RL. Chantranupong L. Saxton RA. Shen K. Scaria SM. Cantor JR. Sabatini DM. Sestrin2 is a leucine sensor for the mTORC1 pathway. *Science* 2016; 351: 43–48.

269 Chantranupong L, Scaria SM, Saxton RA, Gygi MP, Shen K, Wyant GA *et al*. The CASTOR Proteins Are Arginine Sensors for the mTORC1 Pathway. *Cell* 2016; 165: 153-164.

270 Chen J, Ou Y, Luo R, Wang J, Wang D, Guan J *et al*. SAR1B senses leucine levels to regulate mTORC1 signalling. *Nature* 2021; 596: 281-284.

271 Saxton RA. Knockenhauer KE. Wolfson RL. Chantranupong L. *et al*. Structural basis for leucine sensing by the Sestrin2–mTORC1 pathway. *Science* 2016; 351: 53–58.

272 Saxton RA, Chantranupong L, Knockenhauer KE, Schwartz TU, Sabatini DM. Mechanism of arginine sensing by CASTOR1 upstream of mTORC1. *Nature* 2016; 536: 229-233.

273 Gu X. Orozco JM. Saxton RA. Condon KJ. Liu GY *et al*. SAMTOR is an S-adenosylmethionine sensor for the mTORC1 pathway. *Science* 2017; 358: 813–818.

274 Kim SH, Choi JH, Wang P, Go CD, Hesketh GG, Gingras AC *et al*. Mitochondrial Threonyl-tRNA Synthetase TARS2 Is Required for Threonine-Sensitive mTORC1 Activation. *Mol Cell* 2021; 81: 398-407 e394.

275 Yuan HX, Guan KL. The SIN1-PH Domain Connects mTORC2 to PI3K. *Cancer Discov* 2015; 5: 1127-1129.

276 Frias MA. Thoreen CC. Jaffe JD. Schroder W. Sculley T. Carr SA. Sabatini DM. mSin1 is necessary for Akt/PKB phosphorylation, and its isoforms define three distinct mTORC2s. *Curr Biol* 2006; 16: 1865–1870.

277 Yang Q, Inoki K, Ikenoue T, Guan KL. Identification of Sin1 as an essential TORC2 component required for complex formation and kinase activity. *Genes Dev* 2006; 20: 2820-2832.

278 Jacinto E. Facchinetti V. Liu D. Soto N. Wei S. Jung SY. Huang Q. Qin J. Su B *et al*. SIN1/MIP1 maintains rictor–mTOR complex integrity and regulates Akt phosphorylation and substrate specificity. *Cell* 2006; 127: 125–137.

279 Crino PB. Nathanson KL. Henske EP. The Tuberous Sclerosis Complex. *NEJM* 2006; 355: 1345–1356.

280 Okosun J, Wolfson RL, Wang J, Araf S, Wilkins L, Castellano BM *et al*. Recurrent mTORC1-activating RRAGC mutations in follicular lymphoma. *Nat Genet* 2016; 48: 183-188.

281 Nickerson ML. Warren MB. Toro JR. Matrosova V. *et al*. Mutations in a novel gene lead to kidney tumors, lung wall defects, and benign tumors of the hair follicle in patients with the Birt–Hogg–Dube syndrome. *Cancer Cell* 2002; 2: 157–164.

282 Kim LC, Cook RS, Chen J. mTORC1 and mTORC2 in cancer and the tumor microenvironment. *Oncogene* 2017; 36: 2191-2201.

283 Grabiner BC, Nardi V, Birsoy K, Possemato R, Shen K, Sinha S *et al*. A diverse array of cancer-associated MTOR mutations are hyperactivating and can predict rapamycin sensitivity. *Cancer Discov* 2014; 4: 554-563.

284 Benjamin D, Colombi M, Moroni C, Hall MN. Rapamycin passes the torch: a new generation of mTOR inhibitors. *Nat Rev Drug Discov* 2011; 10: 868-880.

285 Tabernero J, Rojo F, Calvo E, Burris H, Judson I, Hazell K *et al*. Dose and schedule dependent inhibition of the mammalian target of rapamycin pathway with everolimus: a phase I tumor pharmacodynamic study in patients with advanced solid tumors. *J Clin Oncol* 2008; 26: 1603-1610.

286 Thoreen CC, Kang SA, Chang JW, Liu Q, Zhang J, Gao Y *et al*. An ATP-competitive mammalian target of rapamycin inhibitor reveals rapamycin-resistant functions of mTORC1. *J Biol Chem* 2009; 284: 8023-8032.

287 Wagle N, Grabiner BC, Van Allen EM, Amin-Mansour A, Taylor-Weiner A, Rosenberg M *et al*. Response and acquired resistance to everolimus in anaplastic thyroid cancer. *N Engl J Med* 2014; 371: 1426-1433.

288 Fan Q, Aksoy O, Wong RA, Ilkhanizadeh S, Novotny CJ, Gustafson WC *et al*. A Kinase Inhibitor Targeted to mTORC1 Drives Regression in Glioblastoma. *Cancer Cell* 2017; 31: 424-435.

289 Zhou X. Clister TL. Lowry PR. Seldin MM. Wong GW. Zhang J. Dynamic visualization of mTORC1 activity in living cells. *Cell Rep* 2015; 10: 1067–1077.

290 Rosner M. Hengstschlager M. mTOR protein localization is cell cycle regulated. *Cell Cycle* 2011; 10: 3608–3610.

291 Zhang X. Shu L. Hosoi H. Murti KG. Houghton PJ. Predominant Nuclear Localization of Mammalian Target of Rapamycin in Normal and Malignant Cells in Culture. *J Biol Chem* 2002; 277: 28127–28134.

292 Kim JE. Chen J. Cytoplasmic-nuclear shuttling of FKBP12-rapamycin associated protein is involved in rapamycin-sensitive signaling and translation initiation. *PNAS* 2000; 97: 14340–14345.

293 Giguere V. Canonical signaling and nuclear activity of mTOR-a teamwork effort to regulate metabolism and cell growth. *FEBS J* 2018; 285: 1572-1588.

294 Cunningham JT, Rodgers JT, Arlow DH, Vazquez F, Mootha VK, Puigserver P. mTOR controls mitochondrial oxidative function through a YY1-PGC-1alpha transcriptional complex. *Nature* 2007; 450: 736-740.

295 Bernardi R, Guernah I, Jin D, Grisendi S, Alimonti A, Teruya-Feldstein J *et al*. PML inhibits HIF-1alpha translation and neoangiogenesis through repression of mTOR. *Nature* 2006; 442: 779-785.

296 Wan W, You Z, Xu Y, Zhou L, Guan Z, Peng C *et al*. mTORC1 Phosphorylates Acetyltransferase p300 to Regulate Autophagy and Lipogenesis. *Mol Cell* 2017; 68: 323-335 e326.

297 Chaveroux C. Eichner LJ. Dufour CR. Shatnawi A. *et al*. Molecular and genetic crosstalks between mTOR and ERRα are key determinants of rapamycin-induced non-alcoholic fatty liver. *Cell Metab* 2013; 17: 586–598.

298 Alayev A, Salamon RS, Berger SM, Schwartz NS, Cuesta R, Snyder RB *et al*. mTORC1 directly phosphorylates and activates ERalpha upon estrogen stimulation. *Oncogene* 2016; 35: 3535-3543.

299 Audet-Walsh E, Dufour CR, Yee T, Zouanat FZ, Yan M, Kalloghlian G *et al*. Nuclear mTOR acts as a transcriptional integrator of the androgen signaling pathway in prostate cancer. *Genes Dev* 2017; 31: 1228-1242.

300 Tsang CK, Liu H, Zheng XF. mTOR binds to the promoters of RNA polymerase I- and III-transcribed genes. *Cell Cycle* 2010; 9: 953-957.

301 Li H, Tsang CK, Watkins M, Bertram PG, Zheng XF. Nutrient regulates Tor1 nuclear localization and association with rDNA promoter. *Nature* 2006; 442: 1058-1061.

302 Kantidakis T, Ramsbottom BA, Birch JL, Dowding SN, White RJ. mTOR associates with TFIIIC, is found at tRNA and 5S rRNA genes, and targets their repressor Maf1. *Proc Natl Acad Sci U S A* 2010; 107: 11823-11828.

303 Wei Y. Tsang CK. Zheng XF. Mechanisms of regulation of RNA polymerase III-dependent transcription by TORC1. *EMBO J* 2009; 28: 2220–2230.

304 Sharma NL, Massie CE, Ramos-Montoya A, Zecchini V, Scott HE, Lamb AD *et al*. The androgen receptor induces a distinct transcriptional program in castration-resistant prostate cancer in man. *Cancer Cell* 2013; 23: 35-47.

305 McMullin RP, Dobi A, Mutton LN, Orosz A, Maheshwari S, Shashikant CS *et al*. A FOXA1-binding enhancer regulates Hoxb13 expression in the prostate gland. *Proc Natl Acad Sci U S A* 2010; 107: 98-103.

306 Xu Y, Chen SY, Ross KN, Balk SP. Androgens induce prostate cancer cell proliferation through mammalian target of rapamycin activation and post-transcriptional increases in cyclin D proteins. *Cancer Res* 2006; 66: 7783-7792.

307 Wu Y. Chhipa RR. Cheng J. Zhang H. Mohler JL. Clement IP. Androgen Receptor-mTOR Crosstalk is Regulated by Testosterone Availability- Implication for Prostate Cancer Cell Survival. *Anticancer Research* 2010; 30: 3895–3901.

308 Cinar B. Benedetti AD. Freeman MR. Post-Transcriptional Regulation of the Androgen Receptor by Mammalian Target of Rapamycin. *Cancer Res* 2005; 65: 2547-2553.

309 Wang Y, Mikhailova M, Bose S, Pan CX, deVere White RW, Ghosh PM. Regulation of androgen receptor transcriptional activity by rapamycin in prostate cancer cell proliferation and survival. *Oncogene* 2008; 27: 7106-7117.

310 Ren QN, Zhang H, Sun CY, Zhou YF, Yang XF, Long JW *et al*. Phosphorylation of androgen receptor by mTORC1 promotes liver steatosis and tumorigenesis. *Hepatology* 2022; 75: 1123-1138.

311 Crumbaker M, Khoja L, Joshua AM. AR Signaling and the PI3K Pathway in Prostate Cancer. *Cancers (Basel)* 2017; 9.

312 Pei H, Li L, Fridley BL, Jenkins GD, Kalari KR, Lingle W *et al*. FKBP51 affects cancer cell response to chemotherapy by negatively regulating Akt. *Cancer Cell* 2009; 16: 259-266.

313 Carver BS, Chapinski C, Wongvipat J, Hieronymus H, Chen Y, Chandarlapaty S *et al*. Reciprocal feedback regulation of PI3K and androgen receptor signaling in PTEN-deficient prostate cancer. *Cancer Cell* 2011; 19: 575-586.

314 Mellinghoff IK, Vivanco I, Kwon A, Tran C, Wongvipat J, Sawyers CL. HER2/neu kinase-dependent modulation of androgen receptor function through effects on DNA binding and stability. *Cancer Cell* 2004; 6: 517-527.

315 Mulholland DJ, Tran LM, Li Y, Cai H, Morim A, Wang S *et al*. Cell autonomous role of PTEN in regulating castration-resistant prostate cancer growth. *Cancer Cell* 2011; 19: 792-804.

316 Castoria G, Lombardi M, Barone MV, Bilancio A, Di Domenico M, Bottero D *et al*. Androgen-stimulated DNA synthesis and cytoskeletal changes in fibroblasts by a nontranscriptional receptor action. *J Cell Biol* 2003; 161: 547-556.

317 Dufour CR, Scholtes C, Yan M, Chen Y, Han L, Li T *et al*. The mTOR chromatin-bound interactome in prostate cancer. *Cell Rep* 2022; 38: 110534.

318 Jung SH, Hwang HJ, Kang D, Park HA, Lee HC, Jeong D *et al*. mTOR kinase leads to PTEN-loss-induced cellular senescence by phosphorylating p53. *Oncogene* 2019; 38: 1639-1650.

319 Sacco F, Perfetto L, Castagnoli L, Cesareni G. The human phosphatase interactome: An intricate family portrait. *FEBS Lett* 2012; 586: 2732-2739.

320 Wang X, Trotman LC, Koppie T, Alimonti A, Chen Z, Gao Z *et al*. NEDD4-1 is a proto-oncogenic ubiquitin ligase for PTEN. *Cell* 2007; 128: 129-139.

321 Maddika S, Kavela S, Rani N, Palicharla VR, Pokorny JL, Sarkaria JN *et al*. WWP2 is an E3 ubiquitin ligase for PTEN. *Nat Cell Biol* 2011; 13: 728-733.

322 Fan H, Wang X, Li W, Shen M, Wei Y, Zheng H *et al*. ASB13 inhibits breast cancer metastasis through promoting SNAI2 degradation and relieving its transcriptional repression of YAP. *Genes Dev* 2020; 34: 1359-1372.

323 Li W, Shen M, Jiang YZ, Zhang R, Zheng H, Wei Y *et al*. Deubiquitinase USP20 promotes breast cancer metastasis by stabilizing SNAI2. *Genes Dev* 2020; 34: 1310-1315.

324 Song MS, Carracedo A, Salmena L, Song SJ, Egia A, Malumbres M *et al*. Nuclear PTEN Regulates the APC-CDH1 Tumor-Suppressive Complex in a Phosphatase-Independent Manner. *Cell* 2011; 144: 187-199.

325 Thomas GE, Egan G, Garcia-Prat L, Botham A, Voisin V, Patel PS *et al*. The metabolic enzyme hexokinase 2 localizes to the nucleus in AML and normal haematopoietic stem and progenitor cells to maintain stemness. *Nat Cell Biol* 2022; 24: 872-884.

326 Zhou X, Zhong Y, Molinar-Inglis O, Kunkel MT, Chen M, Sun T *et al*. Location-specific inhibition of Akt reveals regulation of mTORC1 activity in the nucleus. *Nat Commun* 2020; 11: 6088.

327 Zhong Y, Zhou X, Guan KL, Zhang J. Rheb regulates nuclear mTORC1 activity independent of farnesylation. *Cell Chem Biol* 2022; 29: 1037-1045 e1034.

328 Trotman LC, Wang X, Alimonti A, Chen Z, Teruya-Feldstein J, Yang H *et al*. Ubiquitination regulates PTEN nuclear import and tumor suppression. *Cell* 2007; 128: 141-156.

329 Song MS, Salmena L, Carracedo A, Egia A, Lo-Coco F, Teruya-Feldstein J *et al*. The deubiquitinylation and localization of PTEN are regulated by a HAUSP-PML network. *Nature* 2008; 455: 813-817.

330 Kose S, Furuta M, Imamoto N. Hikeshi, a nuclear import carrier for Hsp70s, protects cells from heat shock-induced nuclear damage. *Cell* 2012; 149: 578-589.

331 Roux KJ, Kim DI, Burke B, May DG. BioID: A Screen for Protein-Protein Interactions. *Curr Protoc Protein Sci* 2018; 91: 19 23 11-19 23 15.

332 Bondeson DP, Mares A, Smith IE, Ko E, Campos S, Miah AH *et al*. Catalytic in vivo protein knockdown by small-molecule PROTACs. *Nat Chem Biol* 2015; 11: 611-617.

333 Schneider M, Radoux CJ, Hercules A, Ochoa D, Dunham I, Zalmas LP *et al*. The PROTACtable genome. *Nat Rev Drug Discov* 2021; 20: 789-797.

334 Zhang X, Crowley VM, Wucherpfennig TG, Dix MM, Cravatt BF. Electrophilic PROTACs that degrade nuclear proteins by engaging DCAF16. *Nat Chem Biol* 2019; 15: 737-746.